

ANALYSIS OF RECTANGULAR AND CIRCULAR WAVEGUIDES

ERIC WONG VUN SHIUNG

**A project report submitted in partial fulfilment of the
requirements for the award of the degree of
Bachelor of Engineering (Hons) Electronic Engineering**

**Faculty of Engineering and Green Technology
Universiti Tunku Abdul Rahman**

May 2016

DECLARATION

I hereby declare that this project report is based on my original work except for citations and quotations which have been duly acknowledged. I also declare that it has not been previously and concurrently submitted for any other degree or award at UTAR or other institutions.

Signature : _____

Name : _____

ID No. : _____

Date : _____

APPROVAL FOR SUBMISSION

I certify that this project report entitled “**ANALYSIS OF RECTANGULAR AND CIRCULAR WAVEGUIDE**” was prepared by **ERIC WONG VUN SHIUNG** has met the required standard for submission in partial fulfilment of the requirements for the award of Bachelor of Engineering (Hons) Electronic Engineering at Universiti Tunku Abdul Rahman.

Approved by,

Signature : _____

Supervisor : Dr. Yeap Kim Ho

Date : _____

The copyright of this report belongs to the author under the terms of the copyright Act 1987 as qualified by Intellectual Property Policy of Universiti Tunku Abdul Rahman. Due acknowledgement shall always be made of the use of any material contained in, or derived from, this report.

© 2016, Eric Wong Vun Shiung. All right reserved.

ACKNOWLEDGEMENTS

I would like to thank everyone who had contributed to the successful completion of this project. I would like to express my gratitude to my research supervisor, Dr. Yeap Kim Ho for his invaluable advice, guidance and his enormous patience throughout the development of the research.

In addition, I would also like to express my gratitude to my loving parent and friends who had helped and given me encouragement

ANALYSIS OF RECTANGULAR AND CIRCULAR WAVEGUIDE

ABSTRACT

Waveguides are generally used to channel the weak cosmic wave to the receiver in a radio telescope. The most commonly used waveguide is the rectangular and circular waveguides. Cosmic waves from distant sources are extremely weak. Hence it is important to minimize the loss in the waveguide. To allow the engineers and scientists to efficiently design a waveguide, it is important to develop a formulation which is able to compute the attenuation in a waveguide accurately.

The transcendental equations developed by Stratton and Yeap to compute losses in waveguides are derived from the first principle. Hence, the equations are able to predict losses with higher accuracy. However, these equations are difficult to solve analytically. Solution to the transcendental equation can only be obtained using a root finding algorithm. Depending on the compiler and the algorithm used, solution may converge or diverge. Besides, it may require long computation time to solve.

On the other hand, closed form solutions are simpler and give more intuitive insights. The resulting equation takes much less time to solve compared to the transcendental equation. Closed form solutions often use assumptions to simplify the equations. Equations such as the power loss method assumes the wall to be perfectly conducting. Such assumption is able to approximate the solution provided the metal is of sufficiently high conductivity. However, the assumption of perfect wall result in an infinite attenuation at cut-off frequency. An infinite conductivity metal prevents wave to propagate when the frequency is below the cut-off frequency. Such case is of course not accurate. Based on the experimental result, the attenuation of the wave increases as the frequency is reduced from the cut-off frequency. However, the attenuation constant is finite.

This thesis primarily focuses on the formulation of a closed form equation that is able to describe wave beyond as well as below the cut-off frequency with reasonable accuracy. The new method developed is based on modification from Yeap's transcendental equation. Unlike Stratton's transcendental equation, which is only restricted to the case of a circular waveguide. Yeap's method is able to be used for circular as well as rectangular waveguide. Hence, the new method proposed here has also the advantage of being applied in waveguides with circular or rectangular geometry. Finite Difference Method is used to approximate the transcendental equation to transform it into a closed form solution. The resulting equation is simpler and gives more intuitive insights than Yeap's transcendental equation. It also requires less computation time.

The results show that the loss computed based on the new method agrees with the experimental result as well as existing theories.

TABLE OF CONTENTS

DECLARATION	ii
APPROVAL FOR SUBMISSION	iii
ACKNOWLEDGEMENTS	v
ABSTRACT	vi
TABLE OF CONTENTS	viii
LIST OF FIGURES	xi
LIST OF ABBREVIATIONS	xiv
LIST OF SYMBOLS	xv
LIST OF APPENDICES	xvii

CHAPTER

1	INTRODUCTION	1
	1.1 Problem Statements	1
	1.2 Aims and Objectives	2
	1.3 Overview of Thesis	2
2	RADIO ASTRONOMY	4
	2.1 Introduction	4
	2.2 Antenna	7
	2.3 Heterodyne Receiver	9
	2.4 Waveguide Coupling	11
3	WAVEGUIDING STRUCTURES	13
	3.1 Introduction	13
	3.2 Transmission Lines	14

	3.2.1	Coaxial Cable	14
	3.2.2	Microstrip	16
	3.3	Waveguide	17
	3.3.1	Metal Waveguide	18
	3.3.2	Dielectric Waveguide	18
4		CIRCULAR WAVEGUIDE	20
	4.1	Introduction	20
	4.2	Fields in Circular Cylindrical Waveguides	23
	4.3	Cutoff Frequency for Circular Waveguide	28
	4.4	A Review of Some Conventional Methods	30
	4.4.1	A Review of the Power Loss Method	30
	4.4.2	A Review of Stratton's Method	34
	4.4.3	A Review of Yeap's Method	41
	4.5	The New Method	43
	4.5.1	Transverse Electric Mode	44
	4.5.2	Transverse Magnetic Mode	46
	4.6	Results and Discussion	47
	4.7	Summary	54
5		RECTANGULAR WAVEGUIDE	56
	5.1	Introduction	56
	5.2	Fields in Rectangular Waveguides	57
	5.3	Cutoff Frequency for Rectangular Waveguide	62
	5.4	Review of Some Conventional Method	64
	5.4.1	A Review of Papadopoulos' Method	64
	5.4.2	A Review of the Power Loss Method	72
	5.4.3	A Review of Yeap's Method	74
	5.5	The New Method	77
	5.5.1	TE ₁₁ Mode	78
	5.5.2	TM ₁₁ Mode	80
	5.5.3	TE ₁₀ Mode	81
	5.6	Results and Discussion	82

		x
5.7	Summary	89
6	CONCLUSION AND RECOMMENDATIONS	90
6.1	Summary	90
6.2	Future Work	92
	REFERENCES	93
	APPENDICES	96

LIST OF FIGURES

FIGURE	TITLE	PAGE
Figure 1	Difference between (a) Optical Telescope and (b) Radio Telescope	5
Figure 2	Atmospheric Opacity (Terahertz region highlighted by red box)	6
Figure 3	SMA Radio Telescope Antenna	7
Figure 4	SMA antenna optics layout	8
Figure 5	Beam waveguide mirrors	8
Figure 6	Receiver optics layout	9
Figure 7	Block Diagram of Heterodyne Receiver	10
Figure 8	Layout of SIS Receiver for ALMA Band 7 Cartridge	11
Figure 9	Mixer Substrate Coupled to Waveguide in ALMA Band 7 Receiver	12
Figure 10	Layout of Quartz Substrate with SIS Mixer Built onto it	12
Figure 11	Coaxial Cable Cutaway (Tkgd2007, 2008)	14
Figure 12	Coaxial Cable Field Pattern	15
Figure 13	Microstrip	16
Figure 14	Microstrip Field Pattern (Al-Raie, 2007)	16
Figure 15	Various Types of Transmission Lines	17
Figure 16	Rectangular Waveguide (Zykure, 2009)	18

Figure 17	Optical Fiber (Gringer, 2008)	19
Figure 18	Normalized Cutoff Frequency for Different Field in a Circular Waveguide (C.S. Lee, 1985)	29
Figure 19	Circular Waveguide (Jin, 2010)	34
Figure 20	Simplified Waveguide Model (Jin, 2010)	35
Figure 21	Modified Bessel's Function of Second Kind	36
Figure 22	Attenuation of TE_{11} mode in a hollow circular waveguide with radius $a = 5.8533$ mm	48
Figure 23	Attenuation of TE_{11} in a circular waveguide with radius $a = 5.8533$ mm	49
Figure 24	Attenuation of TM_{11} in a circular waveguide with radius $a = 8.1$ mm	49
Figure 25	Attenuation of TE_{11} in circular waveguide from 0 GHz to 1000 GHz	50
Figure 26	Attenuation of TM_{11} in circular waveguide from 0 GHz to 800 GHz	51
Figure 27	Comparison of Attenuation of TE_{11} , TE_{01} , TE_{02} , TM_{11} and TM_{01} mode	52
Figure 28	Comparison of different wall conductivity in hollow metal waveguide with radius $a = 5.8533$ mm for TE_{11} mode	52
Figure 29	Difference of Yeap's Solution and the new method at low conductivity. Red solid line is the result from Yeap's method, black dotted line is the result from the new method.	54
Figure 30	Normalized Cutoff Frequency for Different Field in a Rectangular Waveguide (C.S. Lee, 1985)	63
Figure 31	Normalized Cutoff Frequency for Different Field in a Square Waveguide (C.S. Lee, 1985)	63

Figure 32	PPM and Power Loss Method Attenuation (Collin, 1960)	71
Figure 33	Attenuation of TE_{10} Mode in a Hollow Rectangular Waveguide with Width $a = 1.30$ cm, Height, $b = 0.64$ cm	83
Figure 34	Attenuation of TE_{11} and TM_{11} in a Hollow Rectangular Waveguide with Width $a = 2.29$ cm , Height, $b = 1.02$ cm	83
Figure 35	Attenuation of TE_{11} after cutoff in a Hollow Rectangular Waveguide with Width $a = 2.29$ cm, Height, $b = 1.02$ cm	84
Figure 36	Attenuation of TM_{11} after cutoff in a Hollow Rectangular Waveguide with Width $a = 2.29$ cm, Height, $b = 1.02$ cm	85
Figure 37	Attenuation of TE_{10} in a Hollow Rectangular Waveguide with Width $a = 2.29$ cm , Height, $b = 1.02$ cm	85
Figure 38	Tangential Field in a Waveguide	86
Figure 39	Attenuation of TE_{11} around the cutoff frequency in a Hollow Rectangular Waveguide with Width $a = 2.29$ cm, Height, $b = 1.02$ cm	87
Figure 40	Attenuation of TM_{11} around the cutoff frequency in a Hollow Rectangular Waveguide with Width $a = 2.29$ cm, Height, $b = 1.02$ cm	88
Figure 41	Attenuation of TE_{10} around the cutoff frequency in a Hollow Rectangular Waveguide with Width $a = 2.29$ cm , Height, $b = 1.02$ cm	88

LIST OF ABBREVIATIONS

THz	Terahertz
TEM	Transverse Electromagnetic
TE	Transverse Electric
TM	Transverse Magnetic
PPM	Papadopoulos Perturbation Method
FEM	Finite Element Method
EMI	Electromagnetic Interference
IC	Integrated Circuit
PCB	Printed Circuit Board
CPW	Coplanar Waveguide
PCB	Printed Circuit Board
RF	Radio Frequency
IF	Intermediate Frequency
LNA	Low Noise Amplifier
SBD	Schottky Barrier Diode
HEB	Hot Electron Bolometer
SIS	Superconductor-Insulator-Superconductor

LIST OF SYMBOLS

F_s	Input Signal Frequency
F_{LO}	Local Oscillator Signal Frequency
f_c	Cutoff frequency
ω	Angular Frequency
γ	Propagation Constant
β	Phase Constant
α	Attenuation Constant
γ_z	Propagation Constant in z-direction
β_z	Phase Constant in z-direction
β_ρ	Transverse Phase Constant in ρ direction
ϵ	Permittivity of Medium
μ	Permeability of Medium
Z_m	Complex Surface Impedance
R_s	Real Part of Surface Impedance
f	Frequency of Electromagnetic Wave
σ	Conductivity of Waveguide Metal Wall
ρ_v	Electric Charge Density
$\nabla \cdot$	Divergence of vector field
$\nabla \times$	Curl of vector field
J_m	Bessel Function of First Kind
Y_m	Bessel Function of Second Kind
$H_m^{(1)}$	Hankel Function of First Kind
$H_m^{(2)}$	Hankel Function of Second Kind
K_m	Modified Bessel Function

P_z	Average Output Power Flowing through Waveguide
P_o	Average Input Power to the Waveguide
ℓ	Length of the Waveguide
α_c	Attenuation due to Conduction Loss
\mathcal{P}_{ave}	Electromagnetic Wave Average Power
P_c	Average Output Power through Waveguide per unit length
η	Intrinsic Impedance of Medium
∇_T	Transverse Part of Gradient Operator
\overrightarrow{E}_T	Transverse Part of Electric Field in Lossless Waveguide
E_z	Axial Part of Electric Field
\overrightarrow{E}_{Tn}	Transverse Part of Electric Field in Lossy Waveguide
E_{tan}	Tangential Electric Field with Respect to Conductor Wall
\hat{n}	Inward Pointing Vector with Respect to Conductor Wall
Γ_z	Propagation Constant in Lossless Waveguide

LIST OF APPENDICES

APPENDIX	TITLE	PAGE
APPENDIX A:	Helmholtz Equation	96
APPENDIX B:	Conductor Surface Impedance	97

CHAPTER 1

INTRODUCTION

1.1 Problem Statements

This thesis focuses on the theoretical study of waveguide which is important in the design of radio telescopes. Radio telescopes allow scientists to observe the interstellar medium in which visible light fails to do so. In a typical radio telescope, the radiation signal received at the feed horn is usually transmitted to the detector via a circular waveguide and a rectangular waveguide (Yeap, 2011). Due to the low power of electromagnetic wave from distant sources, the design of the waveguide which is capable of minimising signal attenuation is of utmost importance.

Hence a formulation which is able to compute accurately the attenuation in the waveguide below as well as beyond the cutoff frequency is important. Yeap (2011) has developed a set of transcendental equations to solve for the propagation constant of both circular and rectangular waveguides. Since the transcendental equations account for the mode coupling effect, the results have been found to agree closely with the measurements. To solve for the roots of the equations, however, an efficient root-searching algorithm is to be applied on the equations. Moreover, appropriate initial guesses which allow convergence to the correct roots are necessary as well. Because of this reason, applying Yeap's transcendental equation to compute the loss in a waveguide is found to be laborious and time-consuming. The solution in a closed-form equation, on the other hand, can easily be found without the need of a numerical algorithm and appropriate initial guesses. Hence, it may be simpler and more straight-

forward if a closed-form equation which provides solution comparable to Yeap's equation can be applied to compute the loss.

This thesis therefore has its primary objective of formulating an equation which is able to describe the characteristics of wave attenuation above and below the cutoff frequency with reasonably accurate result. The closed form equations illustrated in this thesis would have the simplicity of being applied directly, without the need of an effective root-searching algorithm. They would also give reasonably good prediction of loss in both circular and rectangular waveguides

1.2 Aims and Objectives

In general, this thesis has the objective to

- i) Develop a reasonably accurate equation to describe the propagation of electromagnetic wave in a circular and rectangular waveguide
- ii) Simulate and calculate the attenuation of the electromagnetic wave in circular and rectangular waveguides
- iii) Compare and analyze different equations with the experimental result.

1.3 Overview of Thesis

The thesis is organized as below

Chapter 2 shows the fundamental of radio astronomy. The importance of radio astronomy as well as the difficulty is briefly described. Later, each section of a radio telescope such as the antenna and mixer were briefly described.

Chapter 3 describes different types of wave guiding structures. The difference between transmission lines and waveguides were discussed.

Chapter 4 describes the circular waveguide. This chapter starts with a review of work found in the literature. The derivations of Stratton's method, Yeap's method and power loss perturbation method are illustrated in this chapter. The general review on the comparison between different method describing the advantages as well as disadvantages for each method is well described in this chapter. Later, step by step derivation of a new perturbation method based on Yeap's method were introduced. The chapter ends with the result comparing the new method with the existing method.

Chapter 5 describes the rectangular waveguide. Like the case of the circular waveguide in chapter 4, this chapter starts with a review of existing methods, i.e. the power loss method, Papadopoulos' method, and Yeap's method. The new method modified from Yeap's method is then introduced. The new method is derived using a similar approach like the circular waveguide.

Chapter 6 summarizes all the work done in chapter 4 and chapter 5. Future works with the possibilities of improving the work done in this thesis are briefly explained

CHAPTER 2

RADIO ASTRONOMY

2.1 Introduction

The first ever telescope was invented by Galileo Galilei. It has opened a whole new world to human. Telescope has enabled a better understanding of the world, the earth. It was Galileo, through his invention of telescope, discovers that the earth rotates around the Sun and not vice versa. Through the telescope, Galileo found out that there are other planets exist out there, and our earth is not the sole planet in the galaxy.

The telescope invented by Galileo was made of different optical lenses. Through the combination of the lenses arrangement, it enables distance objects to be viewed clearly. Over the years, the technology and science continue to refine the design of optical telescope, enabling us to have a clearer view of the galaxy. However, one significant drawback of the optical telescope is that it only allows us to “see” within visible spectrum. In reality, an abundance of information is hidden in the other part of the frequency spectrum, such as in the terahertz region. A radio telescope is used instead to observe at the terahertz region and the other longer wavelength radio frequency. Instead of focusing distance light, the radio telescopes are designed specifically to collect electromagnetic radiation at the terahertz and radio frequency regions. Figure 1 shows some space photos that were obtained using the optical telescope and radio telescope. From the picture it can be seen that the radio telescope is able to show more information about the distance galaxy.

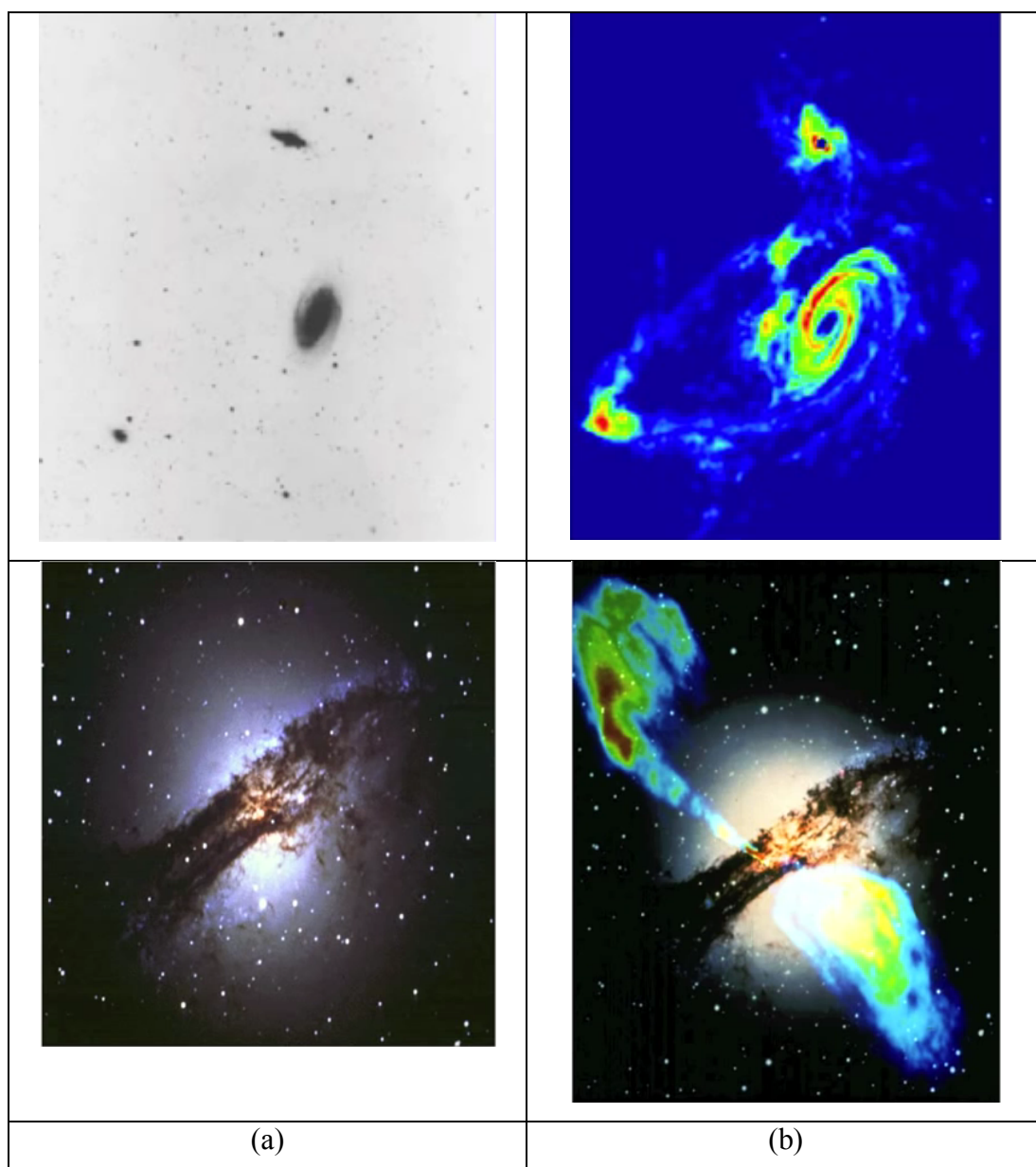


Figure 1 Difference between (a) Optical Telescope and (b) Radio Telescope

Another reason to observe using radio waves is due to the atmospheric opacity. Our Earth is surrounded by a layer of ozone. This ozone protects us from high energy radiation, such as gamma and x-rays. When the electromagnetic radiation from outer space reaches the Earth, some of the radiation is absorbed. The absorption rate of radiation varies with frequency. Figure 2 shows the atmospheric opacity of the Earth. From the figure it can be seen that there are two windows for which the atmospheric condition of the earth allows the signal to pass through. The first window is the narrow visible light spectrum. The other window is the large radio wave window. The large radio wave window has long been studied due to the low atmospheric opacity that

makes it easy to be detected using ground based radio telescopes. In between the visible spectrum and the microwave region, it can be seen numerous narrow window. This is the terahertz region. This region remains largely unexplored due to technological difficulty.

The terahertz region lies in between the optical region and the easily detectable radio waves region. Hence, most of the terahertz region telescopes borrow technology from both the optical and radio region. The radioscope receiver employs a heterodyne design. A heterodyne receiver at such high frequency is difficult to construct. Besides, the atmospheric opacity of the earth adds in another layer of difficulty to the construction of ground based radioscope operating in this region. At the terahertz region, water vapour will absorb incoming radiation. At low elevation, an abundance of water vapour is present in the atmosphere, making detection of terahertz radiation difficult. Hence, most of these detectors are constructed at high altitudes with dry atmosphere to reduce the effect of absorption.

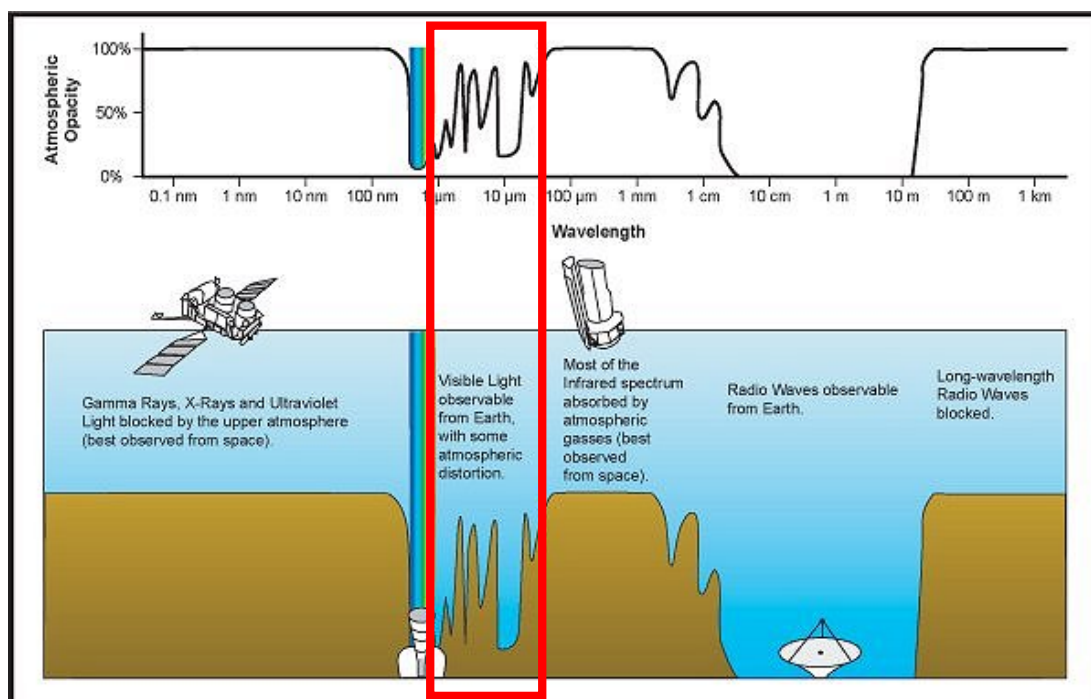


Figure 2 Atmospheric Opacity (Terahertz region highlighted by red box)

2.2 Antenna

The antenna consists of a large parabolic dish. It is used to collect the RF signals. It can be constructed as a single antenna, or used as an antenna array, such as those used as a radio interferometer. An interferometer uses an array of telescopes to achieve higher resolution through interferometry. An example of such interferometer is the Submillimeter Array (SMA), located in Hawaii. The radio telescope antenna is usually located far away from the population to reduce electromagnetic interference (EMI) from other wireless sources, such as television and radio. Figure 3 shows the SMA antenna and its optical configuration (Paine, 1994).

Figure 4 shows the antenna optics layout. The primary reflector with a 6 meter diameter focuses distance RF signal from outer space to the secondary reflector which directs the signals to the beam waveguide.

Figure 5 shows the beam waveguide mirror system. The beam waveguide directs the RF signals from the antenna vertically downward to the receiver optics assembly.



Figure 3 SMA Radio Telescope Antenna

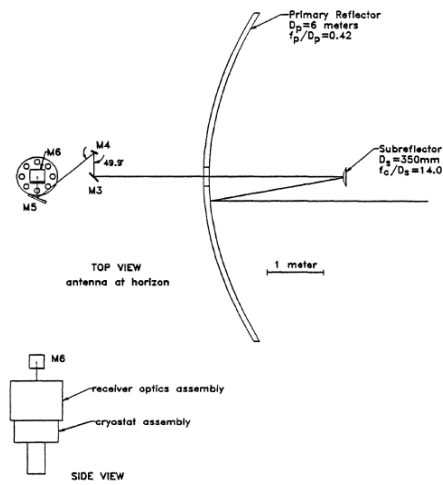


Figure 4 SMA antenna optics layout

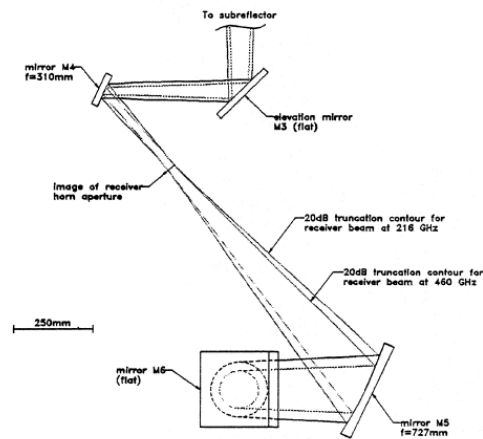


Figure 5 Beam waveguide mirrors

From Figure 6, it can be seen that the beam from the beam waveguide enters the receiver and is splitted into two orthogonally polarized beams by a diplexer. The two orthogonally polarized beams are then directed to a pair of receiver oriented 90° apart.

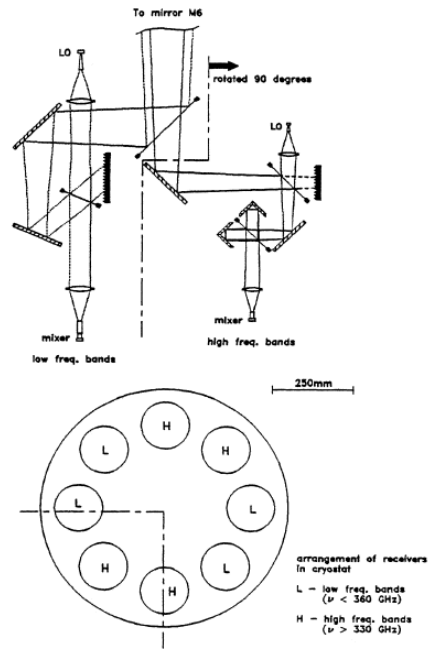


Figure 6 Receiver optics layout

2.3 Heterodyne Receiver

A heterodyne receiver superimposes the weak RF signal from outer space to a strong monochromatic local oscillator in the mixer. Due to the non-linearity of the mixer, a combination of frequency will be generated in the mixer.

Consider that the mixer has an I-V curve according to square law, $I = aV^2$. Let the signal of interest be $V_s = V_s \sin(2\pi F_s t)$ and the local oscillator signal be $V_{LO} = V_{LO} \sin(2\pi F_{LO} t)$. When the two signals are applied to the mixer, the output current generated will be

$$\begin{aligned}
 I &= a(V_0 + V_{LO} \sin(2\pi F_{LO} t) + V_s \sin(2\pi F_s t))^2 \\
 &= aV_0^2 + 2aV_0V_s \sin(2\pi F_s t) + 2aV_0V_{LO} \sin(2\pi F_{LO} t) \\
 &\quad + \frac{1}{2}aV_s^2 \{1 - \cos[2\pi(2F_s)t]\} + \frac{1}{2}aV_{LO}^2 \{1 - \cos[2\pi(2F_{LO})t]\} \\
 &\quad + aV_sV_{LO} \{ \cos[2\pi(F_s - F_{LO})t] - \cos[2\pi(F_s + F_{LO})t] \}
 \end{aligned} \tag{2.1}$$

From (2.1), it can be seen that the mixer produce signals at frequency $F_s, F_{LO}, 2F_s, 2F_{LO}, F_s + F_{LO}$, and $F_s - F_{LO}$. In most cases, only the signal with frequency $F_s - F_{LO}$ will be chosen. The rest of the output frequency are filtered out. If F_{LO} is relatively high, then the mixer will convert the high frequency RF signal (F_s) to a much lower Intermediate Frequency (IF). A lower IF signal is easier to be manipulated and cheaper to amplify than the high frequency signal (F_s).

Figure 7 shows the block diagram of heterodyne receiver. The signal from the antenna is fed to the mixer through a hollow waveguide. The mixer will then combine the signal of interest with the local oscillator signal to produce IF signal. The IF signal then passes through a Low Noise Amplifier (LNA) to amplify the incoming signal. After going through multiple stages of amplification, the IF signal is then fed into the data analysis system such as the spectrometer. The spectrometer will generate the spectral information of the input signal.

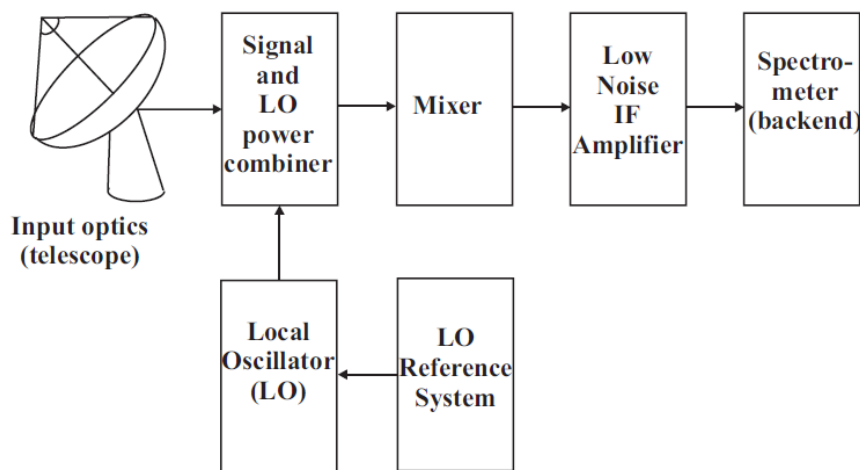


Figure 7 Block Diagram of Heterodyne Receiver

2.4 Waveguide Coupling

There are usually two methods to channel the RF signal from the aperture of a horn down to the SIS mixer, i.e. by quasi-optical coupling or by means of waveguide. This section describes the method of waveguide coupling. It is accomplished by receiving the RF signal from the antenna via a horn and passing it via a waveguide to the waveguide probe where the mixer is located.

The SIS Mixer of ALMA band 7 (Vassilev, et al., 2004) designed by Onsala Space Observatory is used as an example to show the application of waveguide coupling to the receiver system. Figure 8 shows the layout of SIS receiver. The RF signal from the antenna is channelled down to the receiver via waveguide. A corrugated circular horn is used to reduce the sideband signal. After that, the RF signal passes through a circular to rectangular transition waveguide to a rectangular waveguide, before being coupled to the probe. The reason to use a rectangular waveguide to couple to the probe is because of the ease of excitation.

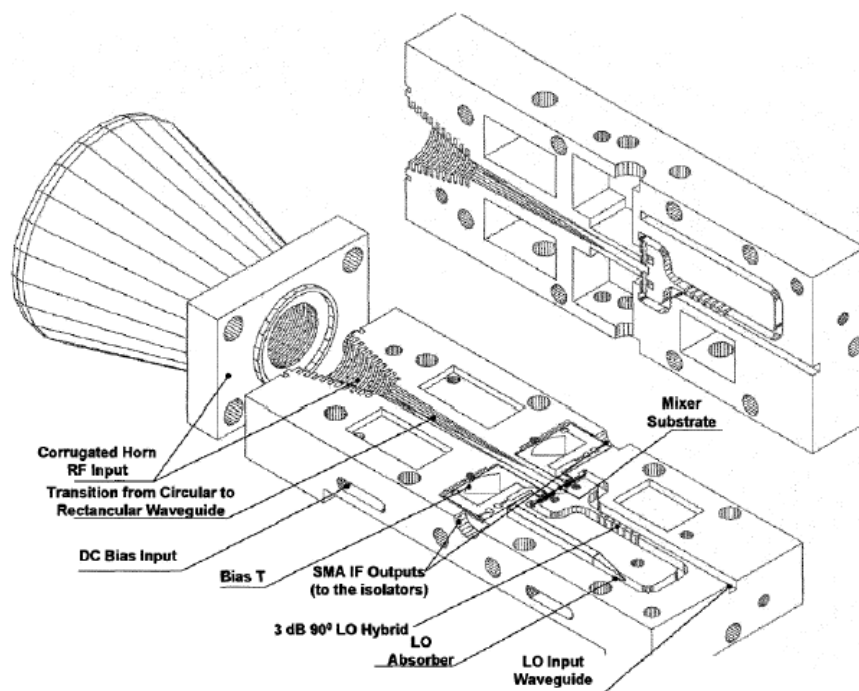


Figure 8 Layout of SIS Receiver for ALMA Band 7 Cartridge

Figure 9 shows the RF signal from the rectangular waveguide coupled to the microstrip probe in the mixer. On the other hand, the LO signal is fed to the mixer via the waveguide branch line coupler. The coupler splits the LO signal into two LO signals with 90° phase difference. The LO signal is then carried to the mixer via the rectangular waveguide and fed to the mixer at both ends.

Figure 10 shows the SIS mixer. The RF and LO signals are fed to the mixer junctions tuning circuitry. At the SIS mixer, both the RF and LO signals are then mixed and down converted to a lower IF signal.

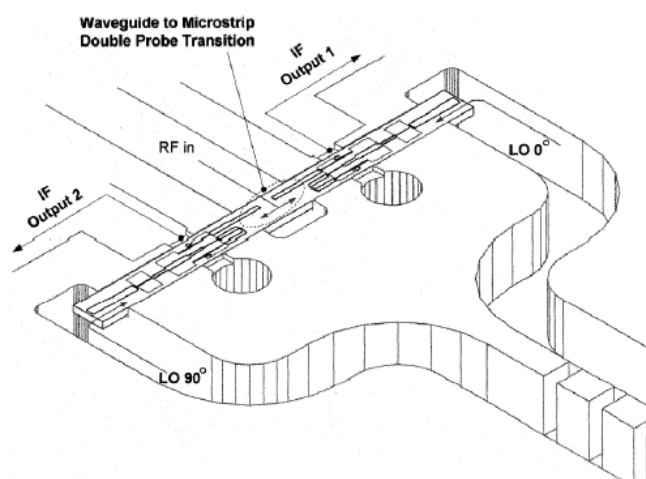


Figure 9 Mixer Substrate Coupled to Waveguide in ALMA Band 7 Receiver

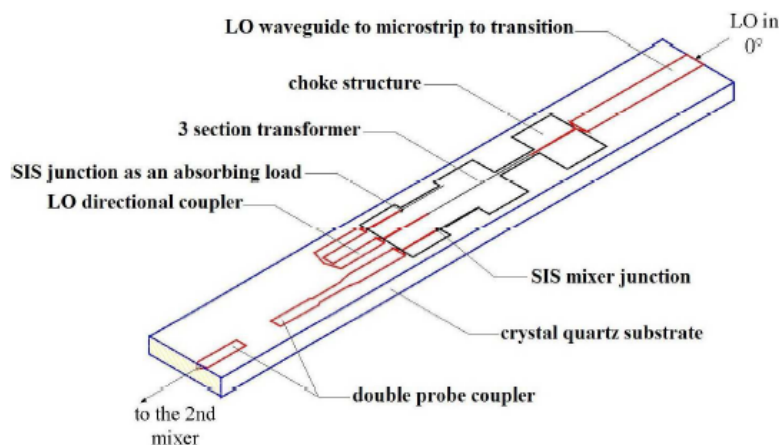


Figure 10 Layout of Quartz Substrate with SIS Mixer Built onto it

CHAPTER 3

WAVEGUIDING STRUCTURES

3.1 Introduction

The nature of electromagnetic wave allows it to propagate in all direction in the form of spherical wave from the source when it is unbounded. Such propagation mode allows the electromagnetic wave to reach all possible destination around the source. This is the principle of transmission antenna such as cell phone tower to maximize the coverage area of receiver. However, waves propagating in such mode has its power reduced according to the inverse square law as the electromagnetic waves expand into the three dimensional space. This is an inefficient method to transmit signals especially for weak signals, where the signal would be attenuated beyond which the recovery of signal would be too difficult and too costly. To efficiently transmit an electromagnetic wave signal with minimum loss, a guiding structure is preferred to confine the wave to travel in one direction. Such guiding structures are widely employed in the receiver system. For such system, the receiver antenna intercepts the weak electromagnetic waves, which is then amplified for signal recovery. This low power electromagnetic wave need to travel from the receiver antenna to the amplifier with minimum attenuation. A guiding structure would therefore be employed to guide the weak wave to the amplifier for further post processing. There are two types of wave guiding structure, waveguides and transmission lines.

3.2 Transmission Lines

Transmission lines are used to convey the signal from the source to the destination. Electromagnetic wave from the source induce current in the conductor of the transmission lines. The signal then travels through the conductor in the form of electric current. Transmission lines can support TEM and quasi-TEM mode. A transmission lines can support direct current (DC) up to high frequency, however, at high frequency, the conductor loss will be too high for the transmission lines to be efficient. There exist different types of transmission lines. Below, some of the more common type of transmission lines are discussed.

3.2.1 Coaxial Cable

Coaxial cable is usually used to transmit signals at the lower radio frequency range. The electromagnetic wave induce alternating current (AC) in the conducting core and it propagates in the form of alternating current in the transmission line. Transmission line differs from an ordinary copper cable in such that transmission line is a specialized structure that is designed to carry AC in the radio frequency range. The impedance of transmission line are matched to the source and destination impedance to maximize power transfer from source to destination. In ordinary copper cable, the discontinuities at the cable end increases standing wave in the cable, therefore reducing its efficiency. A typical coaxial cable is shown in Figure 11.

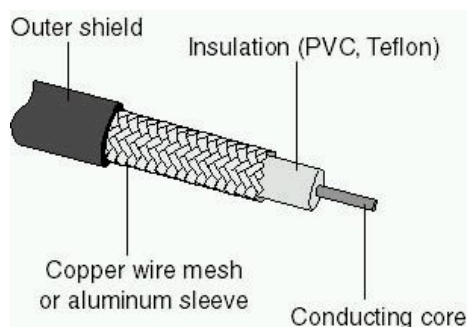


Figure 11 Coaxial Cable Cutaway (Tkgd2007, 2008)

From the cross sectional view of the coaxial cable it can be seen that copper meshes are surrounding the copper conductor. These copper meshes shield the copper conductor, preventing electromagnetic interference (EMI) from the surrounding from affecting the signal of the coaxial cable. It also prevents the signal from the coaxial cable to interfere with other sources. The conductor core is surrounded by a flexible insulating outer shield, protecting the copper core and making the coaxial cable flexible. Hence, coaxial cables are suitable to carry high speed signal, connecting two different devices, externally.

The copper meshes are usually grounded, and the signal voltage is applied to the copper core. The electric field travels from the copper core to the outer copper mesh, through the dielectric, while the magnetic field forms a closed loop around the copper core. Therefore, most of the EM field are confined within the dielectric. The field pattern of the coaxial cable is shown in Figure 12. The fundamental mode of coaxial cable is TEM mode.

In the microwave region, coaxial cable becomes too lossy due to the skin effect of the conductor. Skin effect refers to the imbalance distribution of current density at the outer and inner region of the conductor. High frequency causes current to concentrate near the surface, resulting in lower effective area for the current to pass through, which increases the effective resistance of the coaxial cable, reducing its efficiency.

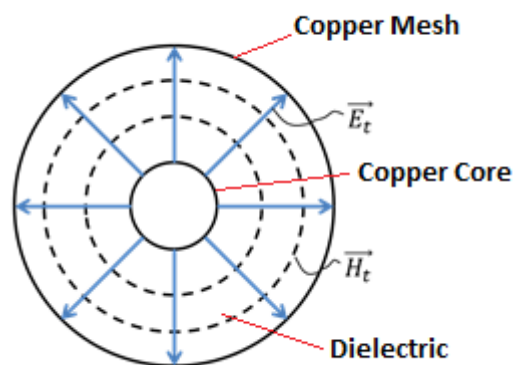


Figure 12 Coaxial Cable Field Pattern

3.2.2 Microstrip

Microstrip is also a type of transmission line. However, microstrip are fabricated for Printed Circuit Board (PCB) and Integrated Circuit (IC). It is used to transmit high frequency signal inside an IC and PCB within the device internally. The structure of a microstrip is shown in Figure 13.

Unlike the coaxial cable, the fields of a microstrip are not confined within the dielectric. Instead, part of the electromagnetic field propagate outside through the air. Hence, extra caution must be taken to protect the circuit from EMI and also to prevent the circuit disturbing other devices. Hence, microstrip would not be suitable for connecting devices externally. It can only be used within a device.

Since the top part of the field travels through air, and the bottom part travels through the substrate, the substrate material constitutive parameters alone are not enough to characterize the microstrip. A combination effect of air and substrate are required to describe the field. The field pattern of a microstrip is shown in Figure 14 .

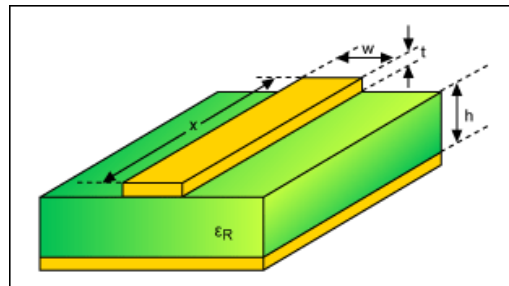


Figure 13 Microstrip

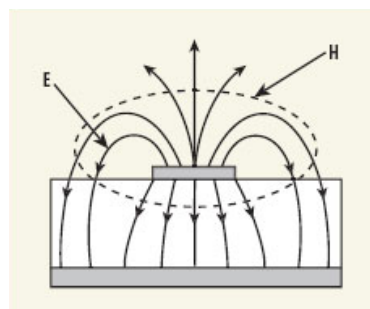


Figure 14 Microstrip Field Pattern (Al-Raie, 2007)

As mentioned previously, the top field of a microstrip propagates through air, while bottom field propagates through the substrate, since both mediums have different permittivity, they would propagate at different speed, and therefore there is a slight phase difference between the two fields. Therefore, a microstrip could not support pure TEM field because of the different mediums. It can only support quasi-TEM mode.

Besides microstrip, there are other different type of waveguide that supports quasi-TEM mode as shown below in Figure 15, all which can be used for PCB or IC.

3.3 Waveguide

Waveguide is preferred for transmission of electromagnetic wave in the microwave region. A waveguide carries signals in the form of wave, while, a transmission line carries signals in the form of current. Unlike transmission lines, a waveguide has a minimum operating frequency, known as the cut-off frequency, f_c . Therefore, waveguide only allows signal with frequency above the cutoff frequency to propagate. Although transmission line can carry signal in the microwave region, however the attenuation is much higher than waveguide.

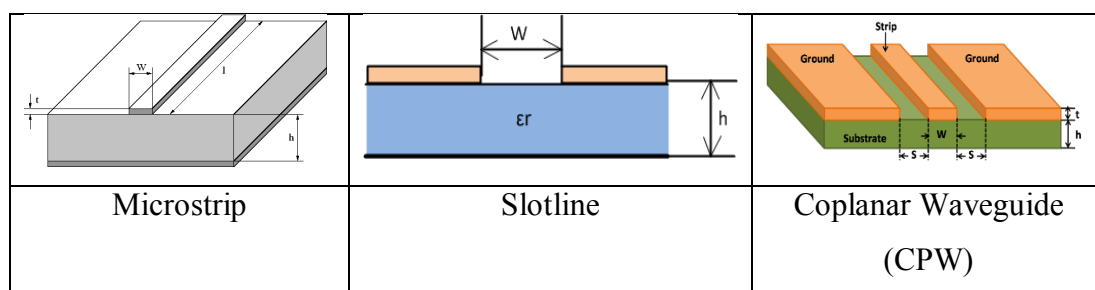


Figure 15 Various Types of Transmission Lines

3.3.1 Metal Waveguide

A metal waveguide consists of a hollow metal layer surrounding the dielectric medium, which is typically air. Electromagnetic wave propagates through the dielectric medium confined by the conductor. Due to the high conductivity of the metal, the penetration of the field into the conductor is negligible. The field is said to be confined within the conductor. A metal waveguide can vary in different shapes and sizes. The most common waveguide used is the circular and rectangular waveguide due to its simplicity to manufacture. A typical rectangular waveguide is shown in Figure 16

The surface impedance of the metal waveguide is given in (3.1) below.

$$Z_s = (1 + j) \sqrt{\frac{\pi f \mu}{\sigma}} \quad (3.1)$$

The equation shows that at high frequency, the metal impedance increases, resulting in higher loss for wave propagation. Hence, a metal waveguide would not be suitable at extremely high frequency signal.

3.3.2 Dielectric Waveguide

An optical waveguide consists of a dielectric material surrounding a lower refractive index dielectric medium. Since there is no metal involved, conductor loss due to skin effect is not applicable to dielectric waveguide. Hence at higher frequency, typically above the optical range, a dielectric waveguide is preferred. Optical fibres used in communication are dielectric waveguides. The photonic signals propagate through the optical fibre. The propagation of light inside an optical fibre is shown in Figure 17.

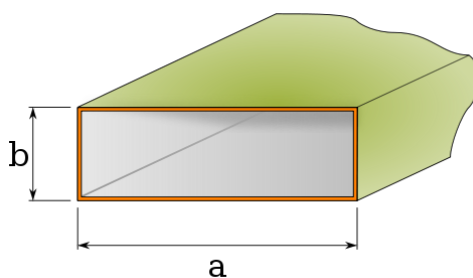


Figure 16 Rectangular Waveguide (Zykure, 2009)

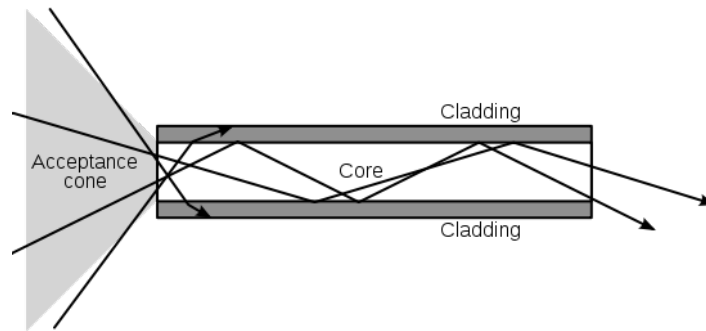


Figure 17 Optical Fiber (Gringer, 2008)

CHAPTER 4

CIRCULAR WAVEGUIDE

4.1 Introduction

The propagation of electromagnetic wave in lossy waveguides has long been studied. The conventional method can be generally divided into two classes, i.e. a rigorous method such as those suggested by Stratton (Stratton, 2007) which can only be solved numerically and the perturbation method which results in a simpler closed form equation. Stratton's rigorous method models the wave penetrating into the wall of the waveguide. This method uses two separate wave functions to model waves in the core of the waveguide as well as in the conductor wall. As waves inside the conductor wall are evanescent and exponentially decaying, Hankel function is used to model this decaying wave inside the conductor. By matching the fields at the boundary of the wall, a set of transcendental equations which can only be solved numerically is derived. The equation is able to include the formulation of the hybrid EH mode and HE mode of the electromagnetic field inside the waveguide. Waves in a lossy waveguide have their magnetic and electric waves closely coupled due to the finite conductivity of the conductor wall. This results in EH mode or HE mode depending either electric field or magnetic field dominates. In contrast, a wave in a perfectly lossless waveguide can be described in TE or TM field where either the longitudinal electric field or magnetic field is zero due to the perfectly conducting wall. Stratton's equation is able to describe these waves in a lossy waveguide, i.e. EH or HE mode, as well as the degenerate modes, making it highly accurate. Stratton's method is by far the most accurate formulation in calculating the attenuation in a circular waveguide. However it possesses a few disadvantages. The solution of Stratton's equation results in a set of transcendental

equation, making it impossible to be solved analytically unless a few approximations are made (Yamaguchi, 1980). The transcendental equation needs to be solved numerically by using some root finding numerical methods. Depending on the numerical method used, some of them may result in divergence in the solution. The numerical method of solving the solution may also take considerable amount of computational time before the solution converges.

Yeap (2011) has developed an alternative approach to compute losses in a waveguide. Instead of matching the propagating waves with the evanescent wave at the boundary, Yeap matches the waves inside the waveguide with the wall impedance. Similarly, this approach results in a set of transcendental equation which can only be solved numerically. Yeap's approach can also be used to calculate the degenerate modes in the waveguide. However, unlike Stratton's approach which can only be applied to circular waveguide, Yeap's approach can be used in both circular and rectangular waveguides. Hence, Yeap's approach is more appropriate to be used in situation where there is transition in waveguides with different geometries and sizes.

Another method to formulate equation describing the attenuation of the wave propagating inside the waveguide is the perturbation method. The most commonly used equation is the power loss method (Balanis, 2012). This method assumes that waves propagating inside the waveguide are identical to those in a lossless waveguide. Hence, the power loss method assumes that waves do not penetrate into the wall. To compute loss, surface resistance is introduced into the equation. The main advantage of the power loss method over Stratton's method is the simplicity of the equation. It is also able to describe the propagation of the wave inside the waveguide with reasonably good accuracy provided that the frequency of the wave is beyond the cutoff frequency. However, singularity exists in the power loss equation at the cutoff frequency resulting in infinite attenuation at the cutoff frequency. From Stratton's equation it is known that when frequency of the wave is below the cut off frequency, the attenuation is high but not infinite. The power loss method therefore does not describe the behaviour of the wave propagation when the frequency is below the cutoff frequency as well as when the frequency is near the cutoff frequency. Another disadvantage of the power loss method is that the equation can only describe TM mode or TE modes separately. Figure 18 from Chapter 4.3 shows that the cutoff frequencies for some TE and TM

modes are the same. These modes are known as degenerate modes. Degenerate modes have their electric field and magnetic field closely coupled together. Imbriale (1998) has shown that when frequency of the electromagnetic wave is equal to such frequency that allows degenerate mode to propagate, the attenuation constant is not simply the addition of TE and TM mode, rather there will be coupling effect between the modes that causes the attenuation constant to be higher. The result of Imbriale's derivation is shown below. As the power loss equation only calculates either TM mode, (where $E_z = 0$), or TE mode (where $H_z = 0$), it fails to take into account the mode coupling effect.

$$\begin{aligned}
P_L = & \frac{1}{2} \mathcal{R} \ell \left(\sum_{m=1}^M |A_m^{TE}|^2 \oint_C \left[|H_{mc}^{TE}|^2 + |H_{mz}^{TE}|^2 \right] dC \right) && \left. \vphantom{\sum_{m=1}^M} \right\} \text{Power loss due to TE mode} \\
& + \sum_{m'=1}^{M'} |A_{m'}^{TM}|^2 \oint_C |H_{m'c}^{TM}|^2 dC && \left. \vphantom{\sum_{m'=1}^{M'}} \right\} \text{Power loss due to TM mode} \\
& + \frac{1}{2} \mathcal{R} \ell \left(\sum_{\substack{m=1 \\ n \neq m}}^M \sum_{n=1}^M A_m^{TE} A_n^{TE*} \oint_C \left[H_{mc}^{TE} H_{nc}^{TE*} + H_{mz}^{TE} H_{nz}^{TE*} \right] dC \left\{ \frac{e^{j(\beta_m^{TE} - \beta_n^{TE})\ell} - 1}{j(\beta_m^{TE} - \beta_n^{TE})\ell} \right\} \right) \\
& \quad \sum_{\substack{m'=1 \\ n' \neq m'}}^{M'} \sum_{n'=1}^{M'} A_{m'}^{TE} A_{n'}^{TE*} \oint_C \left[H_{m'c}^{TM} H_{n'c}^{TM*} \right] dC \left\{ \frac{e^{j(\beta_{m'}^{TM} - \beta_{n'}^{TM})\ell} - 1}{j(\beta_{m'}^{TM} - \beta_{n'}^{TM})\ell} \right\} && \left. \vphantom{\sum_{m'=1}^{M'}} \right\} \text{Power loss due to} \\
& \quad \sum_{m'=1}^M \sum_{n=1}^M A_{m'}^{TM} A_n^{TE*} \oint_C \left[H_{m'c}^{TM} H_{nc}^{TE*} \right] dC \left\{ \frac{e^{j(\beta_{m'}^{TM} - \beta_n^{TE})\ell} - 1}{j(\beta_{m'}^{TM} - \beta_n^{TE})\ell} \right\} && \left. \vphantom{\sum_{m'=1}^M} \right\} \text{coupling effect of TE and TM} \\
& \quad \left. \sum_{m=1}^M \sum_{n'=1}^{M'} A_m^{TE} A_{n'}^{TM*} \oint_C \left[H_{mc}^{TE} H_{n'c}^{TM*} \right] dC \left\{ \frac{e^{j(\beta_m^{TE} - \beta_{n'}^{TM})\ell} - 1}{j(\beta_m^{TE} - \beta_{n'}^{TM})\ell} \right\} \right) && \left. \vphantom{\sum_{m=1}^M} \right\}
\end{aligned}$$

(Eq. 4.1)

A new method which is able to compute the attenuation in a circular waveguide is presented in this chapter. The new method is a closed form solution which is able to compute the attenuation of wave propagating inside a circular waveguide with reasonably high accuracy. The new method is modified from Yeap's method. Yeap's method results in a set of transcendental equation which can only be solved using a root finding algorithm. Here, modifications are made in order to modify Yeap's equations into closed-form.

4.2 Fields in Circular Cylindrical Waveguides

From APPENDIX A: Helmholtz Equation, (A.5), \vec{E} is the electric field vector, which contains three components to describe the behaviour of the electromagnetic wave in three dimensions. In cylindrical coordinate, the field can be decomposed into $\vec{E} = E_\rho \hat{a}_\rho + E_\phi \hat{a}_\phi + E_z \hat{a}_z$. The same is true for the \vec{H} in (A.7). The Laplacian of a vector can be found using the identity as shown below.

$$\nabla^2 A = \nabla(\nabla \cdot A) - \nabla \times \nabla \times A \quad (4.2)$$

Using the Laplacian identity (4.2) above, the Laplacian of electric field can be found as below

$$\begin{aligned} \nabla \times \nabla \times \vec{E} = & \left[\frac{1}{\rho^2} \frac{dE_\phi}{d\phi} + \frac{1}{\rho} \frac{\partial^2 E_\phi}{\partial \rho \partial \phi} - \frac{1}{\rho^2} \frac{\partial^2 E_\rho}{\partial \phi^2} - \frac{\partial^2 E_\rho}{\partial z^2} + \frac{\partial^2 E_z}{\partial \rho \partial z} \right] \cdot \hat{a}_\rho \\ & + \left[\frac{1}{\rho} \frac{\partial^2 E_z}{\partial \phi \partial z} - \frac{\partial^2 E_\phi}{\partial z^2} + \frac{1}{\rho^2} E_\phi - \frac{1}{\rho} \frac{dE_\phi}{d\rho} - \frac{\partial^2 E_\phi}{\partial \rho^2} - \frac{1}{\rho^2} \frac{dE_\rho}{d\phi} + \frac{1}{\rho} \frac{\partial^2 E_\rho}{\partial \phi \partial \rho} \right] \cdot \hat{a}_\phi \\ & + \left[\frac{1}{\rho} \frac{dE_\rho}{dz} + \frac{\partial^2 E_\rho}{\partial z \partial \rho} - \frac{1}{\rho} \frac{dE_z}{d\rho} - \frac{\partial^2 E_z}{\partial \rho^2} - \frac{1}{\rho^2} \frac{\partial^2 E_z}{\partial \phi^2} + \frac{1}{\rho} \frac{\partial^2 E_\phi}{\partial z \partial \phi} \right] \cdot \hat{a}_z \end{aligned} \quad (4.3)$$

$$\begin{aligned} \nabla(\nabla \cdot \vec{E}) = & \left[\left(-\frac{1}{\rho^2} \right) E_\rho + \frac{1}{\rho^2} \frac{dE_\rho}{d\rho} + \frac{\partial^2 E_\rho}{\partial \rho^2} - \frac{1}{\rho^2} \frac{dE_\phi}{d\phi} + \frac{1}{\rho} \frac{\partial^2 E_\phi}{\partial \phi \partial \rho} + \frac{\partial^2 E_z}{\partial z \partial \rho} \right] \cdot \hat{a}_\rho \\ & + \left[\frac{1}{\rho^2} \frac{dE_\rho}{d\phi} + \frac{1}{\rho} \frac{\partial^2 E_\rho}{\partial \rho \partial \phi} + \frac{1}{\rho^2} \frac{\partial^2 E_\phi}{\partial \phi^2} + \frac{1}{\rho} \frac{\partial^2 E_z}{\partial z \partial \phi} \right] \cdot \hat{a}_\phi \\ & + \left[\frac{1}{\rho} \frac{dE_\rho}{dz} + \frac{\partial^2 E_\rho}{\partial \rho \partial z} + \frac{1}{\rho} \frac{\partial^2 E_\phi}{\partial \phi \partial z} + \frac{\partial^2 E_z}{\partial z^2} \right] \cdot \hat{a}_z \end{aligned} \quad (4.4)$$

Substituting the result of (4.3) and (4.4) into the Laplacian identity in (4.2) the Laplacian of the electric field is obtained as shown in (4.5)

$$\begin{aligned} \nabla^2 \vec{E} = & \left[\nabla^2 E_\rho - \frac{2}{\rho^2} \frac{dE_\phi}{d\phi} - \frac{1}{\rho^2} E_\rho \right] \cdot \hat{a}_\rho \\ & + \left[\nabla^2 E_\phi + \frac{2}{\rho^2} \frac{dE_\rho}{d\phi} - \frac{1}{\rho^2} E_\phi \right] \cdot \hat{a}_\phi \\ & + \left[\nabla^2 E_z \right] \cdot \hat{a}_z \end{aligned} \quad (4.5)$$

Using the result of the Laplacian of the electric field (4.5), the Helmholtz vector equation from (A.5) can be decomposed to three separate scalar wave equations as shown below

$$\nabla^2 E_\rho - \frac{2}{\rho^2} \frac{dE_\phi}{d\phi} - \frac{1}{\rho^2} E_\rho = \gamma^2 E_\rho \quad (4.6)$$

$$\nabla^2 E_\phi + \frac{2}{\rho^2} \frac{dE_\rho}{d\phi} - \frac{1}{\rho^2} E_\phi = \gamma^2 E_\phi \quad (4.7)$$

$$\nabla^2 E_z = \gamma^2 E_z \quad (4.8)$$

(4.6) and (4.7) are coupled where each contains more than one electric component which are difficult to solve. Therefore, (4.8) are used for the field derivation. From (4.8), assuming lossless where $\gamma = j\beta$, and given $\beta = \omega^2 \mu\epsilon$

, the wave equation becomes

$$\frac{1}{\rho} \frac{dE_z}{d\rho} + \frac{\partial^2 E_z}{\partial \rho^2} + \frac{1}{\rho^2} \frac{\partial^2 E_z}{\partial \phi^2} + \frac{\partial^2 E_z}{\partial z^2} = -\beta^2 E_z \quad (4.9)$$

The solution to the partial differential equation (4.9) above can be solved analytically using the separation of variables method. Let $E_z = F(\rho)G(\phi)H(z)$, the equation above becomes

$$\frac{1}{\rho} \frac{1}{F} \frac{dF}{d\rho} + \frac{1}{F} \frac{\partial^2 F}{\partial \rho^2} + \frac{1}{\rho^2} \frac{1}{G} \frac{\partial^2 G}{\partial \phi^2} + \frac{1}{H} \frac{\partial^2 H}{\partial z^2} = -\beta^2 \quad (4.10)$$

let

$$\frac{1}{H^2} \frac{\partial^2 H}{\partial z^2} = -\beta_z^2 \quad (4.11)$$

$$\frac{1}{G} \frac{\partial^2 G}{\partial \phi^2} = -m^2 \quad (4.12)$$

(4.10) can be expressed as

$$\rho^2 \frac{\partial^2 F}{\partial \rho^2} + \rho \frac{\partial F}{\partial \rho} + \left[(\beta_\rho \rho)^2 - m^2 \right] F = 0 \quad (4.13)$$

where β_ρ is the wave vector in ρ direction and $\beta^2 = \beta_\rho^2 - \beta_z^2$. Equation (4.13) is the Bessel's Differential Equation and the solution to the differential equation can either be

$$F(\rho) = E_z(\rho) = A_m J_m(\beta_\rho \rho) + B_m Y_m(\beta_\rho \rho) \quad (4.14)$$

or

$$F(\rho) = E_z(\rho) = C_m H_m^{(1)}(\beta_\rho \rho) + D_m H_m^{(2)}(\beta_\rho \rho) \quad (4.15)$$

where, A_m , B_m , C_m and D_m are constants.

$J_m(\beta_\rho \rho)$ is the Bessel's function of the 1st kind. The Bessel's function of 1st kind can be approximated as

$$J_m(\beta_\rho \rho) \approx \sqrt{\frac{2}{\pi \beta_\rho \rho}} \cos\left(\beta_\rho \rho - \frac{m\pi}{2} - \frac{\pi}{4}\right) \quad \text{when } \beta_\rho \rho \gg 1 \quad (4.16)$$

$Y_m(\beta_\rho \rho)$ is the Bessel's function of the 2nd kind. It can be approximated as

$$Y_m(\beta_\rho \rho) \approx \sqrt{\frac{2}{\pi \beta_\rho \rho}} \sin\left(\beta_\rho \rho - \frac{m\pi}{2} - \frac{\pi}{4}\right) \quad \text{when } \beta_\rho \rho \gg 1 \quad (4.17)$$

$H_m^{(1)}(\beta_\rho \rho)$ is the Hankel function of the 1st kind and is defined as

$H_m^{(1)}(\beta_\rho \rho) = J_m(\beta_\rho \rho) + jY_m(\beta_\rho \rho)$. It can be approximated as

$$H_m^{(1)}(\beta_\rho \rho) \approx \sqrt{\frac{2}{\pi \beta_\rho \rho}} e^{j\left(\beta_\rho \rho - \frac{m\pi}{2} - \frac{\pi}{4}\right)} \quad \text{when } \beta_\rho \rho \gg 1 \quad (4.18)$$

$H_m^{(2)}(\beta_\rho \rho)$ is Hankel's function of the 2nd kind and is defined as

$H_m^{(2)}(\beta_\rho \rho) = J_m(\beta_\rho \rho) - jY_m(\beta_\rho \rho)$. It can be approximated as

$$H_m^{(2)}(\beta_\rho \rho) \approx \sqrt{\frac{2}{\pi \beta_\rho \rho}} e^{-j\left(\beta_\rho \rho - \frac{m\pi}{2} - \frac{\pi}{4}\right)} \quad \text{when } \beta_\rho \rho \gg 1 \quad (4.19)$$

From equation(4.11), solution to $H(z)$ is

$$H(z) = E_z(z) = A e^{j\beta_z z} + B e^{-j\beta_z z} \quad (4.20)$$

or

$$H(z) = E_z(z) = C \cos(m\phi) + D \sin(m\phi) \quad (4.21)$$

where A , B , C and D are constants

From equation(4.12), solution to $G(\phi)$ is

$$G(\phi) = E_z(\phi) = E e^{jm\phi} + F e^{-jm\phi} \quad (4.22)$$

or

$$G(\phi) = E_z(\phi) = G \cos(m\phi) + H \sin(m\phi) \quad (4.23)$$

where E , F , G and H are constants

The results above show that there are 2 solutions for each partial differential equation in (4.11), (4.12) and (4.13). The solution are chosen to ease the calculation. For standing wave, boundary conditions are needed to be imposed onto the field. Hence, cosine and sine functions are chosen to represent standing waves as it is easier to impose boundary condition. Exponential solutions are chosen to represent travelling waves. Bessel function from the approximation in (4.16) and (4.17), which contains sine and cosine function is used to represent standing waves. Similarly, Hankel function from the approximation in (4.18) and (4.19), which contains exponential function, is used to represent travelling wave. Bessel function of the 2nd kind possess singularity at $\rho = 0$ therefore B_m needs to be set to zero as the field inside the waveguide must be finite. By assuming wave traveling in the $+z$ direction, the solution for the wave reduces to

$$E_z = A_m J_m(\beta_\rho \rho) \cos(m\phi) e^{-j\beta_z z} \quad (4.24)$$

or

$$E_z = A_m H_m^{(2)}(\beta_\rho \rho) \cos(m\phi) e^{-j\beta_z z} \quad (4.25)$$

Equation (4.24) is used to represent waves travelling within a perfect conductor where the wave does not penetrate into the conductor wall and equation (4.25) is used to model wave in a lossy conductor where waves penetrate into the conductor. The

same solution from equation (4.24) and (4.25) can also be used to represent the z direction magnetic field, H_z inside the waveguide.

Transverse Electromagnetic Field

The solution in (4.24) and (4.25) is used to obtain field in the z direction. The transverse field in the ρ and ϕ direction are obtained from equation (4.26) below. The equation below shows that all the transverse field are obtained by taking the derivative of the axial field, E_z and H_z . The equation shows that either E_z and H_z can be zero, i.e. as in transverse electric (TE) or transverse magnetic (TM), but not both together, i.e. transverse electromagnetic (TEM) field. Therefore a waveguide could not support TEM field as in coaxial cable.

$$\begin{aligned}
 H_\rho &= \frac{j\omega\epsilon}{\rho\beta_\rho^2} \frac{dE_z}{d\phi} - \frac{\gamma}{\beta_\rho^2} \frac{dH_z}{d\rho} \\
 H_\phi &= -\frac{\gamma}{\rho\beta_\rho^2} \frac{dH_z}{d\phi} - \frac{j\omega\epsilon}{\beta_\rho^2} \frac{dE_z}{d\rho} \\
 E_\rho &= -\frac{j\omega\mu}{\rho\beta_\rho^2} \frac{dH_z}{d\phi} - \frac{\gamma}{\beta_\rho^2} \frac{dE_z}{d\rho} \\
 E_\phi &= -\frac{\gamma}{\rho\beta_\rho^2} \frac{dE_z}{d\phi} + \frac{j\omega\mu}{\beta_\rho^2} \frac{dH_z}{d\rho}
 \end{aligned} \tag{4.26}$$

Transverse Electric Field

For transverse electric (TE) field where $E_z = 0$, the corresponding field would be

$$\begin{aligned}
 E_z &= 0 \\
 H_z &= A'_m J_m(\beta_\rho \rho) \cos(m\phi) e^{-\gamma z} \\
 H_\rho &= -\frac{\gamma}{\beta_\rho} A'_m J'_m(\beta_\rho \rho) \cos(m\phi) e^{-\gamma z} \\
 H_\phi &= -\frac{\gamma m}{\rho\beta_\rho^2} A'_m J_m(\beta_\rho \rho) \sin(m\phi) e^{-\gamma z} \\
 E_\rho &= \frac{j\omega\mu m}{\rho\beta_\rho^2} A'_m J_m(\beta_\rho \rho) \sin(m\phi) e^{-\gamma z} \\
 E_\phi &= \frac{j\omega\mu}{\beta_\rho} A'_m J'_m(\beta_\rho \rho) \cos(m\phi) e^{-\gamma z}
 \end{aligned} \tag{4.27}$$

where, A'_m is the constant for TE field. $J'_m(\beta_\rho \rho)$ is the first order derivative of Bessel's function. The electric field tangential to the conductor is zero. Therefore, the boundary condition for TE field would be $E_\phi|_{\rho=a} = 0$ implying that the derivative of the Bessel function is zero, $J'_m(\beta_\rho a) = 0$, $\beta_\rho a = \chi'_{mn}$. Where χ'_{mn} is the n^{th} root of the first order Bessel's function derivative.

Transverse Magnetic Field

For transverse magnetic (TM) field where $H_z = 0$, the corresponding field would be

$$\begin{aligned}
 H_z &= 0 \\
 E_z &= A'_m J_m(\beta_\rho \rho) \cos(m\phi) e^{-\gamma z} \\
 E_\rho &= -\frac{\gamma}{\beta_\rho} A'_m J'_m(\beta_\rho \rho) \cos(m\phi) e^{-\gamma z} \\
 E_\phi &= \frac{\gamma m}{\rho \beta_\rho^2} A'_m J_m(\beta_\rho \rho) \sin(m\phi) e^{-\gamma z} \\
 H_\rho &= -\frac{j\omega\epsilon m}{\rho \beta_\rho^2} A'_m J_m(\beta_\rho \rho) \sin(m\phi) e^{-\gamma z} \\
 H_\phi &= -\frac{j\omega\epsilon}{\beta_\rho} A'_m J'_m(\beta_\rho \rho) \cos(m\phi) e^{-\gamma z}
 \end{aligned} \tag{4.28}$$

where, A_m is the constant for TM field. $J'_m(\beta_\rho \rho)$ is the first order derivative of Bessel's function. Similarly, the electric field tangential to the conductor is zero. Therefore, $J_m(\beta_\rho a) = 0$, $\beta_\rho a = \chi_{mn}$, where χ_{mn} is the n^{th} root of the Bessel's function.

4.3 Cutoff Frequency for Circular Waveguide

As mentioned previously, waveguide acts like a high pass filter where only electromagnetic wave with frequency exceeds the cutoff frequency, f_c are allowed to propagate inside the waveguide. The condition which allows wave to propagate inside waveguide is $\beta > \beta_\rho$, where $\beta = 2\pi f_c \sqrt{\mu\epsilon}$

The cutoff frequency can be obtained as follow

$$f_c = \frac{\beta_\rho}{2\pi\sqrt{\mu\epsilon}} \quad (\text{Eq. 4.29})$$

For TE field where, $\beta_\rho = \frac{\chi'_{mn}}{a}$, The cutoff frequency is

$$f_c = \frac{\chi'_{mn}}{2\pi a\sqrt{\mu\epsilon}} \quad (\text{Eq. 4.30})$$

whereas for TM field, $\beta_\rho = \frac{\chi_{mn}}{a}$, the corresponding cutoff frequency is

$$f_c = \frac{\chi_{mn}}{2\pi a\sqrt{\mu\epsilon}} \quad (\text{Eq. 4.31})$$

The result above shows that the cutoff frequency varies with the diameter of the waveguide, a as well as the propagation mode of the field, m and n . Figure 18 below shows the cutoff frequency for different mode in a circular waveguide. From the figure it can be seen that some modes have the same cutoff frequency such as TM_{11} and TE_{01} . These modes are known as the degenerate mode. Degenerate modes have their field closely coupled together where the H_z field from TE and E_z field from TM are coupled together. The mathematical formulation that shows the coupling effect of TE and TM degenerate modes is studied extensively (W. A. Imbriale, 1998)

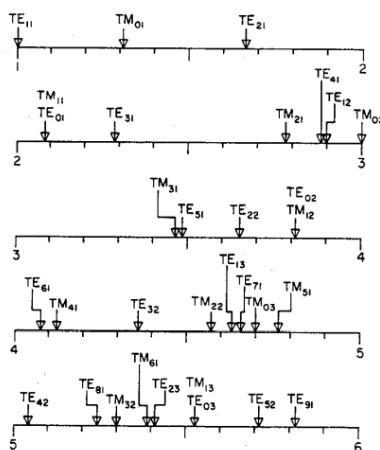


Figure 18 Normalized Cutoff Frequency for Different Field in a Circular Waveguide (C.S. Lee, 1985)

4.4 A Review of Some Conventional Methods

This chapter presents the analysis and comparison among the power loss method, Stratton's method and Yeap's method. Derivations of these methods are presented in a comprehensive and orderly manner.

4.4.1 A Review of the Power Loss Method

The power loss method assumes that most of the losses are due to conduction loss. As current is induced on the conductor wall, the power of the input electromagnetic wave is lost due to the law of conservation of energy. The input to output power of a waveguide can be described from the equation below (4.32)

$$P_z = P_o e^{-2\alpha_c z} \quad (4.32)$$

where, P_z is the average power flowing through the cross section of the conductor wall for a given length ℓ and P_o is the input average power. The average power dissipated per unit length ℓ is obtained by taking the negative derivative of equation (4.32)

$$P_c = -\frac{dP_z}{dz} \quad (4.33)$$

From (4.33), the attenuation due to the conductor, α_c is

$$\alpha_c = \frac{P_c}{2P_z} \quad (4.34)$$

The average power flowing through the cross section of the conductor wall, P_z can be obtained by taking the integral of $\mathcal{P}_{ave} \cdot \hat{a}_z$,

$$P_z = \int_0^a \int_0^{2\pi} \mathcal{P}_{ave} \cdot \hat{a}_z \rho d\rho d\phi \quad (4.35)$$

where \mathcal{P}_{ave} is the average power of the electromagnetic wave, and it is given by

$$\begin{aligned}\mathcal{P}_{ave} &= \frac{1}{2} \{ \vec{E} \times \vec{H}^* \} \\ &= \frac{1}{2} \left[-E_z H_\phi^* \cdot \hat{a}_\rho + E_z H_\rho^* \cdot \hat{a}_\phi + (E_\rho H_\phi^* - E_\phi H_\rho^*) \right] \\ \mathcal{P}_{ave} \cdot \hat{a}_z &= \frac{1}{2} (E_\rho H_\phi^* - E_\phi H_\rho^*)\end{aligned}\quad (4.36)$$

The average power loss at the conductor wall, P_c can be obtained from

$$P_c = \frac{P_L}{\ell} \quad (4.37)$$

where P_L is the total power loss and it is obtained by taking the integral of the current density at the wall surface as shown in (4.38)

$$P_L|_{\rho=a} = \frac{R_s}{2} \iint_A \vec{J}_s \vec{J}_s^* dA \quad (4.38)$$

where the surface current, J_s is calculated from the magnetic field as shown

$$J_s \approx \hat{n} \times H_{surface} \quad (4.39)$$

The calculation using the power loss method is shown below. A separate set of equation for TM and TE are obtained.

Transverse Magnetic Field

The first step is to obtain P_z . Using (4.35) and (4.36) on the TM field equations from (4.28), P_z is obtained as shown

$$P_z = \frac{\omega \epsilon \beta}{2 \beta_\rho^2} A_m^2 \int_0^a \int_0^{2\pi} \left[J_m'^2(\beta_\rho \rho) \cos^2(m\phi) + \left(\frac{m}{\rho \beta_\rho} \right)^2 J_m'^2(\beta_\rho \rho) \sin^2(m\phi) \right] \cdot \rho d\rho d\phi \quad (4.40)$$

Applying trigonometric identities on (4.40) and taking the integral with respect to ϕ , (4.40) becomes

$$P_z = \frac{\omega\epsilon\beta\pi}{2\beta_\rho^2} A_m^2 \int_0^a \left[J_m'^2(\beta_\rho\rho) + \left(\frac{m}{\rho\beta_\rho}\right)^2 J_m^2(\beta_\rho\rho) \right] \rho \, d\rho \quad (4.41)$$

To simplify (4.41), Bessel's recurrence relations are applied. The two Bessel's recurrence relations applied here are

$$\begin{aligned} J_{\nu-1}(z) + J_{\nu+1}(z) &= \frac{2\nu}{z} J_\nu(z) \\ J_{\nu-1}(z) - J_{\nu+1}(z) &= 2J_\nu'(z) \end{aligned} \quad (4.42)$$

Applying Bessel's recurrence relation from (4.42) to (4.41), the equation becomes

$$\begin{aligned} P_z &= \frac{\omega\epsilon\beta\pi}{2\beta_\rho^2} A_m^2 \int_0^a \left[\left(\frac{1}{2} J_{m-1}(\beta_\rho\rho) - \frac{1}{2} J_{m+1}(\beta_\rho\rho) \right)^2 + \left(\frac{m}{\rho\beta_\rho} \right)^2 \left(\left(\frac{\beta_\rho\rho}{2m} \right) \{ J_{m-1}(\beta_\rho\rho) + J_{m+1}(\beta_\rho\rho) \} \right)^2 \right] \rho \, d\rho \\ &= \frac{\omega\epsilon\beta\pi}{4\beta_\rho^2} A_m^2 \int_0^a \left[J_{m-1}^2(\beta_\rho\rho) + J_{m+1}^2(\beta_\rho\rho) \right] \rho \, d\rho \end{aligned} \quad (4.43)$$

The Bessel's Integral Identity in (4.44) is substituted in (4.43) to obtain (4.45)

$$\int_a^b x J_m^2(cx) \, dx = \frac{x^2}{2} \left[J_m(cx) - J_{m-1}(cx) J_{m+1}(cx) \right] \Big|_a^b \quad (4.44)$$

$$P_z = \frac{\omega\epsilon\beta\pi}{4\beta_\rho^2} A_m^2 \frac{a^2}{2} \left[J_{m+1}^2(\beta_\rho a) - J_m(\beta_\rho a) J_{m+2}(\beta_\rho a) + J_{m-1}^2(\beta_\rho a) - J_{m-2}(\beta_\rho a) J_m(\beta_\rho a) \right] \quad (4.45)$$

Applying the boundary condition for TM mode, i.e. $J_m(\beta_\rho a) = 0$ and the Bessel's recurrence relation in (4.42), P_z becomes

$$P_z = \frac{\omega\epsilon\beta\pi a^2}{4\beta_\rho^2} A_m^2 J_{m+1}^2(\beta_\rho a) \quad (4.46)$$

The next step is to find P_L . Substituting the field equation (4.28) into (4.39) and using (4.38) and (4.37), the average power loss at the conductor, P_c is obtained as shown in (4.47)

$$P_c = \frac{R_s a \pi}{2} \left[\frac{\omega \epsilon}{\beta_\rho} A_m J'_m(\beta_\rho a) \right]^2 \quad (4.47)$$

Finally substituting the result from (4.46) and (4.47) into (4.34), the attenuation constant becomes

$$\alpha_c = \frac{R_s \omega \epsilon J_m'^2(\beta_\rho a)}{a \beta J_{m+1}^2(\beta_\rho a)} \quad (4.48)$$

Bessel's recurrence relation:

$$J'_n(\alpha x) + J_{n+1}(\alpha x) = \frac{n}{\alpha x} J_n(\alpha x) \quad (4.49)$$

Substitute $\beta = \omega \sqrt{\mu \epsilon} \sqrt{1 - (f_c/f)^2}$ and apply Bessel's recurrence relation (4.49) into (4.48), the equation becomes (4.50)

$$\alpha_c = \frac{R_s}{a \eta \sqrt{1 - (f_c/f)^2}} \quad (4.50)$$

where, $\eta = \sqrt{\frac{\mu}{\epsilon}}$

Transverse Electric Field

Similarly for TE mode, apply the field equation in (4.27) into (4.35), and apply the Bessel's recurrence relation, the equation for P_z becomes

$$P_z = \frac{\omega \mu \beta \pi}{4 \beta_\rho^2} A_m^2 \frac{a^2}{2} \left[4 J_m'^2(\beta_\rho a) - J_m(\beta_\rho a) J_{m+2}(\beta_\rho a) - J_m(\beta_\rho a) J_{m-2}(\beta_\rho a) + 2 J_{m-1}(\beta_\rho a) J_{m+1}(\beta_\rho a) \right] \quad (4.51)$$

Applying the boundary condition for TE mode, i.e. substituting $J'_m(\beta_\rho a) = 0$ into (4.51), the equation simplifies to

$$P_z = \frac{\omega \mu \beta \pi}{4 \beta_\rho^2} A_m^2 \frac{a^2}{2} \left[2 J_m^2(\beta_\rho a) \left\{ 1 - \left(\frac{m}{\beta_\rho a} \right)^2 \right\} \right] \quad (4.52)$$

To obtain the power loss due to conduction, applying the TE field equation into (4.37) and the result is

$$P_c = \frac{R_s a \pi}{2} [A_m J_m(\beta_\rho \rho)]^2 \left\{ 1 + \left(\frac{\beta m}{\beta_\rho a} \right)^2 \right\} \quad (4.53)$$

Substituting the result from (4.52) and (4.53) into (4.34), with some simplification, the attenuation constant for TE mode is obtained as shown below

$$\alpha_c = \frac{2R_s}{a\eta} \cdot \frac{1}{\sqrt{1 - \left(\frac{f_c}{f}\right)^2}} \cdot \left[\frac{f_c}{f} + \frac{m^2}{\beta_\rho^2 a^2 - m^2} \right] \quad (4.54)$$

4.4.2 A Review of Stratton's Method

This method uses two sets of equation. One sets describing the wave inside the waveguide, i.e. $\rho < a$. Another sets of equation describe the wave in the conductor, i.e. $\rho > a$ as shown in Figure 19.

Wave propagates inside the conducting metal surrounding the waveguide and decays exponentially at the conducting metal layer. To simplify the calculation, the outer layer is approximated as having infinitely large radius as shown Figure 20.

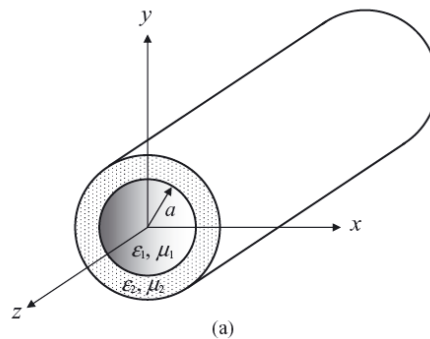


Figure 19 Circular Waveguide (Jin, 2010)

The field equation can therefore be separated into inner layer and outer layer. The inner layer consists of Bessel's function while the outer layer can be described using Modified Bessel's function to describe the exponentially decaying wave. The field equations are obtained from (4.24) and (4.25)

Field equation

$$\left. \begin{aligned} E_{1z} &= A_1 J_m(\beta_{1\rho} \rho) \sin(m\phi) e^{-\gamma_z z} \\ H_{1z} &= B_1 J_m(\beta_{1\rho} \rho) \cos(m\phi) e^{-\gamma_z z} \end{aligned} \right\} \text{Inner layer} \quad (4.55)$$

$$\left. \begin{aligned} E_{2z} &= A_2 H_m^{(2)}(\beta_{2\rho} \rho) \sin(m\phi) e^{-\gamma_z z} \\ H_{2z} &= B_2 H_m^{(2)}(\beta_{2\rho} \rho) \cos(m\phi) e^{-\gamma_z z} \end{aligned} \right\} \text{Outer layer} \quad (4.56)$$

where

$$\beta_{1\rho} = \sqrt{\omega^2 \mu \epsilon_1 - \gamma_z^2} \quad (4.57)$$

$$\beta_{2\rho} = \sqrt{\omega^2 \mu \epsilon_2 - \gamma_z^2} \quad (4.58)$$

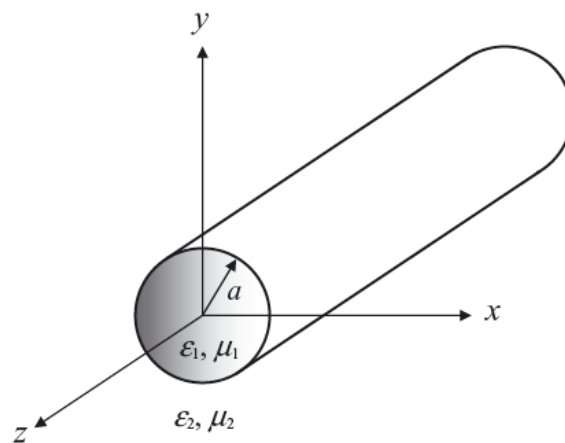


Figure 20 Simplified Waveguide Model (Jin, 2010)

Inside the conducting metal, the wave decays exponentially which implies that $k_z^2 > \omega^2 \mu \epsilon_2$. Therefore, $\beta_{2\rho} = -j\beta_{2\rho}$ and (4.58) can be rewritten as

$$\beta_{2\rho} = \sqrt{\gamma_z^2 - \omega^2 \mu \epsilon_2} \quad (4.59)$$

The Hankel function of imaginary number can also be represented by modified Bessel's function

$$H_m^{(2)}(-j\beta_{2\rho}\rho) = \frac{2}{\pi} j^{m+1} K_m(\beta_{2\rho}\rho) \quad (4.60)$$

Where $K_m(\alpha_{2\rho}\rho)$ is the modified Bessel's function. Figure 21 below shows modified Bessel's function plotted against x which indicate an exponentially decaying function as x increases.

Therefore, the equation for the outer layer can then be written as

$$\left. \begin{aligned} E_{2z} &= A'_2 K_m(\beta_{2\rho}\rho) \sin(m\phi) e^{-\gamma_z z} \\ H_{2z} &= B'_2 K_m(\beta_{2\rho}\rho) \cos(m\phi) e^{-\gamma_z z} \end{aligned} \right\} \text{Outer layer}$$

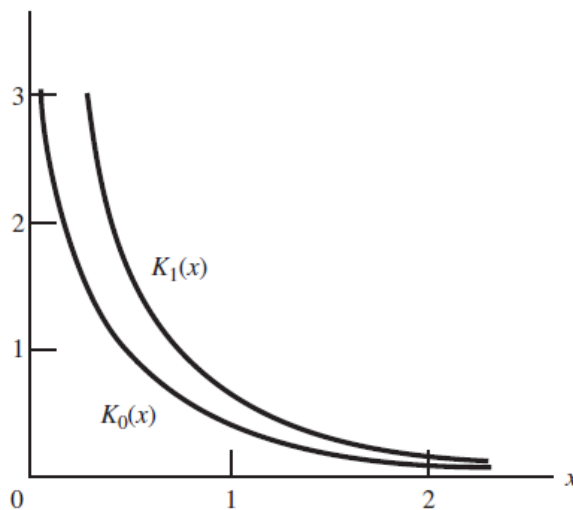


Figure 21 Modified Bessel's Function of Second Kind

The transverse field equation inside the waveguide as well as inside the conducting metal is shown below in (4.61) and (4.62) respectively expressed in matrix form. The field equation for the transverse field are obtained from (4.26).

$$\begin{aligned}
E_{1\rho} &= -\frac{j}{\beta_{1\rho}^2} \begin{bmatrix} A_1 \gamma_z \beta_{1\rho} J'_m(\beta_{1\rho} \rho) & -B_1 \frac{m\omega\mu}{\rho} J_m(\beta_{1\rho} \rho) \end{bmatrix} \begin{bmatrix} \sin(m\phi) \\ \cos(m\phi) \end{bmatrix} e^{-\gamma_z z} \\
E_{1\phi} &= -\frac{j}{\beta_{1\rho}^2} \begin{bmatrix} A_1 \frac{m\gamma_z}{\rho} J_m(\beta_{1\rho} \rho) & -B_1 \omega\mu\beta_{1\rho} J'_m(\beta_{1\rho} \rho) \end{bmatrix} \begin{bmatrix} \cos(m\phi) \\ \sin(m\phi) \end{bmatrix} e^{-\gamma_z z} \\
H_{1\rho} &= -\frac{j}{\beta_{1\rho}^2} \begin{bmatrix} -A_1 \frac{m\omega\epsilon_1}{\rho} J_m(\beta_{1\rho} \rho) & B_1 \gamma_z \beta_{1\rho} J'_m(\beta_{1\rho} \rho) \end{bmatrix} \begin{bmatrix} \cos(m\phi) \\ \sin(m\phi) \end{bmatrix} e^{-\gamma_z z} \\
H_{1\phi} &= -\frac{j}{\beta_{1\rho}^2} \begin{bmatrix} A_1 \omega\epsilon_1 \beta_{1\rho} J'_m(\beta_{1\rho} \rho) & -B_1 \frac{m\gamma_z}{\rho} J_m(\beta_{1\rho} \rho) \end{bmatrix} \begin{bmatrix} \sin(m\phi) \\ \cos(m\phi) \end{bmatrix} e^{-\gamma_z z}
\end{aligned} \tag{4.61}$$

$$\begin{aligned}
E_{2\rho} &= \frac{j}{\beta_{2\rho}^2} \begin{bmatrix} A'_2 \gamma_z \beta_{2\rho} K'_m(\beta_{2\rho} \rho) & -B_2 \frac{m\omega\mu}{\rho} K_m(\beta_{2\rho} \rho) \end{bmatrix} \begin{bmatrix} \sin(m\phi) \\ \cos(m\phi) \end{bmatrix} e^{-\gamma_z z} \\
E_{2\phi} &= \frac{j}{\beta_{2\rho}^2} \begin{bmatrix} A'_2 \frac{m\gamma_z}{\rho} K_m(\beta_{2\rho} \rho) & -B_2 \omega\mu\beta_{2\rho} K'_m(\beta_{2\rho} \rho) \end{bmatrix} \begin{bmatrix} \cos(m\phi) \\ \sin(m\phi) \end{bmatrix} e^{-\gamma_z z} \\
H_{2\rho} &= \frac{j}{\beta_{2\rho}^2} \begin{bmatrix} -A'_2 \frac{m\omega\epsilon_2}{\rho} K_m(\beta_{2\rho} \rho) & B_2 \gamma_z \beta_{2\rho} K'_m(\beta_{2\rho} \rho) \end{bmatrix} \begin{bmatrix} \cos(m\phi) \\ \sin(m\phi) \end{bmatrix} e^{-\gamma_z z} \\
H_{2\phi} &= \frac{j}{\beta_{2\rho}^2} \begin{bmatrix} A'_2 \omega\epsilon_2 \beta_{2\rho} K'_m(\beta_{2\rho} \rho) & -B_2 \frac{m\gamma_z}{\rho} K_m(\beta_{2\rho} \rho) \end{bmatrix} \begin{bmatrix} \sin(m\phi) \\ \cos(m\phi) \end{bmatrix} e^{-\gamma_z z}
\end{aligned} \tag{4.62}$$

The boundary condition is shown below, where the tangential field inside the conductor and outside the conductor must be same, i.e. $E_{T1} = E_{T2}$ and $H_{T1} = H_{T2}$ at the boundary.

$$\begin{aligned}
E_{\phi 1} \Big|_{\rho=a} &= E_{\phi 2} \Big|_{\rho=a} \\
E_{z 1} \Big|_{\rho=a} &= E_{z 2} \Big|_{\rho=a} \\
H_{\phi 1} \Big|_{\rho=a} &= H_{\phi 2} \Big|_{\rho=a} \\
H_{z 1} \Big|_{\rho=a} &= H_{z 2} \Big|_{\rho=a}
\end{aligned} \tag{4.63}$$

Equating the z field result in the equation below

$$\begin{aligned}
A_1 J_m(\beta_{1\rho} a) &= A_2 K_m(\beta_{2\rho} \rho) \\
B_1 J_m(\beta_{1\rho} a) &= B_2 K_m(\beta_{2\rho} \rho)
\end{aligned} \tag{4.64}$$

By matching the boundary condition for ϕ direction, the field equation at the boundary becomes

$$\frac{1}{\beta_{1\rho}^2} \left[A_1 \frac{m\gamma_z}{a} J_m(\beta_{1\rho}a) - B_1 \omega \mu \beta_{1\rho} J'_m(\beta_{1\rho}a) \right] = -\frac{1}{\beta_{2\rho}^2} \left[A'_2 \frac{m\gamma_z}{a} K_m(\beta_{2\rho}\rho) - B'_2 \omega \mu \beta_{2\rho} K'_m(\beta_{2\rho}\rho) \right] \quad (4.65)$$

$$\frac{1}{\beta_{1\rho}^2} \left[A_1 \omega \epsilon_1 \beta_{1\rho} J'_m(\beta_{1\rho}a) - B_1 \frac{m\gamma_z}{a} J'_m(\beta_{1\rho}a) \right] = -\frac{1}{\beta_{2\rho}^2} \left[A'_2 \omega \epsilon_2 \alpha_{2\rho} K'_m(\beta_{2\rho}\rho) - B'_2 \frac{m\gamma_z}{a} K_m(\beta_{2\rho}\rho) \right] \quad (4.66)$$

Using the result from (4.64) to eliminate A_2 and B_2 , the equation (4.65) and (4.66) reduces to (4.67) and (4.68) respectively as shown below.

$$A_1 \frac{m\gamma_z}{\omega a} \left[\frac{1}{\beta_{1\rho}^2} + \frac{1}{\beta_{2\rho}^2} \right] - B_1 \left[\frac{\mu}{\beta_{1\rho}} \frac{J'_m(\beta_{1\rho}a)}{J_m(\beta_{1\rho}a)} + \frac{\mu}{\beta_{2\rho}} \frac{K'_m(\beta_{2\rho}\rho)}{K_m(\beta_{2\rho}\rho)} \right] = 0 \quad (4.67)$$

and

$$A_1 \left[\frac{\epsilon_1}{\beta_{1\rho}} \frac{J'_m(\beta_{1\rho}a)}{J_m(\beta_{1\rho}a)} + \frac{\epsilon_2}{\beta_{2\rho}} \frac{K'_m(\beta_{2\rho}\rho)}{K_m(\beta_{2\rho}\rho)} \right] - B_1 \frac{m\gamma_z}{\omega a} \left[\frac{1}{\beta_{1\rho}^2} + \frac{1}{\beta_{2\rho}^2} \right] = 0 \quad (4.68)$$

Sorting the equation in (4.67) and (4.68) to a single matrix form.

$$\begin{bmatrix} -\frac{m\gamma_z}{\omega a} \left(\frac{1}{\beta_{1\rho}^2} + \frac{1}{\beta_{2\rho}^2} \right) & \frac{\mu}{\beta_{1\rho}} \frac{J'_m(\beta_{1\rho}a)}{J_m(\beta_{1\rho}a)} + \frac{\mu}{\beta_{2\rho}} \frac{K'_m(\beta_{2\rho}\rho)}{K_m(\beta_{2\rho}\rho)} \\ \frac{\epsilon_1}{\beta_{1\rho}} \frac{J'_m(\beta_{1\rho}a)}{J_m(\beta_{1\rho}a)} + \frac{\epsilon_2}{\beta_{2\rho}} \frac{K'_m(\beta_{2\rho}\rho)}{K_m(\beta_{2\rho}\rho)} & -\frac{m\gamma_z}{\omega a} \left(\frac{1}{\beta_{1\rho}^2} + \frac{1}{\beta_{2\rho}^2} \right) \end{bmatrix} \begin{bmatrix} A_1 \\ B_1 \end{bmatrix} = 0 \quad (4.69)$$

To have a non-trivial solution for A_1 and B_1 , the determinant of the coefficient matrix in (4.69) must vanish. Taking the determinant of (4.69) and equating it to zero as shown in (4.70).

$$\det \begin{bmatrix} -\frac{m\gamma_z}{\omega a} \left(\frac{1}{\beta_{1\rho}^2} + \frac{1}{\alpha_{2\rho}^2} \right) & \frac{\mu}{\beta_{1\rho}} \frac{J'_m(\beta_{1\rho} a)}{J_m(\beta_{1\rho} a)} + \frac{\mu}{\beta_{2\rho}} \frac{K'_m(\beta_{2\rho} \rho)}{K_m(\beta_{2\rho} \rho)} \\ \frac{\epsilon_1}{\beta_{1\rho}} \frac{J'_m(\beta_{1\rho} a)}{J_m(\beta_{1\rho} a)} + \frac{\epsilon_2}{\beta_{2\rho}} \frac{K'_m(\beta_{2\rho} \rho)}{K_m(\beta_{2\rho} \rho)} & -\frac{m\gamma_z}{\omega a} \left(\frac{1}{\beta_{1\rho}^2} + \frac{1}{\beta_{2\rho}^2} \right) \end{bmatrix} = 0 \quad (4.70)$$

(4.70) gives a set of transcendental equation shown in (4.71)

$$\begin{aligned} & \left(\frac{m\gamma_z}{\omega a} \right)^2 \left(\frac{1}{\beta_{1\rho}^2} + \frac{1}{\beta_{2\rho}^2} \right)^2 - \left(\frac{\mu}{\beta_{1\rho}} \frac{J'_m(\beta_{1\rho} a)}{J_m(\beta_{1\rho} a)} + \frac{\mu}{\beta_{2\rho}} \frac{K'_m(\beta_{2\rho} \rho)}{K_m(\beta_{2\rho} \rho)} \right) \\ & \times \left(\frac{\epsilon_1}{\beta_{1\rho}} \frac{J'_m(\beta_{1\rho} a)}{J_m(\beta_{1\rho} a)} + \frac{\epsilon_2}{\beta_{2\rho}} \frac{K'_m(\beta_{2\rho} \rho)}{K_m(\beta_{2\rho} \rho)} \right) = 0 \end{aligned} \quad (4.71)$$

let

$$\begin{aligned} \delta &= \frac{\gamma_z}{k_0} \\ u &= \beta_{1\rho} a = k_0 a \sqrt{\epsilon_{r1} - \delta^2} \\ v &= \beta_{2\rho} a = k_0 a \sqrt{\delta^2 - \epsilon_{r2}} \end{aligned} \quad (4.72)$$

where $k_0 = \omega \sqrt{\mu_0 \epsilon_0}$

The equation in (4.71) simplifies to

$$(m\delta)^2 \left(\frac{1}{u^2} + \frac{1}{v^2} \right)^2 - \left(\frac{1}{u} \frac{J'_m(u)}{J_m(u)} + \frac{1}{v} \frac{K'_m(v)}{K_m(v)} \right) \left(\frac{\epsilon_{r1}}{u} \frac{J'_m(u)}{J_m(u)} + \frac{\epsilon_{r2}}{v} \frac{K'_m(v)}{K_m(v)} \right) = 0 \quad (4.73)$$

Expanding the equation in (4.73)

$$\frac{\epsilon_{r1}}{u^2} \left(\frac{J'_m(u)}{J_m(u)} \right)^2 + \frac{\epsilon_{r2}}{v^2} \left(\frac{K'_m(v)}{K_m(v)} \right)^2 + \frac{1}{uv} \frac{J'_m(u)}{J_m(u)} \frac{K'_m(v)}{K_m(v)} (\epsilon_{r1} + \epsilon_{r2}) = (m\delta)^2 \left(\frac{1}{u^2} + \frac{1}{v^2} \right)^2 \quad (4.74)$$

In the case where perfect conductor with infinite conductivity field is assumed, TE and TM mode can propagate, however for a lossy conductor with finite conductivity, such field should not exist, only EH or HE mode exist in lossy waveguide. For simplification, assume a perfect conductor, the field vanishes inside the conductor, where $E_{2\phi} = 0$ From (4.65), let $E_{2\phi} = 0$, the equation now becomes,

$$\frac{1}{\beta_{1\rho}^2} \left[A_1 \frac{m\gamma_z}{a} J_m(\beta_{1\rho}a) - B_1 \omega \mu \beta_{1\rho} J'_m(\beta_{1\rho}a) \right] = 0 \quad (4.75)$$

From (4.55), A_1 represents the electric field while B_1 represents the magnetic field. In the case of TE mode, where $A_1 = 0$, (4.75) indicates that TE mode can be found by finding the root of

$$\frac{J'_m(\beta_{1\rho}a)}{J_m(\beta_{1\rho}a)} = 0 \quad (4.76)$$

On the other hand, for TM mode, $B_1 = 0$, the TM mode can be found by finding the root of

$$\frac{J_m(\beta_{1\rho}a)}{J'_m(\beta_{1\rho}a)} = 0 \quad (4.77)$$

A close inspection of (4.73) shows that the equation can only be used to find TE mode as it contains $\frac{J'_m(\beta_{1\rho}a)}{J_m(\beta_{1\rho}a)}$. The equation needed to be modified for TM mode (G.

Yassin, 2003). By multiplying the equation (4.73) with $\left(\frac{J_m(u)}{J'_m(u)}\right)^2$, the modified equation to calculate TM mode is

$$\frac{\epsilon_{r1}}{u^2} + \frac{\epsilon_{r2}}{v^2} \left(\frac{K'_m(v)}{K_m(v)}\right)^2 \left(\frac{J_m(u)}{J'_m(u)}\right)^2 + \frac{1}{uv} \frac{J_m(u)}{J'_m(u)} \frac{K'_m(v)}{K_m(v)} (\epsilon_{r1} + \epsilon_{r2}) = (m\delta)^2 \left(\frac{1}{u^2} + \frac{1}{v^2}\right)^2 \left(\frac{J_m(u)}{J'_m(u)}\right)^2 \quad (4.78)$$

Case m=0

When $m=0$, where the field is TE_{0n} TM_{0n} , the field is said to be axis symmetric. The equation can be further simplified to

$$\left(\frac{1}{u} \frac{J'_m(u)}{J_m(u)} + \frac{1}{v} \frac{K'_m(v)}{K_m(v)} \right) \left(\frac{\epsilon_{r1}}{u} \frac{J'_m(u)}{J_m(u)} + \frac{\epsilon_{r2}}{v} \frac{K'_m(v)}{K_m(v)} \right) = 0 \quad (4.79)$$

which yields

$$\frac{1}{u} \frac{J'_m(u)}{J_m(u)} + \frac{1}{v} \frac{K'_m(v)}{K_m(v)} = 0 \quad (4.80)$$

or

$$\frac{\epsilon_{r1}}{u} \frac{J'_m(\beta_{1\rho} a)}{J_m(\beta_{1\rho} a)} + \frac{\epsilon_{r2}}{v} \frac{K'_m(\alpha_{2\rho} a)}{K_m(\alpha_{2\rho} a)} = 0 \quad (4.81)$$

(4.80) indicates that $A_1 = 0$; $B_1 \neq 0$, which shows that $E_z \neq 0$; $H_z = 0$, indicating the field is TM_{0n} . Solving the equation in (4.80) together with the relation from (4.72), the propagation constant, γ_z can be obtained. Similarly, (4.81) indicates that $A_1 \neq 0$; $B_1 = 0$ indicating it is a TE_{0n} field.

Case m ≠ 0

In the case where $m \neq 0$, it shows that E_z and H_z fields are coupled, and neither of them can be equal to zero, indicating that neither pure transverse electric (TE) or pure transverse magnetic (TM) can exist inside the waveguide. The field exist in the waveguide are hybrid EH_{mn} or HE_{mn} depending either electric field dominates or otherwise. The propagation constant needed to be solve numerically by finding the root of equation (4.73) for HE_{mn} or equation (4.78) for EH_{mn} mode.

4.4.3 A Review of Yeap's Method

Yeap's method matches the field inside the waveguide to the wall impedance of the waveguide. The surface impedance of the metal wall are given by (Cheng, 1991)

$$\frac{\vec{E}_t}{\vec{a}_n \times \vec{H}_t} = \sqrt{\frac{\mu_c}{\epsilon_c}} \quad (4.82)$$

Where μ_c and ϵ_c is the permeability and permittivity of the conductor wall. The permittivity of conductor is a function of frequency and its given by.

$$\epsilon_c = \epsilon_0 - j \frac{\sigma_c}{\omega} \quad (4.83)$$

The axial field in a circular waveguide is given by

$$E_z = A_m J_m \cos(m\phi) e^{j\omega t - \gamma z} \quad (4.84)$$

$$H_z = A_m' J_m \sin(m\phi) e^{j\omega t - \gamma z} \quad (4.85)$$

To the tangential field inside the waveguide, substitute the axial field in (4.84) into (4.26), following equations which describes the tangential field are obtained.

$$E_\phi = \frac{1}{\beta_\rho^2} \left[\frac{\gamma_z n}{\rho} A_m J_m(\beta_\rho \rho) \sin(m\phi) + j\omega \mu_0 \beta_\rho C_m' J_m'(\beta_\rho \rho) \sin(m\phi) \right] \quad (4.86)$$

$$H_\phi = -\frac{1}{\beta_\rho^2} \left[\frac{\gamma_z n}{\rho} A_m' J_m(\beta_\rho \rho) \cos(m\phi) + j\omega \epsilon_0 \beta_\rho A_m J_m'(\beta_\rho \rho) \cos(m\phi) \right] \quad (4.87)$$

Simplifying the surface impedance equation in (4.82), two set of equations are obtained as follow

$$\frac{E_\phi}{H_z} = \sqrt{\frac{\mu_c}{\epsilon_c}} \quad (4.88)$$

$$-\frac{E_z}{H_\phi} = \sqrt{\frac{\mu_c}{\epsilon_c}} \quad (4.89)$$

Substituting the field equation (4.84), (4.85), (4.86) and (4.87) into (4.88) and (4.89), the following equations are obtained.

$$\left[\frac{\gamma_z m}{\beta_\rho^2 a} \right] A_m + \left[\frac{j\omega \mu_0 J_m'(u)}{\beta_\rho J_m(u)} - \sqrt{\frac{\mu_c}{\epsilon_c}} \right] A_m' = 0 \quad (4.90)$$

$$\left[\frac{j\omega \epsilon_0 J_m'(u)}{\beta_\rho J_m(u)} - \sqrt{\frac{\epsilon_c}{\mu_c}} \right] A_m + \left[\frac{\gamma_z m}{\beta_\rho^2 a} \right] A_m' = 0 \quad (4.91)$$

where

$$u^2 = (\gamma_z^2 + k_0^2) a^2 \quad (4.92)$$

To have a non-trivial solution, the determinant of the equation above must vanish. Solving the determinant of the above equation and equate it to zero, it will result in the following transcendental equation.

$$\left[j\omega\mu_0\beta_\rho \frac{J_m'(u)}{J_m(u)} - \beta_\rho^2 \sqrt{\frac{\mu_c}{\epsilon_c}} \right] \left[j\omega\epsilon_0\beta_\rho \frac{J_m'(u)}{J_m(u)} - \beta_\rho^2 \sqrt{\frac{\epsilon_c}{\mu_c}} \right] = \left[\frac{m\gamma_z}{a} \right]^2 \quad (4.93)$$

Similar to Stratton's approach, the equation are only applicable to TE modes as TM mode will result in singularity in the ratio $\frac{J_m'(u)}{J_m(u)}$. Hence, the equation is multiplied

with $\frac{J_m(u)}{J_m'(u)}$, to remove the singularity. Hence the equation in (4.93) become as

follow

$$\left[j\omega\mu_0\beta_\rho - \beta_\rho^2 \sqrt{\frac{\mu_c}{\epsilon_c}} \frac{J_m(u)}{J_m'(u)} \right] \left[j\omega\epsilon_0\beta_\rho - \beta_\rho^2 \sqrt{\frac{\epsilon_c}{\mu_c}} \frac{J_m(u)}{J_m'(u)} \right] = \left[\frac{m\gamma_z}{a} \frac{J_m(u)}{J_m'(u)} \right]^2 \quad (4.94)$$

4.5 The New Method

The new method proposed here is a modification from Yeap's method, changing it from its transcendental form into closed form. Yamaguchi (1980) has first developed the closed form equation based on the Stratton's equation. Yamaguchi performed approximation to Stratton's equation using the Finite Difference Method. In this new method, his idea was adopted and modified to be used on Yeap's transcendental equation.

To convert the transcendental equation into closed form, several assumptions are imposed to the equation. The first assumption is that the frequency of the signal must be relatively close to the cutoff frequency. Hence, the variable of the Bessel function will be close to the root. The second assumption is that the conductor wall is assumed to be made of a very good conductor with high but finite conductivity. Unlike the power loss method, which results in infinite attenuation at cutoff frequency due to

the perfect conductor assumption, these assumptions result in a finite attenuation at the cutoff frequency,

4.5.1 Transverse Electric Mode

The transcendental equation in (4.93) is first developed, which will result in the following equation.

$$\beta_\rho^4 - j\omega\beta_\rho^3 \left[\epsilon_0 \sqrt{\frac{\mu_c}{\epsilon_c}} + \mu_0 \sqrt{\frac{\epsilon_c}{\mu_c}} \right] \frac{J_m'(u)}{J_m(u)} - \omega^2 \mu_0 \epsilon_0 \beta_\rho^2 \left[\frac{J_m'(u)}{J_m(u)} \right]^2 = \left[\frac{m\gamma_z}{a} \right]^2 \quad (4.95)$$

To simplify the above equation, ignore the $\left[\frac{J_m'(u)}{J_m(u)} \right]^2$ term, as the value will be small for a good conductor. Using the equation (4.92), the simplified equation is shown as follow

$$\frac{J_m'(u)}{J_m(u)} = - \left[\frac{m^2(u^2 - k_0^2 a^2) - u^4}{j\omega u^3 a} \right] \left[\frac{1}{\left[\epsilon_0 \sqrt{\frac{\mu_c}{\epsilon_c}} + \mu_0 \sqrt{\frac{\epsilon_c}{\mu_c}} \right]} \right] \quad (4.96)$$

The first derivative of the Bessel function of a circular waveguide with perfect conductor will have roots at u_{nm} and it's given by

$$J_m'(u_{nm}) = 0 \quad (4.97)$$

However, if the conductor has high but finite conductivity, the Bessel function variable will be close to the root, hence the Bessel function variable can be approximated as follow

$$u = u_{nm} + \Delta u \quad (4.98)$$

where Δu is the perturbation term

The Bessel function then becomes as follow

$$J_m'(u) = J_m'(u_{nm} + \Delta u) \quad (4.99)$$

Using the Finite Difference Method (FDM), the second derivative of the Bessel function can be approximated as follow

$$J_m''(u_{nm}) = \frac{J_m'(u_{nm} + \Delta u) - J_m'(u_{nm})}{\Delta u} \quad (4.100)$$

However, $J'(u_{nm}) = 0$ for TE mode, hence the equation reduced to

$$J_m'(u_{nm} + \Delta u) = J_m''(u_{nm}) \Delta u \quad (4.101)$$

Using the Bessel recursion as follow, the FDM equation can be rewritten by substituting (4.102) into (4.100) and obtained the equation (4.103)

$$J_m''(x) = \left\{ \left(\frac{m}{x} \right)^2 - 1 \right\} J_m(x) \quad (4.102)$$

$$\begin{aligned} J_m'(u_{nm} + \Delta u) &= J_m''(u_{nm}) \Delta u \\ &= \left\{ \frac{m^2}{u_{nm}^2} - 1 \right\} J_m(u_{nm}) \Delta u \end{aligned} \quad (4.103)$$

The Bessel function can be approximated as those with perfect conductor, hence the following can be obtained

$$J_m(u) \approx J_m(u_{nm}) \quad (4.104)$$

The ratio $\frac{J_m'(u)}{J_m(u)}$ can be simplified to as follow

$$\frac{J_m'(u)}{J_m(u)} \approx \left(\frac{m^2}{u_{nm}^2} - 1 \right) \Delta u \quad (4.105)$$

Substituting (4.105) into (4.96), (4.106) can be obtained to calculate Δu

$$\Delta u = - \left[\frac{m^2 (u_{nm}^2 - k_0^2 a^2) - u_{nm}^4}{(j\omega u_{nm} a)(m^2 - u_{nm}^2)} \right] \left[\frac{1}{\left[\epsilon_0 \sqrt{\frac{\mu_c}{\epsilon_c}} + \mu_0 \sqrt{\frac{\epsilon_c}{\mu_c}} \right]} \right] \quad (4.106)$$

From (4.92), the following relation is obtained.

$$\begin{aligned}\gamma_z &= \frac{u^2}{a^2} - k_0^2 \\ &= \frac{u_{nm}^2 + 2u_{nm}\Delta u + \Delta u^2}{a^2} - k_0^2\end{aligned}\quad (4.107)$$

The propagation constant can then be obtained by substituting (4.106) into (4.107)

4.5.2 Transverse Magnetic Mode

A similar approach is used to calculate the equation for the TM mode. First equation (4.94) is expanded as shown below

$$\beta_\rho^4 \left[\frac{J_m(u)}{J_m'(u)} \right]^2 - j\omega\beta_\rho^3 \left[\epsilon_0 \sqrt{\frac{\mu_c}{\epsilon_c}} + \mu_0 \sqrt{\frac{\epsilon_c}{\mu_c}} \right] \frac{J_m(u)}{J_m'(u)} - \omega^2 \mu_0 \epsilon_0 \beta_\rho^2 = \left[\frac{m\gamma_z}{a} \frac{J_m(u)}{J_m'(u)} \right]^2 \quad (4.108)$$

Ignoring the square term and with some simplification (4.109) can be obtained

$$\frac{J_m(u)}{J_m'(u)} = - \left[\frac{\omega\mu_0\epsilon_0}{j\beta_\rho} \right] \left[\frac{1}{\epsilon_0 \sqrt{\frac{\mu_c}{\epsilon_c}} + \mu_0 \sqrt{\frac{\epsilon_c}{\mu_c}}} \right] \quad (4.109)$$

For TM mode with perfect conductor, the Bessel function with root u_{nm} is given by

$$J_m(u_{nm}) = 0 \quad (4.110)$$

The Bessel function with finite conductivity wall can be approximated as follows

$$J_m(u) = J_m(u_{nm} + \Delta u) \quad (4.111)$$

The FDM equation of the first derivative of Bessel function is as follows

$$J_m'(u_{nm}) = \frac{J_m(u_{nm} + \Delta u) - J_m(u_{nm})}{\Delta u} \quad (4.112)$$

The FDM equation can be simplified to follows using (4.110)

$$J_m(u_{nm} + \Delta u) = J_m'(u_{nm}) \Delta u \quad (4.113)$$

The first derivative of the Bessel function can be approximated as those of perfect conductor as follows

$$J_m'(u) \approx J_m'(u_{nm}) \quad (4.114)$$

The ratio $\frac{J_m(u)}{J_m'(u)}$ can then be simplified as follows

$$\frac{J_m(u)}{J_m'(u)} \approx \Delta u \quad (4.115)$$

Substituting (4.115) back to (4.109), it results in equation (4.116)

$$\Delta u = - \left[\frac{\omega \mu_0 \epsilon_0}{j \beta_\rho} \right] \left[\frac{1}{\epsilon_0 \sqrt{\frac{\mu_c}{\epsilon_c}} + \mu_0 \sqrt{\frac{\epsilon_c}{\mu_c}}} \right] \quad (4.116)$$

The propagation constant for TM mode can be obtained by substituting (4.116) into (4.107)

4.6 Results and Discussion

Figure 22 shows the comparison of attenuation of TE₁₁ mode before cutoff computed from Stratton's method, Yeap's method, power loss method, the new method and the experimental result. From the result it can be seen that the power loss fails to describe the attenuation below cutoff as the attenuation diverges to infinity. All the other methods, including the experimental result agrees that the attenuation below cutoff increases sharply, but the values are finite. The solution from the new method is very close to Yeap's transcendental solution, in fact it is indistinguishable from the plot.

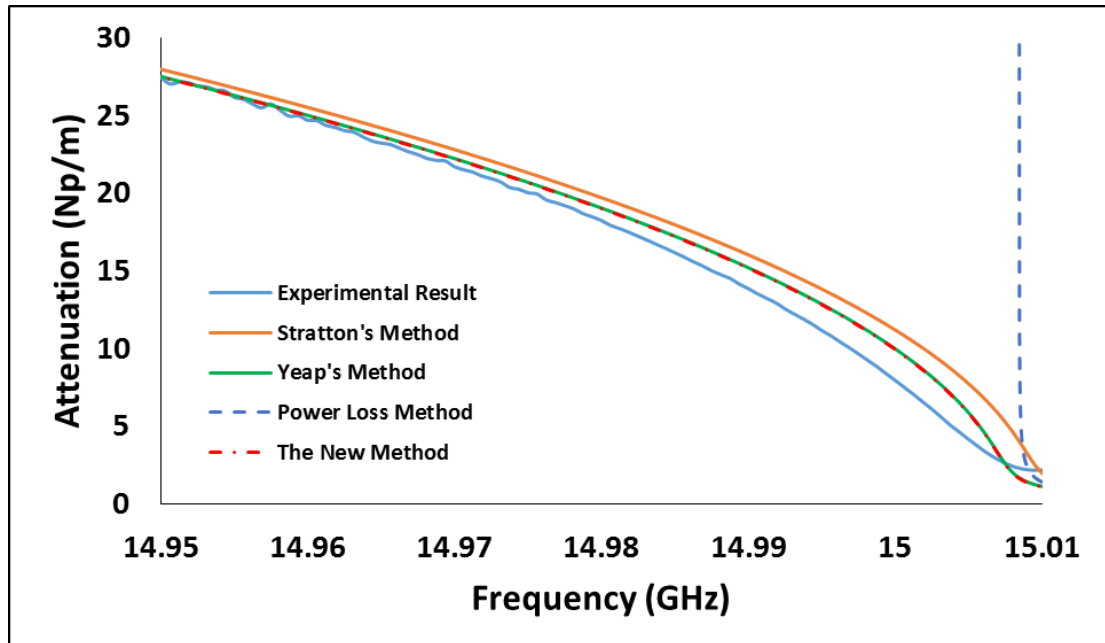


Figure 22 Attenuation of TE_{11} mode in a hollow circular waveguide with radius $a = 5.8533$ mm

Figure 23 and Figure 24 shows the attenuation of TE_{11} and TM_{11} mode computed from the Stratton's method, Yeap's method, power loss method and the new method. From the result it can be seen that the new method is very close to Yeap's method when the frequency of interest is around the cutoff frequency. The power loss method on the other hand diverges in infinity at the cutoff frequency. This solution would deem as invalid. Wave can still propagate even below the cutoff frequency as shown in Figure 22. This implies that the attenuation cannot be infinite.

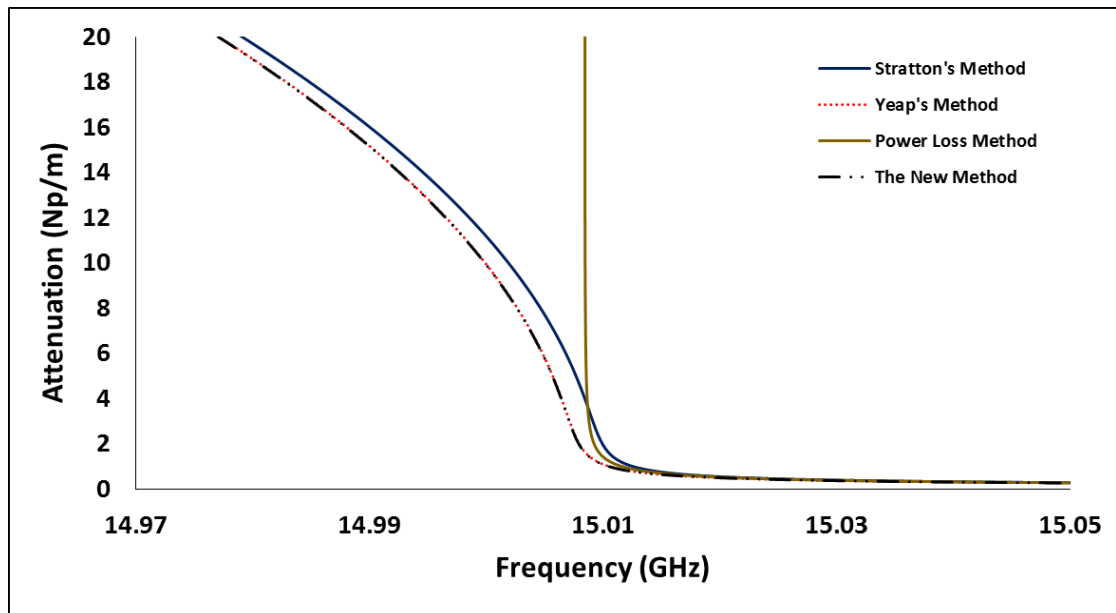


Figure 23 Attenuation of TE_{11} in a circular waveguide with radius $a = 5.8533$ mm

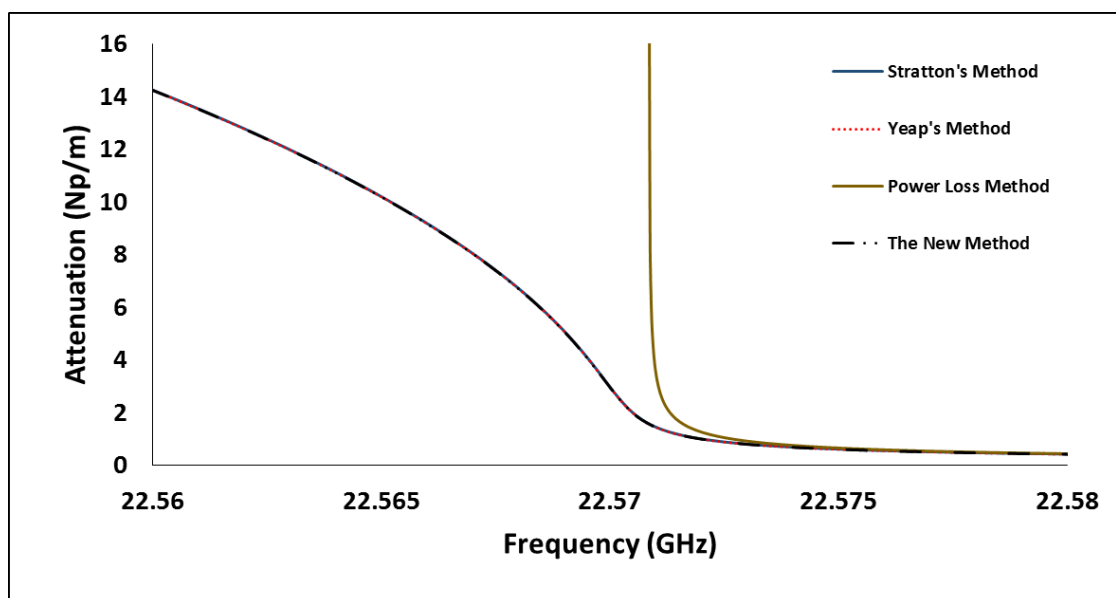


Figure 24 Attenuation of TM_{11} in a circular waveguide with radius $a = 8.1$ mm

Based on the wave-particle duality, electromagnetic waves can be described as particle. According the quantum mechanics, particle can tunnel through a barrier through quantum tunnelling effect. The electromagnetic wave can then be seen as a particle tunnelling through a barrier as it passes through the waveguide with higher cutoff frequency than the wave. As it tunnels through the waveguide, the wave amplitude decreases exponentially. As long as the wave amplitude does not decrease to zero, the wave will propagate. To prevent the wave to travel through the barrier, the

barrier would need to have an infinite potential energy. To create this infinite potential energy, it would require a perfect conductor, such as those assumptions made in the power loss method. Hence it can be seen that the power loss method results in an infinite attenuation at cutoff frequency, which prevents wave propagation below the cutoff frequency.

Figure 25 and Figure 26 show the comparison of various results when applied to higher frequency. From the result it can be seen that as the frequency increases well beyond the cutoff frequency, the result of the new method starts to diverge from Yeap's method. At lower frequency, both the new method and Yeap's method are indistinguishable. However, when the frequency increases, the solution of the new method starts to diverge from Yeap's solution. This is due to the assumption made. The new method assumes that the wave attenuation is the result of a small perturbation term added to the perfect TE or TM mode. However, as the frequency increases, perfect TE and TM modes are no longer a valid assumption. At high frequency, the mode becomes a hybrid EH or HE mode, i.e. $E_z \neq 0, H_z \neq 0$. Hence, the exact solution is no longer a small perturbation added to a perfect TE or TM mode. This causes the solution of the new method to deviate from the exact solution of Yeap's method.

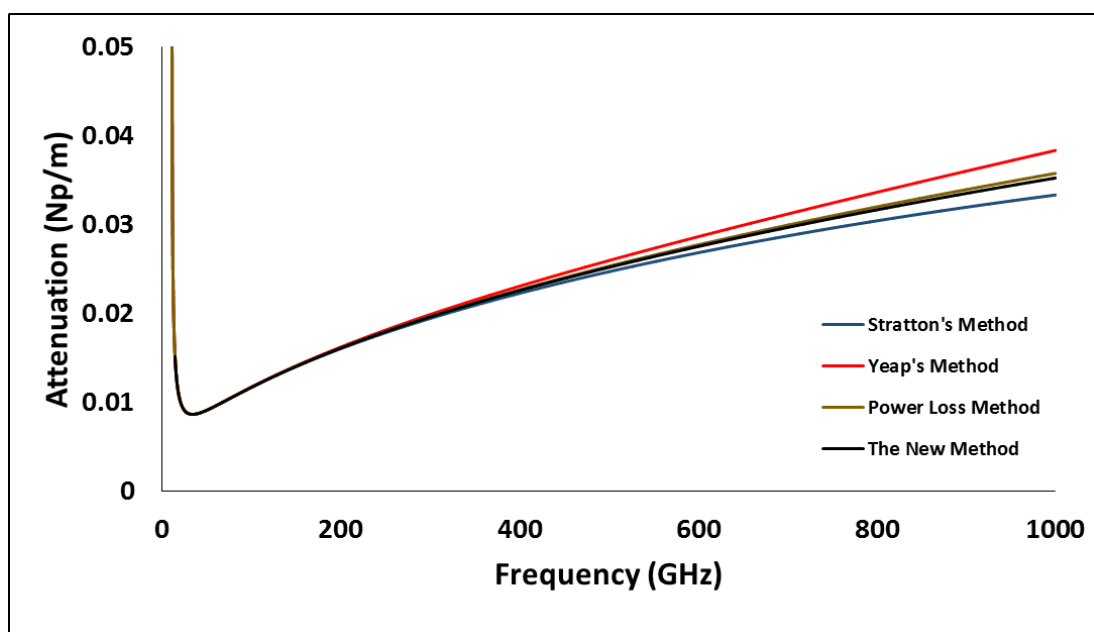


Figure 25 Attenuation of TE_{11} in circular waveguide from 0 GHz to 1000 GHz

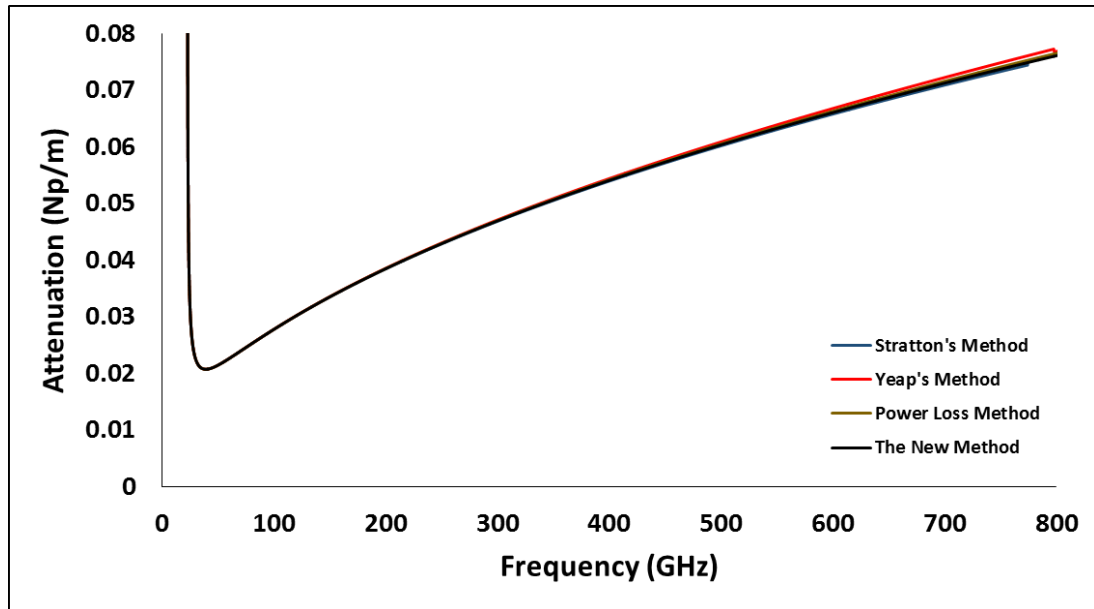


Figure 26 Attenuation of TM_{11} in circular waveguide from 0 GHz to 800 GHz

Figure 27 below shows the attenuation of TE_{11} , TE_{01} , TE_{02} , TM_{11} and TM_{01} mode calculated using the new method. From the result, it can be seen that for a circularly symmetric mode, TE_{0n} will have its attenuation decreases monotonically with frequency. TE_{0n} is known as circularly symmetric mode. In such mode, the electric field lines are circular, while the only magnetic field lines are H_z . However, for a fixed input power, H_z decreases as frequency increases. Simultaneously, the current density and the conductor losses of the waveguide wall decreases. Hence, the attenuation of TE_{0n} decreases as frequency increases.

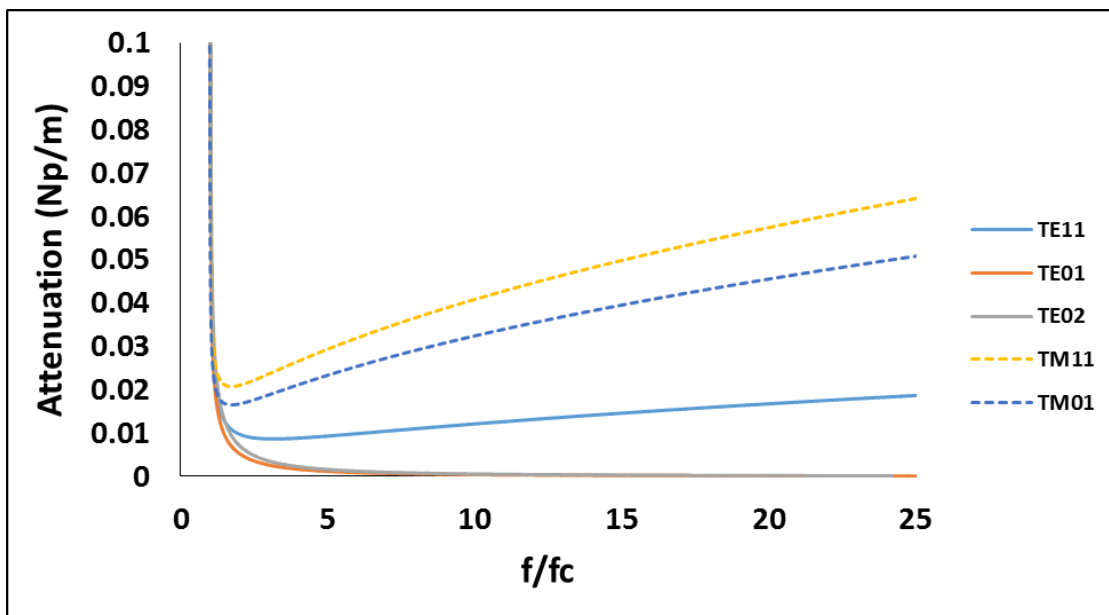


Figure 27 Comparison of Attenuation of TE₁₁, TE₀₁, TE₀₂, TM₁₁ and TM₀₁ mode

Figure 28 shows the attenuation computed using the new method. The figure shows the effect on the attenuation as the conductivity of the wall is varied. From the result it can be seen that lower conductivity results in lower attenuation when the frequency is above the cutoff frequency. Below the cutoff frequency, however, it can be seen that the attenuation is actually lower as conductivity reduces.

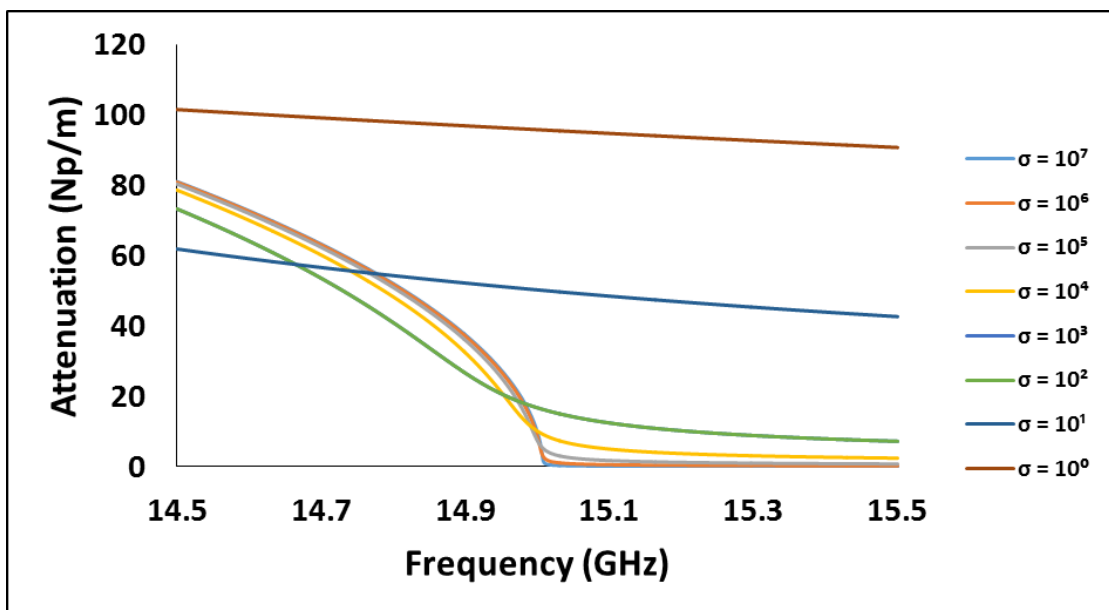


Figure 28 Comparison of different wall conductivity in hollow metal waveguide with radius $a = 5.8533$ mm for TE₁₁ mode

This is because, as the conductivity increases, the metal wall approaches to those of perfect conductor. For a perfect conductor, the attenuation approach infinity at cut-off frequency as shown from the power loss method. Therefore, the attenuation is higher when the frequency is below cut-off for higher conductivity. On the other hand, the attenuation is lower for higher conductivity when frequency is beyond the cut-off frequency. This is because higher conductivity result in lower conductor loss, which decreases the attenuation.

When the conductivity is closer to zero, the attenuation curve approaches a more linear curve. When the wall's conductivity drops, the wave will penetrate more to the wall, i.e. the skin depth will increase. This is similar to those of dielectric waveguide, where the wave penetrate into the wall. This causes attenuation curve more linear. Hence, from the figure it can be seen that at high conductivity, the attenuation curve has a sharp turning point between the evanescent region and propagating region. On the hand, as the conductivity decreases, the evanescent and propagating region become more linear at the cut-off point.

The dielectric used in the waveguide is air which has near zero conductivity. When the conductivity of the wall approaches zero, the boundary between the air and the wall becomes fuzzy. When the conductivity of the wall is same as the air, the wall can no longer confine the wave and act as waveguide. Therefore, there will be no evanescent and propagating region as seen in the figure when conductivity approach zero.

Figure 29 below shows the difference of the new approximate's solution and Yeap's method. From the result it can be seen that as the conductivity decreases, the result from the approximate's solution starts to diverges from Yeap's solution. At lower conductivity, the assumption of perfect TE and TM mode no longer valid. The wave will propagate with a hybrid mode. Similar to the argument made in the high frequency figure, i.e. Figure 25 and Figure 26, based on the assumption made earlier, that the attenuation is equal to those of a small perturbation term added to those of perfect TE and TM is no longer valid. Therefore, as the conductivity decreases, the solution from the new method start to diverge.

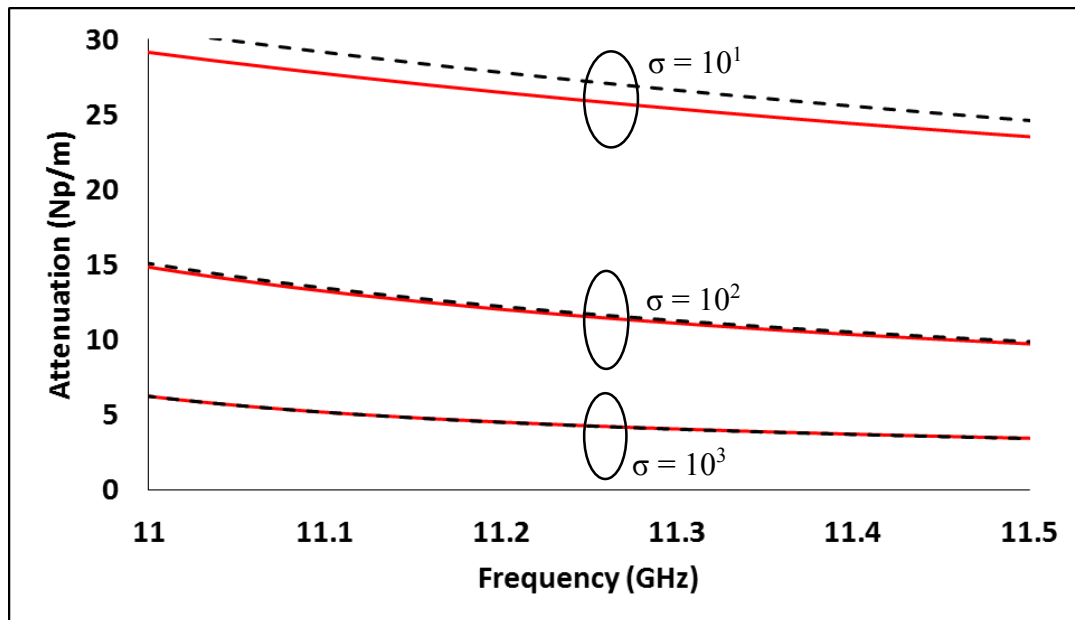


Figure 29 Difference of Yeap's Solution and the new method at low conductivity. Red solid line is the result from Yeap's method, black dotted line is the result from the new method.

4.7 Summary

A new method that is modified from Yeap's transcendental equation has been formulated. The new method transforms the transcendental equation into closed form. This is based on the assumption that wave propagation in a practical conductor can be approximated as in a perfect conductor with an inclusion of a small perturbation term. The new method has the advantage of being simpler and give more intuitive insights than the transcendental equation. A transcendental equation requires a root finding algorithm to solve for the root. Appropriate initial guesses are required in order to allow the solution to converge. A closed form equation has none of these problems and the computation time required to solve the closed form is shorter than the transcendental equation. This allows the closed form equation to be used in real time application.

Based on the result obtained, the loss predicted by the new method is in close agreement with the experimental measurement and those found in Yeap's and

Stratton's methods. The new method is able to give a reasonably accurate solution to compute attenuation in a waveguide.

CHAPTER 5

RECTANGULAR WAVEGUIDE

5.1 Introduction

An equation to calculate the loss in a rectangular waveguide is difficult to formulate rigorously due to the difficulty in boundary matching. Stratton's equation is therefore not available for rectangular waveguide for this reason.

The power loss method for rectangular waveguide is similar to that mentioned in the circular waveguide. Hence it would not be able to compute the attenuation when the signal frequency is below the cutoff frequency of the waveguide due to the assumption of perfect conductor. It is also unable to take into consideration of the presence of cross coupling effect in degenerate modes.

Papadopoulos (1953) has developed a method which accounts for the mode coupling effect. It is a perturbation method where it assumes that the fields in a lossy waveguide can be expressed as a linear combination of fields in a lossless waveguide. It is to be noted, however, that the loss for TM_{11} mode computed using Papadopoulos' method is found to be lower than that using the power loss method. The result contradicts what has been expected theoretically, i.e. the loss should be higher due to mode coupling effect

The formulation developed by Yeap (2011) does not assume a perfect conductor. Hence, it is able to obtain a more realistic result, compared to the power loss method. Yeap's method is able to take into consideration of the mode coupling

effect in degenerate modes. This makes Yeap's method more accurate than the perturbation method. However, similarly Yeap's method result in a transcendental equation which can only be solved with a root finding algorithm.

A new method will be presented in this chapter. The new method is able to calculate attenuation in the wave propagating inside a rectangular waveguide. Similar to the circular waveguide, the new method is based on Yeap's method. It converts the transcendental equation of Yeap's method to a closed form solution. The new method is able to give a reasonable accuracy to compute attenuation.

5.2 Fields in Rectangular Waveguides

To obtain the longitudinal field equation, first expand the Helmholtz Equation from (A.5) in the Cartesian coordinates to obtain the following equation:

$$\frac{\partial^2 E_z}{\partial x^2} + \frac{\partial^2 E_z}{\partial y^2} + \frac{\partial^2 E_z}{\partial z^2} + \gamma^2 E_z = 0 \quad (5.1)$$

The partial differential equation above can be solved using the method of separation of variables. The variable E_z can be separated into the x , y and z variables as shown below.

$$E_z = X(x)Y(y)Z(z) \quad (5.2)$$

Substituting (5.2) into (5.1) and rearranging the equation, the following equation is obtained

$$\frac{X''}{X} + \frac{Y''}{Y} + \frac{Z''}{Z} = -\gamma^2 \quad (5.3)$$

Since the x , y and z variables are independent of each other, (5.3) can be separated into (5.4), (5.5) and (5.6)

$$X'' + k_x^2 X = 0 \quad (5.4)$$

$$Y'' + k_y^2 Y = 0 \quad (5.5)$$

$$Z'' - \gamma^2 Z = 0 \quad (5.6)$$

where, k_x^2 , k_y^2 and γ^2 are the separation constant and their relation with one with another is shown in (5.7) below.

$$-k_x^2 - k_y^2 + \gamma^2 = -k^2 \quad (5.7)$$

The solution to the differential equation in (5.4),(5.5) and (5.6) are in (5.8),(5.9) and (5.10).

$$X(x) = c_1 \cos(k_x x) + c_2 \sin(k_x x) \quad (5.8)$$

$$Y(y) = c_3 \cos(k_y y) + c_4 \sin(k_y y) \quad (5.9)$$

$$Z(z) = c_5 e^{\gamma z} + c_6 e^{-\gamma z} \quad (5.10)$$

Substituting all the solution into (5.2) the solution of the longitudinal electric field, E_z is found to be as follow

$$E_z = (c_1 \cos(k_x x) + c_2 \sin(k_x x))(c_3 \cos(k_y y) + c_4 \sin(k_y y))(c_5 e^{\gamma z} + c_6 e^{-\gamma z}) \quad (5.11)$$

Assuming that the field travels in the forward direction only, the $c_5 e^{\gamma z}$ term can be ignored, the field equation can then be reduced to as follow

$$E_z = (A_1 \cos(k_x x) + A_2 \sin(k_x x))(A_3 \cos(k_y y) + A_4 \sin(k_y y))e^{-\gamma z} \quad (5.12)$$

Similarly, the magnetic field can be shown as follows

$$H_z = (B_1 \cos(k_x x) + B_2 \sin(k_x x))(B_3 \cos(k_y y) + B_4 \sin(k_y y))e^{-\gamma z} \quad (5.13)$$

Transverse Field

The transverse field in the x and y direction can be obtained using the following equations

$$E_x = -\frac{\gamma}{h^2} \frac{\partial E_z}{\partial x} - \frac{j\omega\mu}{h^2} \frac{\partial H_z}{\partial y} \quad (5.14)$$

$$E_y = -\frac{\gamma}{h^2} \frac{\partial E_z}{\partial y} + \frac{j\omega\mu}{h^2} \frac{\partial H_z}{\partial x} \quad (5.15)$$

$$H_x = \frac{j\omega\epsilon}{h^2} \frac{\partial E_z}{\partial y} - \frac{\gamma}{h^2} \frac{\partial H_z}{\partial x} \quad (5.16)$$

$$H_y = -\frac{j\omega\epsilon}{h^2} \frac{\partial E_z}{\partial x} - \frac{\gamma}{h^2} \frac{\partial H_z}{\partial y} \quad (5.17)$$

where;

$$h^2 = \gamma^2 + k^2 = k_x^2 + k_y^2 \quad (5.18)$$

Transverse Magnetic (TM) Mode

The TM mode will have the following boundary conditions. The longitudinal electric field must vanish at the boundary of the waveguide.

Boundary condition:

$$\begin{aligned} E_z &= 0 \text{ at } y = 0 \\ E_z &= 0 \text{ at } y = b \\ E_z &= 0 \text{ at } x = 0 \\ E_z &= 0 \text{ at } x = a \end{aligned} \quad (5.19)$$

This requires that the cosine term to be zero, hence A_1 and A_3 must vanish, resulting in the following equation

$$E_z = E_0 \sin(k_x x) \sin(k_y y) e^{-\gamma z} \quad (5.20)$$

The boundary equation also requires the field to vanish at the end of the x and y , hence this implies that

$$k_x a = m\pi, \quad m = 1, 2, 3, \dots \quad (5.21)$$

$$k_y b = n\pi, \quad n = 1, 2, 3, \dots \quad (5.22)$$

which can be rearrange to the following

$$k_x = \frac{m\pi}{a} \quad (5.23)$$

$$k_y = \frac{n\pi}{b} \quad (5.24)$$

Substituting the equation above (5.23) and (5.24) into (5.20) will result in the following equation

$$E_z = E_0 \sin\left(\frac{m\pi x}{a}\right) \sin\left(\frac{n\pi y}{b}\right) e^{-\gamma z} \quad (5.25)$$

To obtain the transverse field, substitute the longitudinal field (5.25) into (5.14), (5.15), (5.16) and (5.17) and noting that the longitudinal magnetic field, H_z is zero for TM mode. The following equation summarize the field equation for TM mode in a rectangular waveguide.

$$E_z = E_0 \sin\left(\frac{m\pi x}{a}\right) \sin\left(\frac{n\pi y}{b}\right) e^{-\gamma z} \quad (5.26)$$

$$H_z = 0 \quad (5.27)$$

$$E_x = -\frac{\gamma}{h^2} \left(\frac{m\pi}{a}\right) E_0 \cos\left(\frac{m\pi x}{a}\right) \sin\left(\frac{n\pi y}{b}\right) e^{-\gamma z} \quad (5.28)$$

$$E_y = -\frac{\gamma}{h^2} \left(\frac{n\pi}{b}\right) E_0 \sin\left(\frac{m\pi x}{a}\right) \cos\left(\frac{n\pi y}{b}\right) e^{-\gamma z} \quad (5.29)$$

$$H_x = -\frac{j\omega\epsilon}{h^2} \left(\frac{n\pi}{b}\right) E_0 \sin\left(\frac{m\pi x}{a}\right) \cos\left(\frac{n\pi y}{b}\right) e^{-\gamma z} \quad (5.30)$$

$$H_y = -\frac{j\omega\epsilon}{h^2} \left(\frac{m\pi}{a}\right) E_0 \cos\left(\frac{m\pi x}{a}\right) \sin\left(\frac{n\pi y}{b}\right) e^{-\gamma z} \quad (5.31)$$

Transverse Electric (TE) Mode

TE mode has the following boundary conditions

Boundary Conditions:

$$\begin{aligned}
 E_x &= 0 \text{ at } y = 0 \\
 E_x &= 0 \text{ at } y = b \\
 E_y &= 0 \text{ at } x = 0 \\
 E_y &= 0 \text{ at } x = a
 \end{aligned} \tag{5.32}$$

$$\begin{aligned}
 \frac{\partial H_z}{\partial y} &= 0 \text{ at } y = 0 \\
 \frac{\partial H_z}{\partial y} &= 0 \text{ at } y = b \\
 \frac{\partial H_z}{\partial x} &= 0 \text{ at } x = 0 \\
 \frac{\partial H_z}{\partial x} &= 0 \text{ at } x = a
 \end{aligned} \tag{5.33}$$

Imposing the boundary condition to the longitudinal magnetic field, (5.34) can be obtained

$$H_z = H_0 \cos\left(\frac{m\pi x}{a}\right) \cos\left(\frac{n\pi y}{b}\right) e^{-\gamma z} \tag{5.34}$$

The following equation show the summary of the field equation for TE mode

$$H_z = H_0 \cos\left(\frac{m\pi x}{a}\right) \cos\left(\frac{n\pi y}{b}\right) e^{-\gamma z} \tag{5.35}$$

$$E_z = 0 \tag{5.36}$$

$$E_x = \frac{j\omega\mu}{h^2} \left(\frac{n\pi}{b}\right) H_0 \cos\left(\frac{m\pi x}{a}\right) \sin\left(\frac{n\pi y}{b}\right) e^{-\gamma z} \tag{5.37}$$

$$E_y = -\frac{j\omega\mu}{h^2} \left(\frac{m\pi}{a}\right) H_0 \sin\left(\frac{m\pi x}{a}\right) \cos\left(\frac{n\pi y}{b}\right) e^{-\gamma z} \tag{5.38}$$

$$H_x = \frac{\gamma}{h^2} \left(\frac{m\pi}{a}\right) H_0 \sin\left(\frac{m\pi x}{a}\right) \cos\left(\frac{n\pi y}{b}\right) e^{-\gamma z} \tag{5.39}$$

$$H_y = \frac{\gamma}{h^2} \left(\frac{n\pi}{b}\right) H_0 \cos\left(\frac{m\pi x}{a}\right) \sin\left(\frac{n\pi y}{b}\right) e^{-\gamma z} \tag{5.40}$$

5.3 Cutoff Frequency for Rectangular Waveguide

The cutoff frequency can be obtained from the dispersion relation equation. Rearranging the dispersion relation in (5.18), the following equation is obtained.

$$\gamma = \sqrt{\left[\frac{m\pi}{a}\right]^2 + \left[\frac{n\pi}{b}\right]^2} - k^2 \quad (5.41)$$

At the cutoff frequency, the propagation constant is zero, which implies that

$$k^2 = \left[\frac{m\pi}{a}\right]^2 + \left[\frac{n\pi}{b}\right]^2 = \omega^2 \mu \epsilon \quad (5.42)$$

Rearranging the equation the following equation to compute the cutoff frequency of a rectangular waveguide is obtained.

$$f_c = \frac{1}{2\pi\sqrt{\mu\epsilon}} \sqrt{\left[\frac{m\pi}{a}\right]^2 + \left[\frac{n\pi}{b}\right]^2} \quad (5.43)$$

The following diagram shows the cutoff frequency of different modes for a rectangular waveguide. From the diagram it can be seen that TE₁₀ is the fundamental mode for rectangular waveguide. From the diagram below it can be seen that TE_{mn} and TM_{mn} have the same cut-off frequency. These modes are said to be the degenerate mode. Degeneracy results in higher attenuation as mentioned in previous chapter. The total attenuation is not simply the addition of the attenuation of two modes. There are coupling effect between the TE and TM mode which results in higher attenuation.

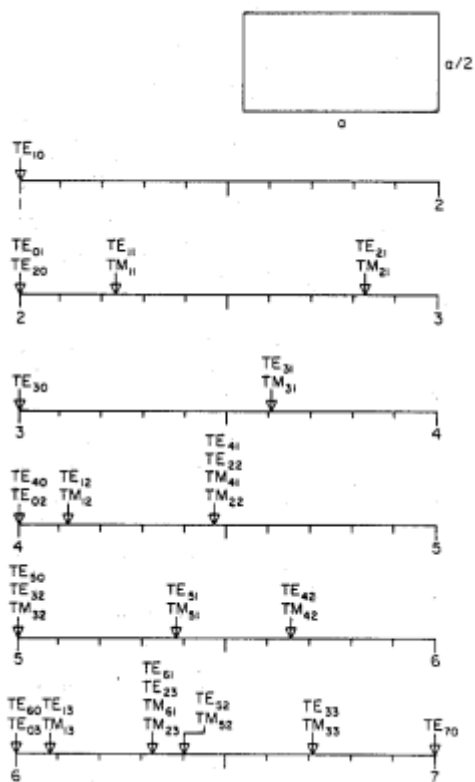


Figure 30 Normalized Cutoff Frequency for Different Field in a Rectangular Waveguide (C.S. Lee, 1985)

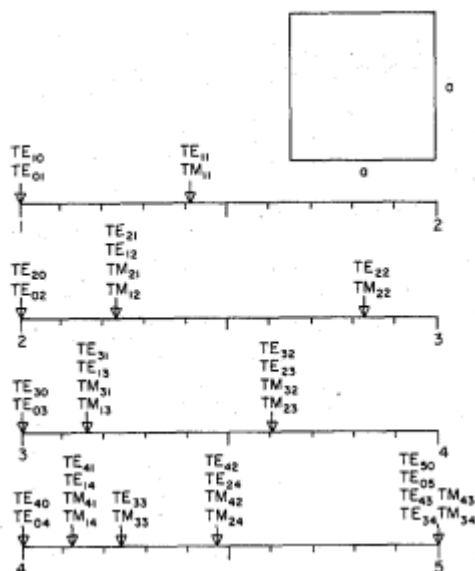


Figure 31 Normalized Cutoff Frequency for Different Field in a Square Waveguide (C.S. Lee, 1985)

5.4 Review of Some Conventional Method

This chapter presents the analysis and comparison among the power loss method, Papadopoulos' method (PPM) and Yeap's method. Derivations of the mentioned methods are presented in a comprehensive and orderly manner.

5.4.1 A Review of Papadopoulos' Method

Papadopoulos' method expresses field in lossy waveguide as a linear combination of field in lossless waveguide. The field in the waveguide is first separated into transverse and axial part

$$\vec{E} = \vec{E}_T e^{-\gamma z} + E_Z e^{-\gamma z} \hat{a}_z \quad (5.44)$$

$$\vec{H} = \vec{H}_T e^{-\gamma z} + H_Z e^{-\gamma z} \hat{a}_z \quad (5.45)$$

Where \vec{E}_T and \vec{H}_T both represents the transverse field and E_Z and H_Z represent the axial field. Using the above field equation, the Maxwell's equation is separated into transverse and axial equation. Substituting (5.44) into (A.1), and splitting the gradient, $\nabla = \nabla_T + \hat{a}_z \frac{\partial}{\partial z}$, the result is shown below in (5.46)

$$\left(\nabla_T + \hat{a}_z \frac{\partial}{\partial z} \right) \cdot \left(\vec{E}_T e^{-\gamma z} + E_Z e^{-\gamma z} \hat{a}_z \right) = 0 \quad (5.46)$$

$$\nabla_T \cdot \vec{E}_T = \gamma_z E_Z$$

Equation below (5.47) is obtained by substituting (5.44) into (A.3)

$$\left(\nabla_T + \hat{a}_z \frac{\partial}{\partial z} \right) \times \left(\vec{E}_T e^{-\gamma z} + E_Z e^{-\gamma z} \hat{a}_z \right) = -j\omega\mu \left(\vec{H}_T e^{-\gamma z} + H_Z e^{-\gamma z} \hat{a}_z \right) \quad (5.47)$$

$$\nabla_T \times \vec{E}_T e^{-\gamma z} + \nabla_T \times \hat{a}_z E_Z e^{-\gamma z} - \gamma_z \hat{a}_z \times \vec{E}_T e^{-\gamma z} = -j\omega\mu \left(\vec{H}_T e^{-\gamma z} + H_Z e^{-\gamma z} \hat{a}_z \right)$$

The above equation(5.47) can be separated into transverse and axial field as shown below.

Transverse field

$$\hat{a}_z \times \nabla_T \cdot E_Z + \gamma_z \hat{a}_z \times \vec{E}_T = j\omega\mu \vec{H}_T \quad (5.48)$$

Axial field

$$\nabla_T \times \overline{E_T} = -j\omega\mu H_z \hat{a}_z \quad (5.49)$$

Similarly for magnetic field, substitute (5.45) into (A.2) and (A.4) results in the equation shown below

$$\nabla_T \cdot \overline{H_T} = \gamma_z H_z \quad (5.50)$$

$$\nabla_T \times \overline{H_T} e^{-\gamma_z z} + \nabla_T \times H_z e^{-\gamma_z z} \hat{a}_z - \gamma_z \hat{a}_z \times \overline{H_T} e^{-\gamma_z z} = j\omega\epsilon \left(\overline{E_T} e^{-\gamma_z z} + E_z e^{-\gamma_z z} \hat{a}_z \right) \quad (5.51)$$

Equation (5.51) can be divided into axial and transverse field

Transverse field

$$\hat{a}_z \times \nabla_T \cdot H_z + \gamma_z \hat{a}_z \times \overline{H_T} = -j\omega\epsilon \overline{E_T} \quad (5.52)$$

Axial field

$$\nabla_T \times \overline{H_T} = j\omega\epsilon E_z \hat{a}_z \quad (5.53)$$

The Helmholtz equation can also be separated into transverse and axial field. Substituting (5.44) into (A.5), the equation becomes

$$\left(\nabla_T^2 + \hat{a}_z \frac{\partial^2}{\partial z^2} \right) \left(\overline{E_T} e^{-\gamma_z z} + E_z e^{-\gamma_z z} \hat{a}_z \right) + \beta^2 \left(\overline{E_T} e^{-\gamma_z z} + E_z e^{-\gamma_z z} \hat{a}_z \right) = 0 \quad (5.54)$$

Expand (5.54) and separates the equation into transverse part and axial part, the equation becomes (5.55) and (5.56)

Transverse Helmholtz equation

$$\nabla_T^2 \overline{E_T} + (\beta^2 + \gamma_z^2) \overline{E_T} = 0 \quad (5.55)$$

Axial Helmholtz equation

$$\nabla_T^2 E_z + (\beta^2 + \gamma_z^2) E_z = 0 \quad (5.56)$$

Since the Papadopoulos' method includes both wave in lossy waveguide as well as lossless waveguide, a separate set of wave equation from (5.55) is required. One for a lossless waveguide, another for lossy waveguide. The lossless wave equation dot with

lossy field, and vice versa, resulting two sets of equation shown below. \overline{E}_T represents the electric field in lossy waveguide while \overline{E}_{Tn} represents the field in lossless waveguide.

Lossy wave equation dot with lossless field

$$\begin{aligned}\nabla_T^2 \overline{E}_T + (\beta^2 + \gamma_z^2) \overline{E}_T &= 0 \\ \overline{E}_{Tn} \cdot \nabla_T^2 \overline{E}_T + (\beta^2 + \gamma_z^2) \overline{E}_T \cdot \overline{E}_{Tn} &= 0\end{aligned}\quad (5.57)$$

Lossless wave equation dot with lossy field

$$\begin{aligned}\nabla_T^2 \overline{E}_{Tn} + (\beta^2 + \Gamma_z^2) \overline{E}_{Tn} &= 0 \\ \overline{E}_T \cdot \nabla_T^2 \overline{E}_{Tn} + (\beta^2 + \Gamma_z^2) \overline{E}_{Tn} \cdot \overline{E}_T &= 0\end{aligned}\quad (5.58)$$

Where Γ_z is the propagation constant of the field in lossless waveguide. Take the difference between the two equations(5.57) and (5.58)

$$(\gamma_z^2 - \Gamma_z^2) \overline{E}_T \cdot \overline{E}_{Tn} = \overline{E}_T \cdot \nabla_T^2 \overline{E}_{Tn} - \overline{E}_{Tn} \cdot \nabla_T^2 \overline{E}_T \quad (5.59)$$

Take the integral of (5.59) over the conductor cross sectional area, the equation becomes

$$(\gamma_z^2 - \Gamma_z^2) \iint_A \overline{E}_T \cdot \overline{E}_{Tn} dA = \iint_A (\overline{E}_T \cdot \nabla_T^2 \overline{E}_{Tn} - \overline{E}_{Tn} \cdot \nabla_T^2 \overline{E}_T) dA \quad (5.60)$$

The magnitude of the field is normalized using the orthogonal property of the field shown below

$$\iint_A e_{in} \cdot e_{im} \cdot da = \delta_{m,n}$$

Where

$$\delta_{m,n} = \begin{cases} 1 & \text{when } m = n \\ 0 & \text{when } m \neq n \end{cases}$$

The equation becomes

$$(\gamma_z^2 - \Gamma_z^2) a_n = \iint_A (\overline{E}_T \cdot \nabla_T^2 \overline{E}_{Tn} - \overline{E}_{Tn} \cdot \nabla_T^2 \overline{E}_T) dA \quad (5.62)$$

Apply Green's function(5.63) onto (5.62)

$$\iint_A [(\nabla^2 A) \cdot B - A \cdot (\nabla^2 B)] dA = \oint_C [(\hat{n} \times A) \cdot (\nabla \times B) + (\hat{n} \times \nabla \times A) \cdot B + \hat{n} \cdot A \nabla \cdot B - \hat{n} \cdot B \nabla \cdot A] d\ell \quad (5.63)$$

The equation becomes

$$(\gamma_z^2 - \Gamma_z^2) a_n = \oint_C [(\hat{n} \times \overline{E_{Tn}}) \cdot (\nabla_T \times \overline{E_T}) + (\hat{n} \times \nabla_T \times \overline{E_{Tn}}) \cdot \overline{E_T} + \hat{n} \cdot \overline{E_{Tn}} \nabla_T \cdot \overline{E_T} - \hat{n} \cdot \overline{E_T} \nabla_T \cdot \overline{E_{Tn}}] d\ell \quad (5.64)$$

Where, \hat{n} is the radially inward pointing unit vector and the integral is taken around the conductor wall perimeter.

Boundary condition for lossy waveguide

The section below shows the steps to obtain the boundary condition for a lossy waveguide based on the current density equation

$$E_{tan} = Z_m J e^{-\gamma_z z} \quad (5.65)$$

where Z_m is the surface impedance. J is the current density flowing in the metal conductor wall. E_{tan} is the tangential electric field with respect to the conductor wall and it can be separated into the \hat{a}_ϕ direction and \hat{a}_z direction. Therefore (5.65) can be decomposed into these two direction as shown below.

For \hat{a}_ϕ direction:

$$\begin{aligned} \hat{a}_\phi \cdot \overline{E_T} &= Z_m \hat{a}_\phi \cdot J_\phi \\ &= Z_m H_z \end{aligned} \quad (5.66)$$

Substitute (5.49) into (5.66), the equation becomes

$$\hat{a}_\phi \cdot \overline{E_T} = -\frac{Z_m}{j\omega\mu} \hat{a}_z \cdot \nabla_T \times \overline{E_T} \quad (5.67)$$

For \hat{a}_z direction:

$$E_z = Z_m J_z \cdot \hat{a}_z \quad (5.68)$$

Substitute (5.46) into (5.68)

$$\nabla_T \cdot \frac{\vec{E}_T}{\gamma} = Z_m J_z \cdot \hat{a}_z \quad (5.69)$$

Substitute (5.48) into the above equation, the equation now becomes

$$\nabla_T \cdot \vec{E}_T = \frac{Z_m}{j\omega\mu} \left(\hat{n} \cdot \nabla_T \times \nabla_T \times \vec{E}_T - \beta^2 \hat{n} \cdot \vec{E}_T \right) \quad (5.70)$$

Applying boundary condition for lossy and lossless field onto (5.64), the lossy waveguide boundary condition are obtained from (5.67) and (5.69)

$$\left. \begin{aligned} \hat{a}_\phi \cdot \vec{E}_{Tn} &= 0 \\ \hat{n} \cdot \vec{E}_{Tn} &= 0 = E_{zn} \\ \nabla_T \times \vec{E}_{Tn} &= 0 \end{aligned} \right\} \text{lossless waveguide boundary condition}$$

$$\left. \begin{aligned} \hat{a}_\phi \cdot \vec{E}_T &= -\frac{Z_m}{j\omega\mu} \hat{a}_z \cdot \nabla_T \times \vec{E}_T \\ \nabla_T \cdot \vec{E}_T &= \frac{Z_m}{j\omega\mu} \hat{n} \cdot \nabla_T \times \nabla_T \times \vec{E}_T - \beta^2 \hat{n} \cdot \vec{E}_T \end{aligned} \right\} \text{boundary condition for lossy waveguide}$$

The field equation becomes

$$\left(\gamma_z^2 - \Gamma_z^2 \right) a_n = -\frac{Z_m}{j\omega\mu} \oint_C \left[\left(\nabla_T \times \vec{E}_{Tn} \right) \cdot \left(\nabla_T \times \vec{E}_T \right) - \hat{n} \cdot \vec{E}_{Tn} \left(\hat{n} \cdot \nabla_T \times \nabla_T \times \vec{E}_T - \beta^2 \hat{n} \cdot \vec{E}_T \right) \right] d\ell \quad (5.71)$$

Papadopoulos' method postulates that a field in a lossy waveguide can be expressed as a linear combination of field in a lossless waveguide, where

$$\vec{E}_T = \sum_k^{TE, TM} a_k \vec{E}_{Tk} \quad (5.72)$$

Express the lossy field, \overline{E}_T as a linear combination of lossless field by substituting (5.72) into (5.71) and the equation becomes

$$(\gamma_z^2 - \Gamma_z^2) a_n = -\frac{Z_m}{j\omega\mu} \sum_k a_k \oint_C \left[(\nabla_T \times \overline{E}_{Tn}) \cdot (\nabla_T \times \overline{E}_{Tk}) - \hat{n} \cdot \overline{E}_{Tn} (\hat{n} \cdot \nabla_T \times \nabla_T \times \overline{E}_{Tk} - \beta^2 \hat{n} \cdot \overline{E}_{Tk}) \right] d\ell \quad (5.73)$$

This essentially becomes an eigenvalue problem where

$$\underbrace{(\gamma_z^2 - \Gamma_z^2)}_{\lambda} \underbrace{a_n}_E = -\frac{Z_m}{j\omega\mu} \sum_k \underbrace{a_k}_E \underbrace{\oint_C \left[(\nabla_T \times \overline{E}_{Tn}) \cdot (\nabla_T \times \overline{E}_{Tk}) - \hat{n} \cdot \overline{E}_{Tn} (\hat{n} \cdot \nabla_T \times \nabla_T \times \overline{E}_{Tk} - \beta^2 \hat{n} \cdot \overline{E}_{Tk}) \right] d\ell}_A \quad (5.74)$$

$\lambda E = AE$

For an eigenvalue problem

$$(\lambda I - A)E = 0 \quad (5.75)$$

The determinant of the matrix in (5.75) must vanish in order to have a trivial solution. By equating the determinant to zero, the equation becomes the characteristic polynomial of the matrix

$$|\lambda I - A| = 0 = P(\lambda_n) \quad (5.76)$$

Solving the characteristics polynomial gives n number of eigenvalue, indicating that n number of modes exist in the waveguide.

The equation (5.73) shows that there are an infinite number linear equation for the unknown coefficient a_n , leading to an infinite number of mode propagate in the waveguide. Calculation of such infinite linear equation would be impossible. Therefore a perturbation is made on the equation to ease the calculation. The perturbation made is shown below.

For $\gamma_z \neq \Gamma_z$, a_n is small since Z_m is small for a good conductor, therefore it can be ignored

For $\gamma_z = \Gamma_z$, a_n is not small and it cannot be ignored

When $\gamma_z = \Gamma_z$, it implies that all the field has the same propagation constant.

For the case when all the field has the same propagation constant, if $\vec{E}_{T_k} = \vec{E}_{T_n}$ the solution is trivial. Therefore, the electric field must be different, such that $\vec{E}_{T_k} \neq \vec{E}_{T_n}$ which only occurs for the degenerate mode where for a given cutoff frequency, both the TE and TM field has the same propagation constant. Since there are only two mode for a degenerate mode, i.e. TE and TM, the summation now only has two components. The summation can be expanded as shown below. The equation (5.73) is divided into 2 sets of equation

$$\begin{aligned}
 (\gamma_z^2 - \Gamma_z^2) a_1 = & - \frac{Z_m}{j\omega\mu} a_1 \oint_C \left[\underbrace{(\nabla_T \times \vec{E}_{T1}) \cdot (\nabla_T \times \vec{E}_{T1}) - \hat{n} \cdot \vec{E}_{T1} (\hat{n} \cdot \nabla_T \times \nabla_T \times \vec{E}_{T1} - \beta^2 \hat{n} \cdot \vec{E}_{T1})}_{\text{Due to } \vec{E}_{T1}} \right] d\ell \\
 & - \frac{Z_m}{j\omega\mu} a_2 \oint_C \left[\underbrace{(\nabla_T \times \vec{E}_{T1}) \cdot (\nabla_T \times \vec{E}_{T2}) - \hat{n} \cdot \vec{E}_{T1} (\hat{n} \cdot \nabla_T \times \nabla_T \times \vec{E}_{T2} - \beta^2 \hat{n} \cdot \vec{E}_{T2})}_{\text{Coupling of } \vec{E}_{T1} \text{ and } \vec{E}_{T2}} \right] d\ell
 \end{aligned} \quad (5.77)$$

and

$$\begin{aligned}
 (\gamma_z^2 - \Gamma_z^2) a_2 = & - \frac{Z_m}{j\omega\mu} a_1 \oint_C \left[\underbrace{(\nabla_T \times \vec{E}_{T2}) \cdot (\nabla_T \times \vec{E}_{T1}) - \hat{n} \cdot \vec{E}_{T2} (\hat{n} \cdot \nabla_T \times \nabla_T \times \vec{E}_{T1} - \beta^2 \hat{n} \cdot \vec{E}_{T1})}_{\text{Coupling of } \vec{E}_{T2} \text{ and } \vec{E}_{T1}} \right] d\ell \\
 & - \frac{Z_m}{j\omega\mu} a_2 \oint_C \left[\underbrace{(\nabla_T \times \vec{E}_{T2}) \cdot (\nabla_T \times \vec{E}_{T2}) - \hat{n} \cdot \vec{E}_{T2} (\hat{n} \cdot \nabla_T \times \nabla_T \times \vec{E}_{T2} - \beta^2 \hat{n} \cdot \vec{E}_{T2})}_{\text{Due to } \vec{E}_{T2}} \right] d\ell
 \end{aligned} \quad (5.78)$$

To obtain an equation describing the propagation constant for rectangular waveguide, let E_{T1} = TE field and E_{T2} = TM field, the transverse equation becomes

$$E_{T1} = \frac{j\omega\mu}{\beta_\rho^2} \left[\left(\frac{n\pi}{b} \right) \cos\left(\frac{m\pi x}{a} \right) \sin\left(\frac{n\pi y}{b} \right) \hat{a}_x - \left(\frac{m\pi}{a} \right) \sin\left(\frac{m\pi x}{a} \right) \cos\left(\frac{n\pi y}{b} \right) \hat{a}_y \right] \quad (5.79)$$

and

$$E_{T2} = \frac{-\gamma_z}{\beta_\rho^2} \left[\left(\frac{m\pi}{a} \right) \cos\left(\frac{m\pi x}{a} \right) \sin\left(\frac{n\pi y}{b} \right) \hat{a}_x + \left(\frac{n\pi}{b} \right) \sin\left(\frac{m\pi x}{a} \right) \cos\left(\frac{n\pi y}{b} \right) \hat{a}_y \right] \quad (5.80)$$

Substitute the field equation (5.79) and (5.80) into equation (5.77) and (5.78). Take the integral around the waveguide in x and y direction. The result would produce 2 sets of equation as shown below.

$$a_1 \left\{ \frac{(\gamma_z^2 + \beta_{zmn}^2) j \omega \mu}{Z_m} + \omega^2 \mu^2 (a+b) + \left(\frac{\omega \mu}{\beta_\rho} \right)^2 \left(\frac{\beta_{zmn}}{\beta_\rho} \right)^2 \left[\left(\frac{n\pi}{b} \right)^2 b + \left(\frac{m\pi}{a} \right)^2 a \right] \right\} \\ + a_2 \left\{ \left(-\frac{\omega \mu \beta^2 \beta_{zmn}}{\beta_\rho^4} \right) \left(\frac{mn\pi^2}{ab} \right) (b-a) \right\} = 0 \quad (5.81)$$

and

$$a_1 \left\{ -\frac{\omega \mu \beta_{zmn}}{\beta_\rho} \left(\frac{\beta_{zmn}}{\beta_\rho} \right)^2 \left(\frac{mn\pi^2}{ab} \right) (b-a) \right\} \\ + a_2 \left\{ \frac{(\gamma_z^2 + \beta_{zmn}^2) j \omega \mu}{Z_m} - \left(\frac{\beta \beta_{zmn}}{\beta_\rho^2} \right)^2 \left(\left(\frac{m\pi}{a} \right)^2 b + \left(\frac{n\pi}{b} \right)^2 a \right) \right\} = 0 \quad (5.82)$$

where γ_z is the propagation constant, β_{zmn} is the phase constant and it is equal to $\beta_{zmn} = \beta \sqrt{1 - \frac{f_c^2}{f^2}}$, $\beta = \omega \sqrt{\mu \epsilon}$, m and n is the propagating mode, and a , b is the length of the rectangular waveguide in x and y direction. Solving the above two linear equation (5.81) and (5.82) to obtain γ_z would produce the result shown in Figure 32 below

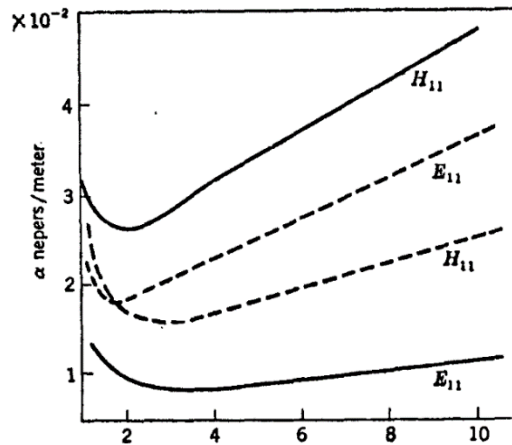


Figure 32 PPM and Power Loss Method Attenuation (Collin, 1960)

Solid line is the result for PPM and broken like is from the power loss Method. The above comparison shows that there are differences between the PPM and power loss method. This is due to PPM taking consideration of the coupling effect of TE and TM mode in the calculation.

5.4.2 A Review of the Power Loss Method

The concept of power loss method for rectangular waveguide is the same as that for circular waveguide in section 4.4.1. To develop the formulation for the propagation constant of a rectangular waveguide, the fields in the waveguide is substituted into (4.34)

Transverse Magnetic (TM) Mode

The first step is to obtain \mathcal{P}_{ave} . It can be obtained by substituting the TM field equation from (5.26) to (5.31) into (4.36) which will result in the following

$$\mathcal{P}_{ave} \cdot \hat{a}_z = \frac{\omega\epsilon\beta}{2h^4} E_0^2 \left[\left(\frac{m\pi}{a} \right)^2 \cos^2 \left(\frac{m\pi x}{a} \right) \sin^2 \left(\frac{n\pi y}{b} \right) + \left(\frac{n\pi}{b} \right)^2 \sin^2 \left(\frac{m\pi x}{a} \right) \cos^2 \left(\frac{n\pi y}{b} \right) \right] \quad (5.83)$$

Next, P_z can be found by substituting (5.83) into (4.35) which gives the following

$$P_z = \frac{\omega\epsilon\beta E_0^2 ab}{8 \left(\left[\frac{m\pi}{a} \right]^2 + \left[\frac{n\pi}{b} \right]^2 \right)} \quad (5.84)$$

The current density can be found as follow

$$\begin{aligned} J_{s(x=0)} = J_{s(x=a)} &= \hat{a}_z \cdot \left[-\frac{j\omega\epsilon}{h^2} E_0 \left(\frac{m\pi}{a} \right) \sin \left(\frac{n\pi y}{b} \right) \right] \\ J_{s(y=0)} = J_{s(y=b)} &= \hat{a}_z \cdot \left[-\frac{j\omega\epsilon}{h^2} E_0 \left(\frac{n\pi}{b} \right) \sin \left(\frac{m\pi x}{a} \right) \right] \end{aligned} \quad (5.85)$$

Substituting the current density equation into (4.38) to obtain the power loss for each wall in the x and y direction as follow

$$P_{c(x=0)} = \frac{1}{2} \left(\frac{\omega\epsilon}{h^2} \right)^2 \left(\frac{m\pi}{a} \right)^2 E_0^2 R_s \left(\frac{b}{2} \right) \quad (5.86)$$

$$P_{c(y=0)} = \frac{1}{2} \left(\frac{\omega\epsilon}{h^2} \right)^2 \left(\frac{n\pi}{b} \right)^2 E_0^2 R_s \left(\frac{a}{2} \right) \quad (5.87)$$

The total power loss can be obtained by adding the power loss in all the wall as shown below

$$\begin{aligned} P_c &= 2 \left[P_{L(x=0)} \right] + 2 \left[P_{L(y=0)} \right] \\ &= \left(\frac{\omega\epsilon}{h^2} \right)^2 E_0^2 R_s \left(\frac{\pi^2}{2} \right) \left[\frac{m^2 b}{a^2} + \frac{n^2 a}{b^2} \right] \end{aligned} \quad (5.88)$$

The attenuation can be obtained by substituting (5.88) and (5.84) into (4.34) and with some simplification, it will result in the following equation

$$\alpha_c = \frac{2R_s (m^2 b^3 + n^2 a^3)}{\eta ab \sqrt{1 - \left(\frac{f_c}{f} \right)^2} (m^2 b^2 + n^2 a^2)} \quad (5.89)$$

where,

$$\eta = \sqrt{\frac{\mu}{\epsilon}} \quad (5.90)$$

Transverse Electric (TE) Mode

A similar approach is used to find the attenuation constant for TE mode. The average power can be found as follow

$$\mathcal{P}_{ave} \cdot \hat{a}_z = \frac{\omega\mu\beta}{2h^4} H_0^2 \left[\left(\frac{n\pi}{b} \right)^2 \cos^2 \left(\frac{m\pi x}{a} \right) \sin^2 \left(\frac{n\pi y}{b} \right) + \left(\frac{m\pi}{a} \right)^2 \sin^2 \left(\frac{m\pi x}{a} \right) \cos^2 \left(\frac{n\pi y}{b} \right) \right] \quad (5.91)$$

The total power can be then be obtained as follow

$$P_z = \frac{\omega\mu\beta}{8h^2} H_0^2 ab \quad (5.92)$$

The total power loss is as shown below

$$P_c = R_s H_0^2 \left[\frac{a}{2} + \frac{b}{2} + \frac{\beta^2}{2h^4} \left\{ \frac{(m\pi)^2}{a} + \frac{(n\pi)^2}{b} \right\} \right] \quad (5.93)$$

The attenuation constant for TE mode can be showed as follow

$$\alpha_c = \frac{2R_s}{\beta\eta\sqrt{1-\left(\frac{f_c}{f}\right)^2}} \cdot \left\{ \left(1+\frac{b}{a}\right)\left(\frac{f_c}{f}\right)^2 + \frac{b}{a} \left[1-\left(\frac{f_c}{f}\right)^2\right] \cdot \left[\frac{m^2ab+(na)^2}{(mb)^2+(na)^2} \right] \right\} \quad (5.94)$$

5.4.3 A Review of Yeap's Method

The longitudinal field is first obtained. However, the field equations derived in Section 5.2 were assumed to be those in a lossless waveguide. To impose the criterion of good conductor wall with high but finite conductivity, a correction factor, ϕ is introduced into the longitudinal field equation as shown below. Due to the non-perfect conductor condition, neither E_z nor H_z is zero.

$$E_z = E_0 \sin(k_x x + \phi_x) \sin(k_y y + \phi_y) \quad (5.95)$$

$$H_z = H_0 \cos(k_x x + \phi_x) \cos(k_y y + \phi_y) \quad (5.96)$$

The tangential field has to be maximum at half the length of x and y wall.

$$\sin\left(\frac{k_x a}{2} + \phi_x\right) = \sin\left(\frac{k_y b}{2} + \phi_y\right) = \pm 1 \text{ or } 0 \quad (5.97)$$

Imposing the condition above, the correction fact can be obtained as follow

$$\phi_x = \frac{m\pi - k_x a}{2} \quad (5.98)$$

$$\phi_y = \frac{n\pi - k_y b}{2} \quad (5.99)$$

Substituting the longitudinal field equation into (5.95) and (5.96) into (5.14) to (5.17), the following tangential field equations are obtained.

$$H_x = -\frac{j}{h^2} (j\gamma k_x H_0 - \omega\epsilon_0 k_y E_0) \sin(k_x x + \phi_x) \cos(k_y y + \phi_y) \quad (5.100)$$

$$H_y = -\frac{j}{h^2} [j\gamma k_y H_0 + \omega\epsilon_0 k_x E_0] \cos(k_x x + \phi_x) \sin(k_y y + \phi_y) \quad (5.101)$$

$$E_x = \frac{j}{h^2} [j\gamma k_x E_0 + \omega\mu_0 k_y H_0] \cos(k_x x + \phi_x) \sin(k_y y + \phi_y) \quad (5.102)$$

$$E_y = \frac{j}{h^2} [j\gamma k_y E_0 - \omega\mu_0 k_x H_0] \sin(k_x x + \phi_x) \cos(k_y y + \phi_y) \quad (5.103)$$

Using the relation of (4.82), the following relation in the Cartesian coordinates is obtained.

$$\frac{E_z}{H_x} = -\frac{E_x}{H_z} = \sqrt{\frac{\mu_c}{\epsilon_c}} \quad (5.104)$$

Substituting the field equation into (5.104), the following equations are obtained

$$-\frac{E_x}{H_z} = -\frac{j}{h^2} \left(j \frac{E_0}{H_0} \gamma k_x + \omega\mu_0 k_y \right) \tan(k_y b + \phi_y) = \sqrt{\frac{\mu_c}{\epsilon_c}} \quad (5.105)$$

$$\frac{H_x}{E_z} = -\frac{j}{h^2} \left(j \frac{H_0}{E_0} \gamma k_x - \omega\epsilon_0 k_y \right) \cot(k_y b + \phi_y) = \sqrt{\frac{\epsilon_c}{\mu_c}} \quad (5.106)$$

$$\frac{E_y}{H_z} = \frac{j}{h^2} \left(j \frac{E_0}{H_0} \gamma k_y - \omega\mu_0 k_x \right) \tan(k_x a + \phi_x) = \sqrt{\frac{\mu_c}{\epsilon_c}} \quad (5.107)$$

$$-\frac{H_y}{E_z} = \frac{j}{h^2} \left(j \frac{H_0}{E_0} \gamma k_y + \omega\epsilon_0 k_x \right) \cot(k_x a + \phi_x) = \sqrt{\frac{\epsilon_c}{\mu_c}} \quad (5.108)$$

Rearranging the equation (5.105) and (5.106), the following equations are obtained

$$\left(\frac{\gamma k_x \tan(k_y b + \phi_y)}{h^2} \right) E_0 + \left(-\frac{j\omega\mu_0 k_y \tan(k_y b + \phi_y)}{h^2} - \sqrt{\frac{\mu_c}{\epsilon_c}} \right) H_0 = 0 \quad (5.109)$$

$$\left(\frac{\gamma k_x \cot(k_y b + \phi_y)}{h^2} \right) H_0 + \left(\frac{j\omega\epsilon_0 k_y \cot(k_y b + \phi_y)}{h^2} - \sqrt{\frac{\epsilon_c}{\mu_c}} \right) E_0 = 0 \quad (5.110)$$

Rearranging the equation above into matrix form, (5.111) is obtained

$$\begin{bmatrix} \left(\frac{\gamma k_x \tan(k_y b + \phi_y)}{h^2} \right) & \left(-\frac{j\omega\mu_0 k_y \tan(k_y b + \phi_y)}{h^2} - \sqrt{\frac{\mu_c}{\epsilon_c}} \right) \\ \left(\frac{j\omega\epsilon_0 k_y \cot(k_y b + \phi_y)}{h^2} - \sqrt{\frac{\epsilon_c}{\mu_c}} \right) & \left(\frac{\gamma k_x \cot(k_y b + \phi_y)}{h^2} \right) \end{bmatrix} \begin{bmatrix} E_0 \\ H_0 \end{bmatrix} = 0 \quad (5.111)$$

Similarly, rearranging the equation (5.107) and (5.108), the following equations are obtained

$$\left(-\frac{\gamma k_y \tan(k_x a + \phi_x)}{h^2} \right) E_0 + \left(-\frac{j\omega\mu_0 k_x \tan(k_x a + \phi_x)}{h^2} - \sqrt{\frac{\mu_c}{\epsilon_c}} \right) H_0 = 0 \quad (5.112)$$

$$\left(-\frac{\gamma k_y \cot(k_x a + \phi_x)}{h^2} \right) H_0 + \left(\frac{j\omega\epsilon_0 k_x \cot(k_x a + \phi_x)}{h^2} - \sqrt{\frac{\epsilon_c}{\mu_c}} \right) E_0 = 0 \quad (5.113)$$

Rearranging the above equation into matrix form, (5.114) is obtained

$$\begin{bmatrix} \left(-\frac{\gamma k_y \tan(k_x a + \phi_x)}{h^2} \right) & \left(-\frac{j\omega\mu_0 k_x \tan(k_x a + \phi_x)}{h^2} - \sqrt{\frac{\mu_c}{\epsilon_c}} \right) \\ \left(\frac{j\omega\epsilon_0 k_x \cot(k_x a + \phi_x)}{h^2} - \sqrt{\frac{\epsilon_c}{\mu_c}} \right) & \left(-\frac{\gamma k_y \cot(k_x a + \phi_x)}{h^2} \right) \end{bmatrix} \begin{bmatrix} E_0 \\ H_0 \end{bmatrix} = 0 \quad (5.114)$$

To obtain a non-trivial solution, the determinant of the matrix must vanish. Hence the following equations are obtained from (5.111) and (5.114) which is the transcendental equation in the y and x direction respectively

$$\left[\sqrt{\frac{\mu_c}{\epsilon_c}} + \frac{j\omega\mu_0 k_y \tan(k_y b + \phi_y)}{h^2} \right] \left[\sqrt{\frac{\epsilon_c}{\mu_c}} - \frac{j\omega\epsilon_0 k_y \cot(k_y b + \phi_y)}{h^2} \right] = \left[\frac{\gamma k_x}{h^2} \right]^2 \quad (5.115)$$

$$\left[\sqrt{\frac{\mu_c}{\epsilon_c}} + \frac{j\omega\mu_0 k_x \tan(k_x a + \phi_x)}{h^2} \right] \left[\sqrt{\frac{\epsilon_c}{\mu_c}} - \frac{j\omega\epsilon_0 k_x \cot(k_x a + \phi_x)}{h^2} \right] = \left[\frac{\gamma k_y}{h^2} \right]^2 \quad (5.116)$$

TE₁₀

For TE₁₀ mode, the equations can be simplified by substituting, $m=1$. $n=1$ into the penetration factor. The following expression is obtained for TE₁₀

$$\left[\sqrt{\frac{\mu_c}{\epsilon_c}} + \frac{j\omega\mu_0 k_y \tan\left(k_y \frac{b}{2}\right)}{h^2} \right] \left[\sqrt{\frac{\epsilon_c}{\mu_c}} - \frac{j\omega\epsilon_0 k_y \cot\left(k_y \frac{b}{2}\right)}{h^2} \right] = \left[\frac{\gamma k_x}{h^2} \right]^2 \quad (5.117)$$

$$\left[\sqrt{\frac{\mu_c}{\epsilon_c}} - \frac{j\omega\mu_0 k_x \cot\left(k_x \frac{a}{2}\right)}{h^2} \right] \left[\sqrt{\frac{\epsilon_c}{\mu_c}} + \frac{j\omega\epsilon_0 k_x \tan\left(k_x \frac{a}{2}\right)}{h^2} \right] = \left[\frac{\gamma k_y}{h^2} \right]^2 \quad (5.118)$$

TE₁₁ and TM₁₁ Mode

For TE₁₁ and TM₁₁ mode, by substituting $m=1$ $n=1$ into the penetration factor the following equations are obtained. In such case, both the mode result in a pair of identical equation. Hence, such equation has the ability to include the effect of degenerate mode into the calculation of the attenuation constant. To compute the value for each mode, the initial guesses for the root searching algorithm has to be varied slightly so that the algorithm can converge into two different root, which gives the TE and TM mode.

$$\left[\sqrt{\frac{\mu_c}{\epsilon_c}} - \frac{j\omega\mu_0 k_y \cot\left(k_y \frac{b}{2}\right)}{h^2} \right] \left[\sqrt{\frac{\epsilon_c}{\mu_c}} + \frac{j\omega\epsilon_0 k_y \tan\left(k_y \frac{b}{2}\right)}{h^2} \right] = \left[\frac{\gamma k_x}{h^2} \right]^2 \quad (5.119)$$

$$\left[\sqrt{\frac{\mu_c}{\epsilon_c}} - \frac{j\omega\mu_0 k_x \cot\left(k_x \frac{a}{2}\right)}{h^2} \right] \left[\sqrt{\frac{\epsilon_c}{\mu_c}} + \frac{j\omega\epsilon_0 k_x \tan\left(k_x \frac{a}{2}\right)}{h^2} \right] = \left[\frac{\gamma k_y}{h^2} \right]^2 \quad (5.120)$$

5.5 The New Method

The new method derivations is similar to those presented in the circular waveguide. It uses the FDM to approximate a function, hence to simplify the transcendental equation into closed form solution.

5.5.1 TE₁₁ Mode

To obtain the closed form solution, first expand (5.119), which gives the following equation

$$1 + \frac{j\omega k_y}{h^2} \left[\epsilon_0 \sqrt{\frac{\mu_c}{\epsilon_c}} \tan\left(k_y \frac{b}{2}\right) - \mu_0 \sqrt{\frac{\epsilon_c}{\mu_c}} \cot\left(k_y \frac{b}{2}\right) \right] + \frac{\omega^2 \mu_0 \epsilon_0 k_y^2}{h^4} = \left[\frac{\gamma^2 k_x^2}{h^4} \right] \quad (5.121)$$

With some simplification and make use of the dispersion relation (5.7), (5.122) can be obtained.

$$\begin{aligned} \left[\epsilon_0 \sqrt{\frac{\mu_c}{\epsilon_c}} \tan\left(k_y \frac{b}{2}\right) - \mu_0 \sqrt{\frac{\epsilon_c}{\mu_c}} \cot\left(k_y \frac{b}{2}\right) \right] &= \frac{h^2}{j\omega k_y} \left[\frac{\gamma^2 k_x^2 - k_0^2 k_y^2 - h^4}{h^4} \right] \\ &= \frac{h^2}{j\omega k_y} \left[\frac{-k_0^2 k_x^2 + h^2 k_x^2 - k_0^2 k_y^2 - h^4}{h^4} \right] \\ &= \left[\frac{-k_0^2 - k_y^2}{j\omega k_y} \right] \end{aligned} \quad (5.122)$$

A perfect conductor will have $k_y \frac{b}{2} = \frac{\pi}{2}$. This gives an infinity to the tangent function.

To remove the singularity, substitution for the tangent function is required. Hence, the following assumption is made

For TE mode, $E_0 = 0$, hence from (5.109), it can be simplified as below.

$$-\frac{E_x}{H_z} = \left(-\frac{j\omega\mu_0 k_y \tan(k_y b + \phi_y)}{h^2} - \sqrt{\frac{\mu_c}{\epsilon_c}} \right) H_0 = 0 \quad (5.123)$$

Since, $H_0 \neq 0$, this implies that the term inside the H_0 have to be zero

$$-\frac{j\omega\mu_0 k_y \tan(k_y b + \phi_y)}{h^2} - \sqrt{\frac{\mu_c}{\epsilon_c}} = 0 \quad (5.124)$$

Rearranging the equation in (5.124), the following is obtained

$$\tan\left(k_y \frac{b}{2}\right) = \frac{j\omega\mu_0 k_y}{h^2} \sqrt{\frac{\epsilon_c \mu_c}{\mu_c}} \quad (5.125)$$

Substituting (5.125) into (5.122) and rearranging the equation, (5.126) can be obtained

$$\cot\left(k_y \frac{b}{2}\right) = \frac{1}{\mu_0} \left[\frac{k_0^2 + k_y^2}{j\omega k_y} + \frac{j\omega\epsilon_0\mu_0 k_y}{h^2} \right] \sqrt{\frac{\mu_c}{\epsilon_c}} \quad (5.126)$$

With the assumption that for a good conductor with finite conductivity, it can be assumed that the wave number is very close to those of perfect conductor with infinite conductivity. Hence, the wave number can be assumed as a small perturbation term added to the wave number of perfect conductor as shown below, where k_{y-p} is the wave number of perfect conductor in the y direction.

$$k_y = k_{y-p} + \delta_y \quad \text{where} \quad k_{y-p} = \frac{n\pi}{b} \quad (5.127)$$

Substituting (5.127) into the cotangent function, (5.128) can be obtained

$$\cot\left(k_y \frac{b}{2}\right) = \cot\left((k_{y-p} + \delta_y) \frac{b}{2}\right) = \cot\left(k_{y-p} \frac{b}{2} + \delta_y \frac{b}{2}\right) = \cot\left(k_{y-p} \frac{b}{2} + \Delta y\right) \quad (5.128)$$

Using the FDM, the following relation in (5.129) can be obtained.

$$\cot'\left(k_{y-p} \frac{b}{2}\right) = \frac{\cot\left(k_{y-p} \frac{b}{2} + \Delta y\right) - \cot\left(k_{y-p} \frac{b}{2}\right)}{\Delta y} \quad (5.129)$$

Noting that $\cot\left(k_{y-p} \frac{b}{2}\right) = 0$, it can be further simplified results in (5.130).

$$\begin{aligned} \cot\left(k_{y-p} \frac{b}{2} + \Delta y\right) &= \cot'\left(k_{y-p} \frac{b}{2}\right) \Delta y \\ &= -\frac{\Delta y}{\sin^2\left(k_{y-p} \frac{b}{2}\right)} \end{aligned} \quad (5.130)$$

Substituting the equation (5.130) back to (5.126) and rearranging the equation, the following can be obtained. Note that $\Delta y = \delta_y \frac{b}{2}$ from (5.128)

$$\delta_y = -\frac{2}{b\mu_0} \left[\frac{k_0^2 + k_{y-p}^2}{j\omega k_{y-p}} + \frac{j\omega\epsilon_0\mu_0 k_{y-p}}{h^2} \right] \left[\sin^2\left(k_{y-p} \frac{b}{2}\right) \right] \sqrt{\frac{\mu_c}{\epsilon_c}} \quad (5.131)$$

δ_y is the small perturbation term. To obtain the wave number, the perturbation term is added to the wave number of perfect conductor as shown in (5.127). Similar steps can be used to obtain the wavenumber for x direction. The perturbation term for x direction is shown below

$$\delta_x = -\frac{2}{a\mu_0} \left[\frac{k_0^2 + k_{x-p}^2}{j\omega k_{x-p}} + \frac{j\omega\epsilon_0\mu_0 k_{x-p}}{h^2} \right] \left[\sin^2 \left(k_{x-p} \frac{a}{2} \right) \right] \sqrt{\frac{\mu_c}{\epsilon_c}} \quad (5.132)$$

To obtain the propagation constant, substitute the wavenumber in x and y direction into the dispersion relation in (5.7)

5.5.2 TM₁₁ Mode

For TM mode, $H_z = 0$, hence the equation (5.113) can be reduced to the following

$$-\frac{H_y}{E_z} = \left(\frac{j\omega\epsilon_0 k_x \cot(k_x a + \phi_x)}{h^2} - \sqrt{\frac{\epsilon_c}{\mu_c}} \right) E_0 = 0 \quad (5.133)$$

Since $E_0 \neq 0$, the term inside E_0 have to be zero which give the following equation after some simplification

$$\tan \left(k_y \frac{b}{2} \right) = -\frac{h^2}{j\omega\epsilon_0 k_y} \sqrt{\frac{\epsilon_c}{\mu_c}} \quad (5.134)$$

Substituting (5.134) into (5.122) the following equation is obtained

$$\cot \left(k_y \frac{b}{2} \right) = \frac{1}{\mu_0} \left[\frac{k_0^2 + k_y^2}{j\omega k_y} - \frac{h^2}{j\omega k_y} \right] \sqrt{\frac{\mu_c}{\epsilon_c}} \quad (5.135)$$

Using the FDM from (5.130), (5.136) is obtained

$$\cot \left(k_y \frac{b}{2} \right) = \cot \left(k_{y-p} \frac{b}{2} + \Delta y \right) = -\frac{\Delta y}{\sin^2 \left(k_{y-p} \frac{b}{2} \right)} = \frac{1}{\mu_0} \left[\frac{k_0^2 + k_y^2}{j\omega k_y} - \frac{h^2}{j\omega k_y} \right] \sqrt{\frac{\mu_c}{\epsilon_c}} \quad (5.136)$$

Hence the perturbation term for TM₁₁ mode is shown below

$$\delta_y = -\frac{2}{b\mu_0} \left[\frac{k_0^2 + k_{y-p}^2}{j\omega k_{y-p}} - \frac{h^2}{j\omega k_{y-p}} \right] \left[\sin^2 \left(k_{y-p} \frac{b}{2} \right) \right] \sqrt{\frac{\mu_c}{\epsilon_c}} \quad (5.137)$$

$$\delta_x = -\frac{2}{a\mu_0} \left[\frac{k_0^2 + k_{x-p}^2}{j\omega k_{x-p}} - \frac{h^2}{j\omega k_{x-p}} \right] \left[\sin^2 \left(k_{x-p} \frac{a}{2} \right) \right] \sqrt{\frac{\mu_c}{\epsilon_c}} \quad (5.138)$$

5.5.3 TE₁₀ Mode

Due to the singularity exist in (5.122) when $k_{y-p} = 0$, an alternate steps is required to remove the singularity. To derive TE₁₀ mode, expand (5.117) will give the following

$$\epsilon_0 \sqrt{\frac{\mu_c}{\epsilon_c}} \tan \left(k_y \frac{b}{2} \right) - \mu_0 \sqrt{\frac{\epsilon_c}{\mu_c}} \cot \left(k_y \frac{b}{2} \right) = - \left[\frac{k_0^2 + k_y^2}{j\omega k_y} \right] \quad (5.139)$$

Take the inverse of the equation (5.139) to remove the singularity gives the following.

$$\frac{1}{\epsilon_0 \sqrt{\frac{\mu_c}{\epsilon_c}} \tan \left(k_y \frac{b}{2} \right) - \mu_0 \sqrt{\frac{\epsilon_c}{\mu_c}} \cot \left(k_y \frac{b}{2} \right)} = - \left[\frac{j\omega k_y}{k_0^2 + k_y^2} \right] \quad (5.140)$$

Multiply the equation with the conjugate and with some simplification, the equation then becomes as follow

$$\frac{\epsilon_0 \sqrt{\frac{\mu_c}{\epsilon_c}} \tan \left(k_y \frac{b}{2} \right) + \mu_0 \sqrt{\frac{\epsilon_c}{\mu_c}} \cot \left(k_y \frac{b}{2} \right)}{\frac{\mu_0^2 \epsilon_c}{\mu_c} \tan^2 \left(k_y \frac{b}{2} \right) - \frac{\epsilon_0^2 \mu_c}{\epsilon_c} \cot^2 \left(k_y \frac{b}{2} \right)} = - \left[\frac{j\omega k_y}{k_0^2 + k_y^2} \right] \quad (5.141)$$

From (5.124) the following is obtained

$$\cot \left(k_y \frac{b}{2} \right) = - \frac{j\omega \mu_0 k_y}{h^2} \sqrt{\frac{\epsilon_c}{\mu_c}} \quad (5.142)$$

Substitute (5.142) into (5.141), (5.143) is obtained

$$\frac{\epsilon_0 \sqrt{\frac{\mu_c}{\epsilon_c}} \tan\left(k_{y-p} \frac{b}{2}\right) - \mu_0 \sqrt{\frac{\epsilon_c}{\mu_c}} \frac{j\omega\mu_0 k_{y-p}}{h^2} \sqrt{\frac{\epsilon_c}{\mu_c}}}{\frac{\mu_0^2 \epsilon_c}{\mu_c} \tan^2\left(k_{y-p} \frac{b}{2}\right) + \frac{\epsilon_0^2 \mu_c}{\epsilon_c} \frac{j\omega\mu_0 k_{y-p}}{h^2} \sqrt{\frac{\epsilon_c}{\mu_c}}} = - \left[\frac{j\omega k_{y-p}}{k_0^2 + k_{y-p}^2} \right] \quad (5.143)$$

Substituting $k_{y-p} = 0$ into (5.143), the following result is obtained for the wavenumber in y direction

$$\delta_y = 0 \quad (5.144)$$

For the x direction, the perturbation term is shown below

$$\delta_x = -\frac{2}{a\mu_0} \left[\frac{k_0^2 + k_{x-p}^2}{j\omega k_{x-p}} + \frac{j\omega\epsilon_0\mu_0 k_{x-p}}{h^2} \right] \left[\sin^2\left(k_{x-p} \frac{a}{2}\right) \right] \sqrt{\frac{\mu_c}{\epsilon_c}} \quad (5.145)$$

5.6 Results and Discussion

Figure 33 shows the comparison among the experimental result, the power loss method, PPM, Yeap's method and the new method. From the result it can be seen that except the power loss method, all the other method agrees with the experimental result. The attenuation increases exponentially as the frequency decreases from the cutoff frequency. The power loss method on the other hand has its attenuation diverges to infinity at the cutoff frequency. All the other methods have very close result, in fact it is indistinguishable from the graph. There are slight differences between the experimental result and the theoretical value. These small discrepancies might be due error from the standing wave. In deriving the theoretical equation, a waveguide with infinite length is assumed. However this cannot be done in the experiment. A finite length waveguide will result in standing wave, which will cause an inaccurate measurement.

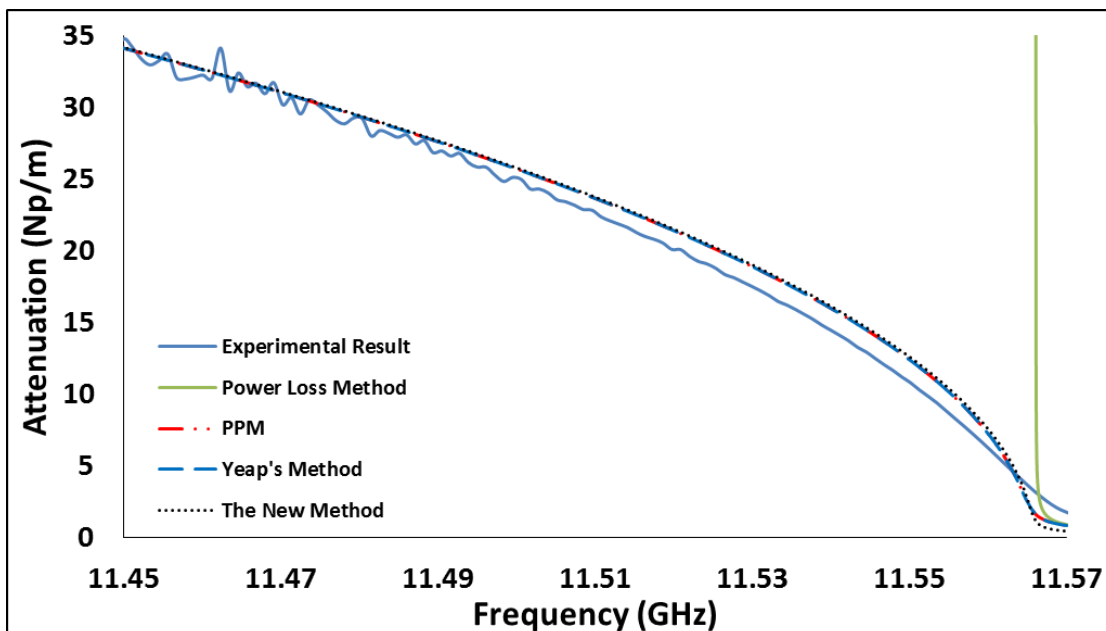


Figure 33 Attenuation of TE_{10} Mode in a Hollow Rectangular Waveguide with Width $a = 1.30$ cm, Height, $b = 0.64$ cm

Figure 34 shows the attenuation of both TE_{11} and TM_{11} . Both these modes have the same cutoff frequency. TE_{11} attenuation is slightly larger than the TM_{11} mode which can be seen from the Yeap's method. The new method agrees with the result

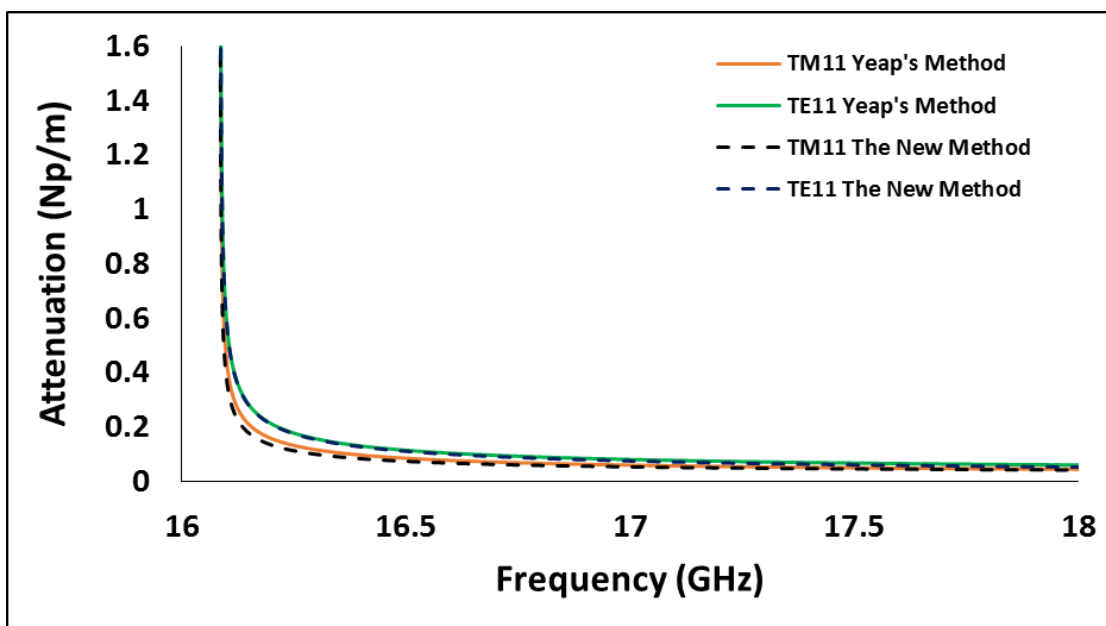


Figure 34 Attenuation of TE_{11} and TM_{11} in a Hollow Rectangular Waveguide with Width $a = 2.29$ cm, Height, $b = 1.02$ cm

Figure 35 and Figure 36 shows the comparison of power loss method, PPM, Yeap's method and the new method, focusing on the propagating region. From the result it can be seen that, all the method are very close to each other. This shows that the new method agrees with the existing theory.

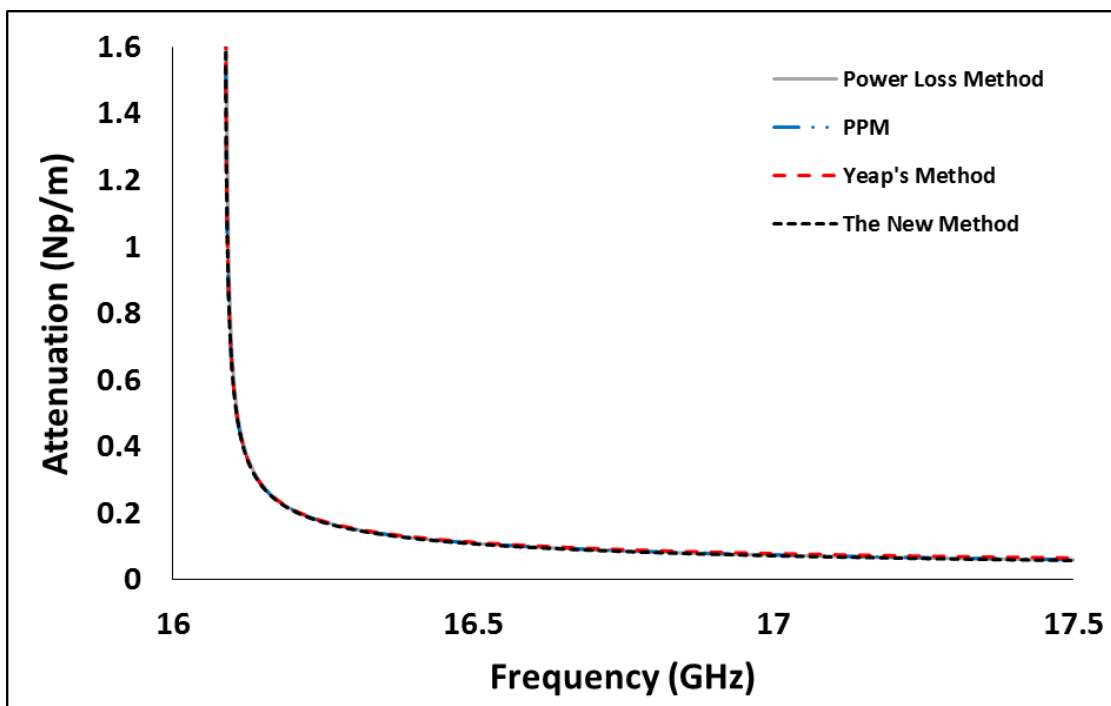


Figure 35 Attenuation of TE_{11} after cutoff in a Hollow Rectangular Waveguide with Width $a = 2.29$ cm, Height, $b = 1.02$ cm

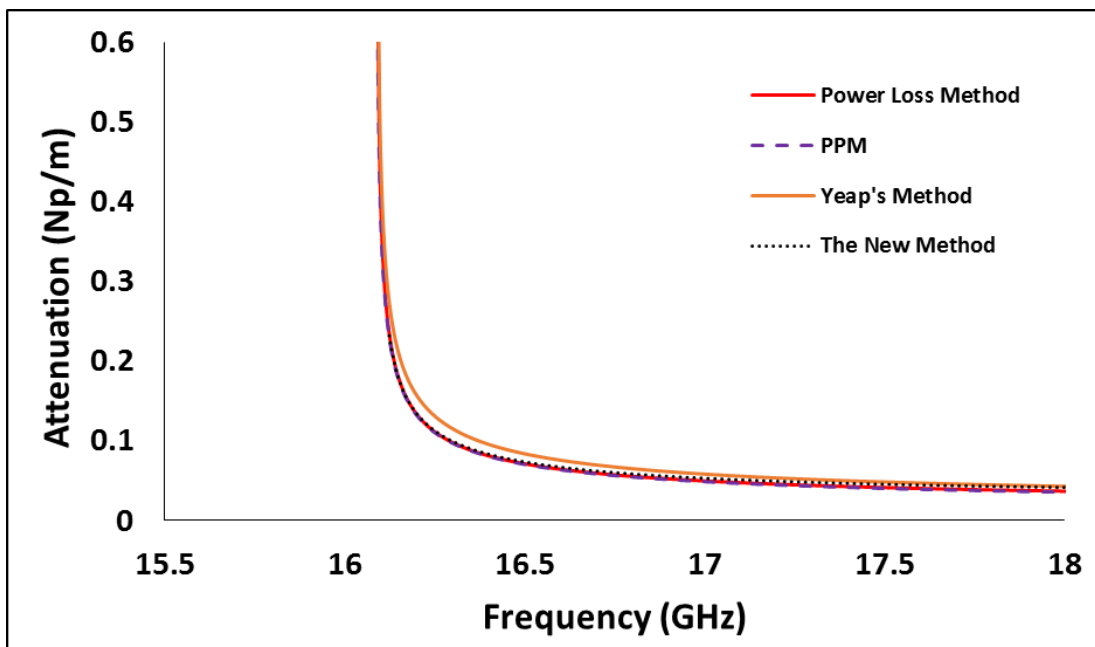


Figure 36 Attenuation of TM_{11} after cutoff in a Hollow Rectangular Waveguide with Width $a = 2.29$ cm, Height, $b = 1.02$ cm

Figure 37 shows the result from power loss method, Yeap's method and the new method. From the result, it can be seen that the new method gave a lower attenuation compared to the power loss and the Yeap's method for TE_{10} mode.

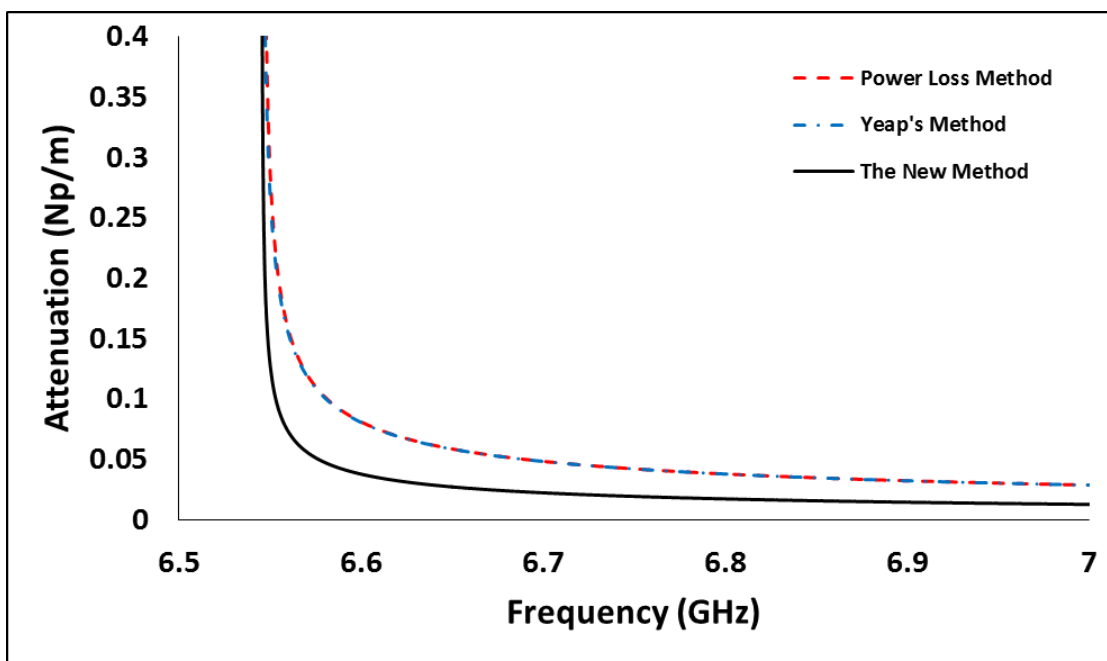


Figure 37 Attenuation of TE_{10} in a Hollow Rectangular Waveguide with Width $a = 2.29$ cm, Height, $b = 1.02$ cm

From the derivation of the new method for TE₁₀ mode, the wave number for the y direction is zero. The reason that it gave a zero value is from the fundamental idea in deriving the new method. The tangential field equation is given by

$$\sin\left(\frac{m\pi x}{a}\right)\sin\left(\frac{n\pi y}{b}\right) \quad (5.146)$$

or

$$\cos\left(\frac{m\pi x}{a}\right)\cos\left(\frac{n\pi y}{b}\right) \quad (5.147)$$

The equation shows that the tangential field is a sinusoidal wave. From the diagram below, it can be seen that due to the finite conductivity of the metal, there are phase difference between the transverse wave due to the lossy conductor and the perfect conductor. The idea behind the new method is that the wavenumber is the summation of a perfect conductor and phase difference.

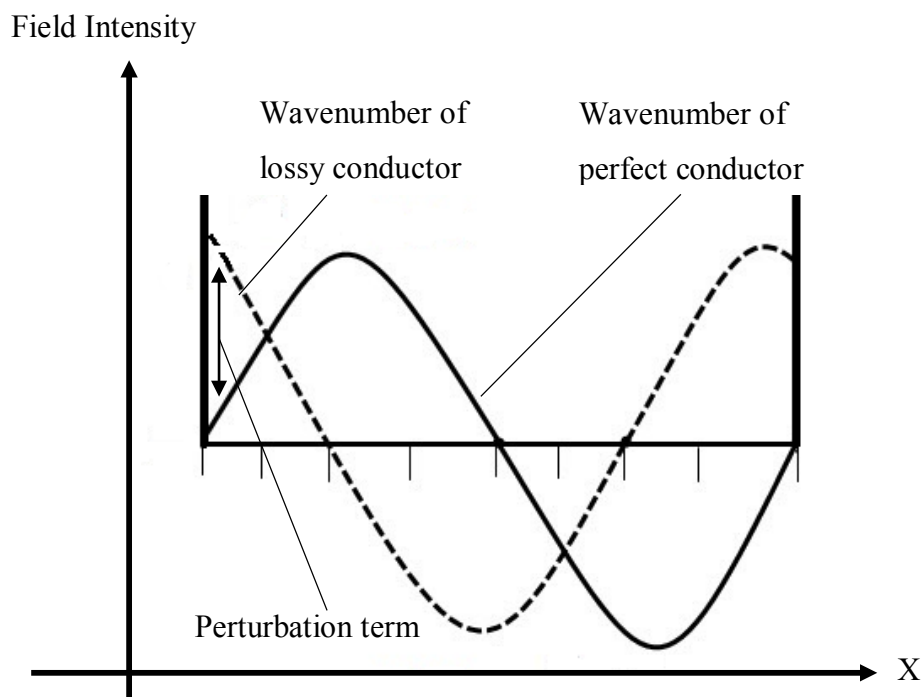


Figure 38 Tangential Field in a Waveguide

However, for TE₁₀ mode, the wavenumber for the perfect conductor in the y direction is zero. Hence, there are no sine wave in the y direction of the waveguide. As there are no sine wave, there are no phase difference in the y direction between the wave due to the lossy conductor and those of perfect conductor. Hence k_y is zero. However, this is not true. There are still losses contributed by k_y . This causes the inaccuracy from the new method

Figure 39, Figure 40 and Figure 41 shows the attenuation of TE₁₁, TM₁₁ and TE₁₀ mode around the cutoff frequency. From the result it can be seen that the new method is in close agreement with the Yeap's method and PPM. The power loss method on the other hand diverge to infinity at the cutoff frequency.

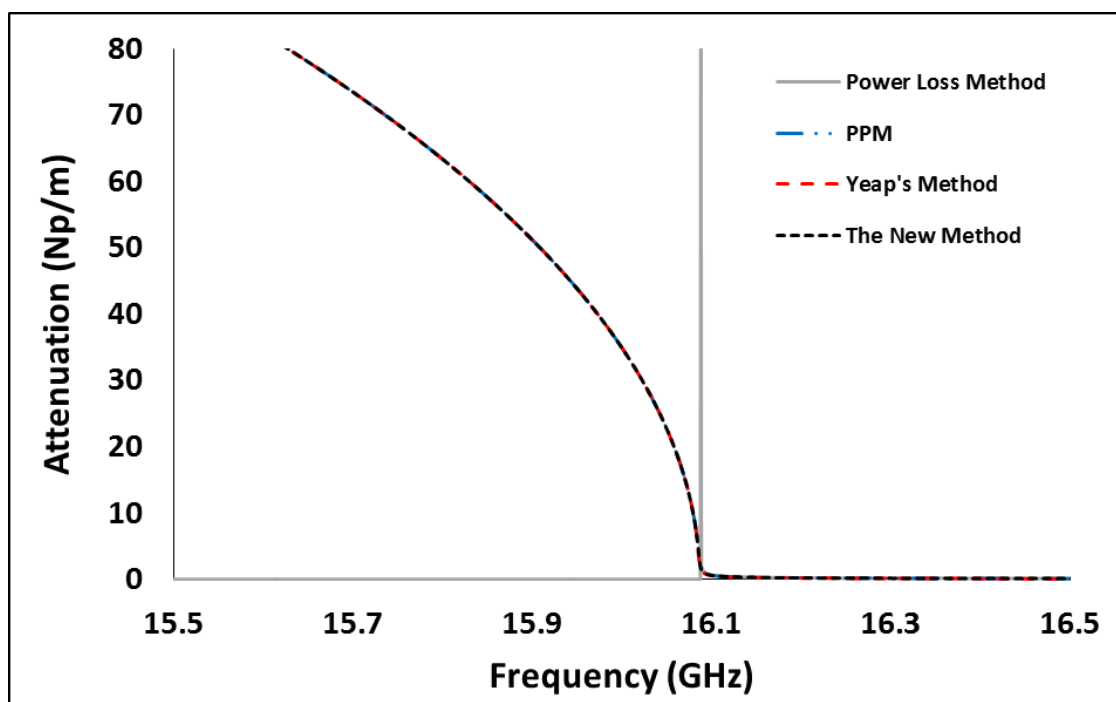


Figure 39 Attenuation of TE₁₁ around the cutoff frequency in a Hollow Rectangular Waveguide with Width $a = 2.29$ cm, Height, $b = 1.02$ cm

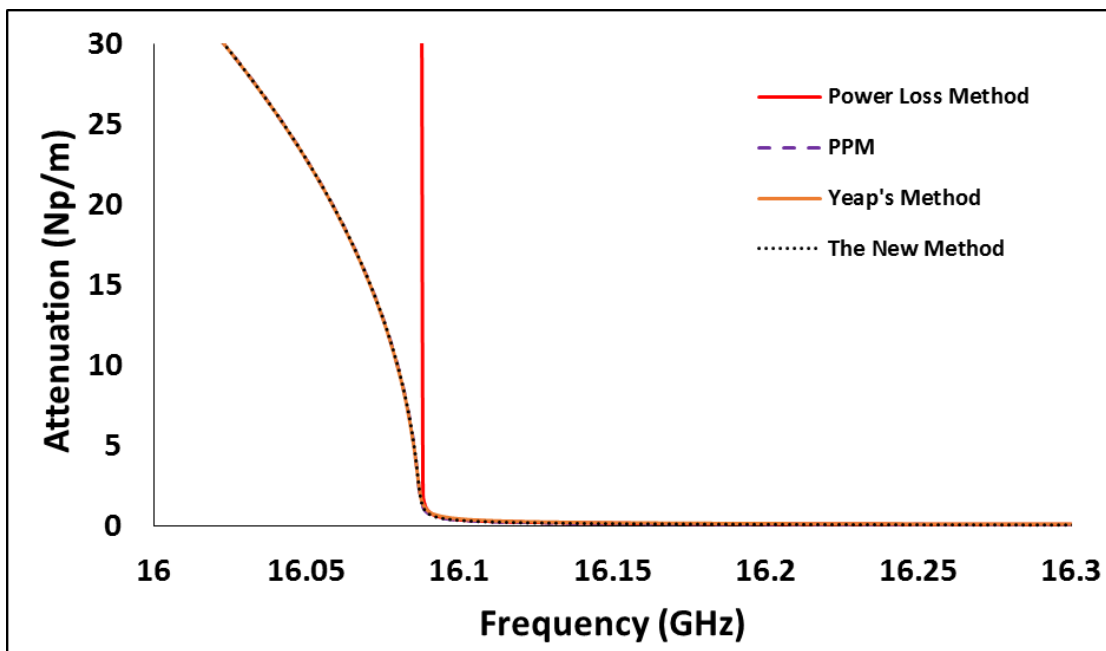


Figure 40 Attenuation of TM_{11} around the cutoff frequency in a Hollow Rectangular Waveguide with Width $a = 2.29$ cm, Height, $b = 1.02$ cm

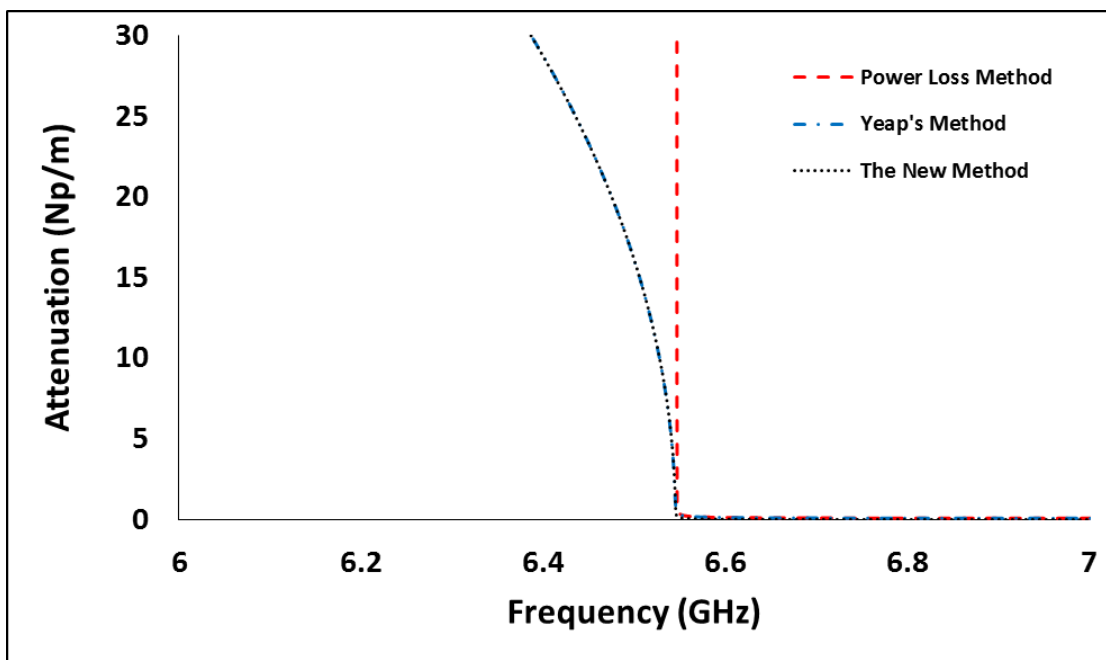


Figure 41 Attenuation of TE_{10} around the cutoff frequency in a Hollow Rectangular Waveguide with Width $a = 2.29$ cm, Height, $b = 1.02$ cm

5.7 Summary

The result of the new method shown are in close agreement with the previous theory. The attenuation when the signal is below the cutoff frequency also tally with the experimental result. The new theory transform the transcendental equation of Yeap's method to a closed form solution. The resulting closed form solution does not need a root searching algorithm to solve, which reduces the computation time dramatically. Besides, it also doesn't have the problem of diverging due to the root searching algorithm. However, for TE₁₀ mode the attenuation computed using the new method are lower than Yeap's method and power loss method. The inability to include the perturbation term into TE₁₀ in k_y made it to be inaccurate. The resulting attenuation therefore is lower.

CHAPTER 6

CONCLUSION AND RECOMMENDATIONS

6.1 Summary

The invention of the radio telescope has given the privilege to mankind to study the largely unexplored galaxy. Radio telescope is used to collect these cosmic radio frequency wave. However, the magnitude of these cosmic radio frequency is very much lower than the radio frequency in our surrounding. This makes detection and analysis of these waves laborious. A waveguide is used to channel these waves from the antenna to the detector circuit. In order to reduce the loss and to increase the efficiency in this process, it is of utmost importance to minimize the loss in the waveguide. Therefore, in order to aid engineers and scientist to design an efficient waveguide, an accurate formulation which able to compute attenuation in a waveguide is important.

Existing formulations can be generally divided into two classes, a more accurate transcendental equation and a simpler closed form equation. Transcendental equation provides a more accurate description of the wave inside a waveguide. However, solving the transcendental equation is laborious. A root finding algorithm is required to solve the equation. An initial guess is therefore required to initiate the algorithm. Besides, depending on the algorithm and the compiler used, the solution may diverge. The computation time required to solve the transcendental equation is also very much longer.

A closed form solution on the other hand is simpler and gives more intuitive insights. A closed form solution usually employs some sort of perturbation to simplify the equation. It usually assumes a perfect waveguide as in the power loss method. The conventional power loss method equation is simple and easy to solve. It does not require the root finding algorithm to solve, hence resulting in a much lower computation time. The power loss method gives a reasonable accuracy provided that the frequency of the signal is higher than the cutoff frequency. However, the equation possesses a flaw. It contains singularity at the cutoff frequency, which results in an infinite attenuation when the frequency of the signal approach the cutoff frequency of the waveguide. This makes the equation fails to describe the propagation of wave when the frequency is below the cutoff frequency.

This thesis provides an alternative to compute the attenuation in the waveguide. It is derived from Yeap's method. Yeap's method results in a set of transcendental equation which requires the use of root finding algorithm to solve. In this new method, the transcendental equation is converted into closed form based on the perturbation theory. The Finite Difference Method is used to approximate a function, which is used to convert the transcendental equation into close form. The resulting close form equation is simpler. It able to factor in the lossy properties of metal. This prevents singularity in the equation such as those in the power loss method. The new method hence able to compute the attenuation when the frequency is below the cutoff.

Based on the result, the new method agrees with the experimental result. The experimental result shows that the attenuation increases dramatically as the frequency decreases from the cutoff frequency. The new method able to show this accurately, together with the existing method except the power loss method. The power loss method diverge to infinity at the cutoff frequency.

The new method however is unable to describe the attenuation of the fundamental mode of rectangular waveguide, TE_{10} mode accurately. The result shows that the attenuation computed from the new method is lower than Yeap's method and the power loss method when the frequency is beyond the cutoff frequency. This is because the wavenumber in the y direction is found out to be zero using the new

method. This is of course not true in the case of lossy metal. Hence, this cause the computed attenuation to be lower than Yeap's method and the power loss method.

6.2 Future Work

Inaccuracy of TE_{10} Mode

The new method presented in this thesis able to calculate the attenuation of the circular waveguide accurately. For rectangular waveguide on the other hand, it able to calculate the TE_{11} and TM_{11} mode accurately but not the fundamental mode, TE_{10} . A refinement of the equation is needed to include the computation of wavenumber in the y direction. The inclusion of a non-zero wavenumber in the y direction is believe will increase the attenuation, allowing it describe the TE_{10} mode much more accurate.

Dielectric Waveguide

The transcendental equation developed by Stratton and Yeap can be used to solve both metal and dielectric waveguide. The new method proposed assumes that the waveguide wall is made of good conductor to simplify the equation. This restricts the new method to be used only for metal waveguide. The new method can be extended so it can be apply to dielectric waveguide.

Bending Loss

The new method assumes that the metal waveguide is a uniformly straight waveguide. Studies have shown that a bend waveguide will result in higher loss (Miyagi, et al., 1984). The new method can be extended by including the bending loss into the equation.

REFERENCES

- Al-Raie, F. M. A., 2007. *Microwaves&RF*. [Online]
 Available at: <http://mwrf.com/components/estimate-microstrip-substrate-relative-dielectric-constant>
 [Accessed 16 March 2016].
- Balanis, C. A., 2012. *Advanced Engineering Electromagnetics*. Second Edition ed. s.l.:John Wiley & Sons, Inc.
- C.S. Lee, S. L. a. S. C., 1985. Plot of Modal Field Distribution in Rectangular and Circular Waveguides. *IEEE. Transactions on Microwave Theory and Techniques*, p. 271.
- Cheng, D. K., 1991. *Field and Wave Electromagnetics*. s.l.:Addison-Wesley Publishing Company, Inc.
- Collin, R. E., 1960. *Field Theory of Guided Waves*. 1st ed. s.l.:McGraw-Hill Book Company, Inc.
- G. Yassin, C. T. a. S. W., 2003. Propagation in Lossy and Superconducting Cylindrical Waveguides. *Proceedings of the 14th International Symposium on Space Terahertz Technology*.
- Gringer, 2008. *Wikipedia*. [Online]
 Available at: <https://commons.wikimedia.org/wiki/File:Optical-fibre.svg>
 [Accessed 20 August 2015].
- Jin, J.-M., 2010. *Theory and Computation of Electromagnetic Fields*. s.l.:John Wiley & Sons, Inc.

- Marcuvitz, N., 1951. *Waveguide Handbook*. s.l.:McGraw-Hill Book Company, Inc.
- Miyagi, M., Harada, K. & Kawakami, S., 1984. Wave propagation and attenuation in the general class of circular hollow waveguides with uniform curvature.. *IEEE Transactions on Microwave Theory and Techniques*, pp. 513-521.
- Paine, S., 1994. Beam Waveguide and Receiver Optics for the SMA. *Fifth International Symposium on Space Terahertz Technology*, pp. 811-823.
- Papadopoulos, V. M., 1953. Propagation of Electromagnetic Waves in Cylindrical Waveguides With Imperfectly Conducting Walls. *The Quarterly Journal of Mechanics and Applied Mathematics*.
- Sadiku, M. N., 2009. *Principles of Electromagnetics Fourth Edition*, s.l.: Oxford University Press.
- Stratton, J. A., 2007. *Electromagnetic Theory*. s.l.:John Wiley & Sons, Inc.
- Tkgd2007, 2008. *Wikipedia*. [Online]
Available at:
https://commons.wikimedia.org/wiki/File:Coaxial_cable_cutaway.svg
[Accessed 20 August 2015].
- Vassilev, V. et al., 2004. *Design and characterization of a sideband separating SIS mixer for 85 - 115 GHz*. Hotel Northampton, Northampton, Massachusetts, Proceedings of the 15th International Symposium on Space Terahertz Technology.
- W. A. Imbriale, T. Y. O. a. C. Y., 1998. Power Loss for Multimode Waveguides and Its Application to Beam-Waveguide System. *IEEE Transactions on Microwave Theory and Techniques*, 46(5), p. 523.
- Yamaguchi, T. A. a. Y., 1980. Propagation Constant Below Cutoff Frequency in a Circular Waveguide with Conducting Medium. *IEEE Transaction on Microwave Theory and Techniques*, p. 707.
- Yeap, K. H., 2011. *Boundary Matching Techniques for Terahertz Lossy Guiding Structures*, s.l.: s.n.

Zykure, 2009. *Wikipedia*. [Online]

Available at: <https://commons.wikimedia.org/wiki/File:Waveguide.svg>

[Accessed 8 August 2015].

APPENDICES

APPENDIX A: Helmholtz Equation

Axial Field

A correct formulation of wave equation inside a circular waveguide is the first step to describe the characteristic of circular waveguide. The derivation of all electromagnetic wave start from the four fundamental Maxwell equation as shown below.

$$\nabla \cdot \vec{E} = \frac{\rho_v}{\epsilon} \quad (\text{A.1})$$

$$\nabla \cdot \vec{B} = 0 \quad (\text{A.2})$$

$$\nabla \times \vec{E} = -\mu \frac{\partial \vec{H}}{\partial t} \quad (\text{A.3})$$

$$\nabla \times \vec{H} = \vec{J} + \epsilon \frac{\partial \vec{E}}{\partial t} \quad (\text{A.4})$$

The derivation of equation that describes the propagation of electromagnetic wave can be done by taking the curl of (A.3) and the result is shown below which is the classical Helmholtz equation to describe the field changes with time and space

$$\nabla^2 \vec{E} = \gamma^2 \vec{E} \quad (\text{A.5})$$

Where γ is the propagation constant of the electromagnetic wave.

$$\begin{aligned} \gamma &= \alpha + j\beta \\ &= j\omega\sqrt{\mu\epsilon_c} \\ &= j\omega\sqrt{\mu\epsilon} \left(1 + \frac{\sigma}{j\omega\epsilon}\right)^{\frac{1}{2}} \end{aligned} \quad (\text{A.6})$$

ϵ_c is the complex permittivity of the medium and can be described as $\epsilon_c = 1 + \frac{\sigma}{j\omega\epsilon}$

The same can be done by taking the curl of (A.4) which will lead to the equation as shown below

$$\nabla^2 \vec{H} = \gamma^2 \vec{H} \quad (\text{A.7})$$

APPENDIX B: Conductor Surface Impedance

The metal conductor surrounding the waveguide plays an important role in the formulation of the waveguide efficiency. Most of the power loss in the waveguide are due to the characteristic of the conductor. As most metal conductor has very high conductivity, based on this assumption, some approximations can be made to simplify the calculation (Cheng, 1991), Referring to (A.6), for a good conductor $\frac{\sigma}{j\omega\epsilon} \gg 1$.

The propagation constant, γ can then be approximated as

$$\gamma \approx \sqrt{j\omega\mu\sigma} \quad (\text{B.8})$$

From the Euler's identity,

$$\begin{aligned} \sqrt{j} &= \left(e^{\frac{j\pi}{2}} \right)^{\frac{1}{2}} \\ &= \frac{(1+j)}{\sqrt{2}} \end{aligned} \quad (\text{B.9})$$

Substitute the result of the Euler's identity (B.9) into (B.8), γ can be represented as

$$\gamma \approx (1+j)\sqrt{\pi f\mu\sigma} \quad (\text{B.10})$$

Since γ can be expressed as $\gamma = \alpha + j\beta$, from (B.10) $\alpha = \beta = \sqrt{\pi f\mu\sigma}$, indicates that for a good conductor, α and β are approximately equal.

The surface impedance, Z_m of the conductor is given as

$$Z_m = \sqrt{\frac{\mu}{\epsilon_c}} \quad (\text{B.11})$$

From (B.11), using the approximation of $\epsilon_c \approx \frac{\sigma}{j\omega\epsilon}$ for a good conductor, the equation can be approximated as

$$Z_m \approx (1+j) \sqrt{\frac{\pi f \mu}{\sigma}} \quad (\text{B.12})$$

The equation for (B.12) is only valid for conductor where it gives a reasonable accuracy to calculate the surface impedance for good conductor, and should not be used for dielectric as such approximation fails to provide an accurate representation of the medium.